

The Role of the Tropical Indian Ocean in Global Climate

Dissertation
zur Erlangung des Doktorgrades
der Naturwissenschaften im Fachbereich
Geowissenschaften
der Universität Hamburg

vorgelegt von

Jürgen Bader

aus Osnabrück

Hamburg

2005

Als Dissertation angenommen vom Fachbereich Geowissenschaften
der Universität Hamburg

auf Grund der Gutachten von Professor Dr. Hartmut Graß
und Professor Dr. Mojib Latif

Hamburg, den 02.02.2005

Prof. Dr. Schleicher
Dekan
des Fachbereichs Geowissenschaften

Abstract

Among the most striking decadal climatic trends of the last century are the strengthening of the NAO index and the decreasing summer monsoon rainfall over sub-Saharan West Africa.

This thesis focuses on the role of tropical sea surface temperatures (SSTs) driving these changes. Both of these changes are investigated by conducting experiments with the atmospheric general circulation model ECHAM4.5 – run in stand-alone mode – and the global ocean-atmosphere-sea ice model MPI-OM/ECHAM5.

These experiments provide evidence that the Indian Ocean warming in the last decades is of paramount importance in driving the recent observed drying trend over the West Sahel. The model West Sahel dried more when tropical seas were warmer during the past half-century than when they were cooler. When sea surface temperatures were changed in one ocean basin at a time, it was the tropical Indian Ocean that dominated. The warming of the Indian Ocean produces through atmospheric teleconnections mid-tropospheric large-scale subsidence over sub-Saharan West Africa.

The Indian and eastern tropical Atlantic Oceans are key ocean areas for driving the two basic rainfall anomaly patterns over sub-Saharan West Africa in summer. This could improve the ability to predict sub-Saharan West African rainfall variability on interannual time-scales.

It is found further that the progressive warming of the tropical Indian Ocean is a principal contributor to the strengthening of the North Atlantic Oscillation via the jet stream waveguide.

Contents

| | | |
|----------|---|-----------|
| 1 | Introduction | 1 |
| 1.1 | Sub-Saharan rainfall variability | 1 |
| 1.1.1 | What are the mechanisms which govern the sub-Saharan West African rainfall variability? | 3 |
| 1.2 | The North Atlantic Oscillation | 6 |
| 1.2.1 | What are the mechanisms which govern the NAO variability? | 10 |
| 1.3 | Scientific Objectives | 12 |
| 1.4 | Contents of my Ph. D. thesis | 14 |
| 1.5 | References | 15 |
| 2 | The Impact of Decadal-Scale Indian Ocean Sea Surface Temperature Anomalies on Sahelian Rainfall and the North Atlantic Oscillation | 23 |
| 2.1 | Introduction | 24 |
| 2.2 | Model and experiments | 27 |
| 2.3 | Results | 29 |
| 2.4 | Summary | 33 |
| 2.5 | References | 35 |
| 3 | Combined Tropical Oceans Drive Anomalous Sub-Saharan West African Rainfall | 39 |
| 3.1 | Introduction | 40 |
| 3.2 | Observations | 41 |
| 3.3 | Model and experiments | 45 |
| 3.4 | Results | 48 |

| | | |
|----------|---|-----------|
| 3.5 | Conclusions | 61 |
| 3.6 | References | 64 |
| 4 | North Atlantic Oscillation response to anomalous Indian Ocean SST in a coupled GCM | 69 |
| 4.1 | Introduction | 70 |
| 4.2 | Model and Experiments | 72 |
| 4.3 | Results | 78 |
| 4.4 | Conclusions | 89 |
| 4.5 | References | 92 |
| 5 | Summary | 95 |
| 5.1 | Conclusions | 95 |
| 5.2 | Discussion | 99 |
| 5.3 | Additional Results | 101 |
| 5.3.1 | Is there a relation between the secular rainfall variability over West Africa north and south of the Sahara desert? | 101 |
| 5.3.2 | Indian Ocean impact on the thermohaline circulation (THC) | 104 |
| 5.4 | References | 109 |

Chapter 1

Introduction

The climate of the 20th century exhibited some rather strong decadal-scale changes. One example is the drying trend in the Sahelian region from the 1950s to the 1990s. Another is the strengthening of the North Atlantic Oscillation (NAO; Hurrell 1995a), the leading mode of North Atlantic climate variability, from the 1970s onward. Both phenomena are the subject of many observational and modelling papers (e.g., Folland et al. 1986, Hurrell 1995a), but it remains controversial which processes lead to the decadal climate fluctuations.

In the following two sections, I will shortly summarize/review the understanding of sub-Saharan West African rainfall variability – especially Sahelian rainfall variability – and NAO variability on seasonal to decadal timescales until the year 2002. The summary is given as a basis for the scientific objectives of my thesis and as background information for the reader.

1.1 Sub-Saharan rainfall variability

The climates of North Africa are still relatively poorly known and understood. The regions north and south of the Sahara desert are regions with climates that are among the most variable in the world (Ward et al. 1999). The Sahel is the semi-arid transition zone situated between the arid to hyper-arid Sahara and humid tropical Africa. The term "Sahel" derives from an Arabic word meaning the "fringe" or "shore" of the desert (Nicholson 1995). The Sahel

region is characterized by a strong north-south rainfall gradient and high interannual rainfall variability, with annual rainfall amounts varying from 600 mm in the south to 100 mm in the north (e.g., Hulme 1992). The rainfall is delivered by a monsoon, or seasonal wind, that originates over the tropical Atlantic, passes over the southwestern coast of West Africa, and gradually pushes north and east over sub-Saharan West Africa (Lamb 1986). Most rainfall – about eighty percent of the annual rainfall – occurs in the period July to September – the rainy season – as a result of the generation of lines of organized convective disturbances often referred to as squall lines (Rowell and Milford, 1993). The Sahel may be viewed as the latitudinal band spanning the African continent from 12°N to 20°N . The Sahel rainfall index shows strong interannual to decadal variability (Lamb 1992; Figure 1.1). A sharp

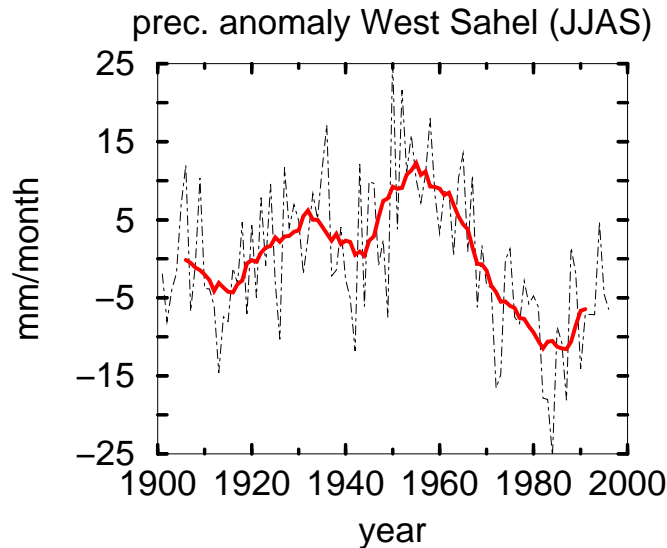


Figure 1.1: *Observed JJAS rainfall anomaly over the West Sahel, based on the Climate Research Unit dataset (mm/month). The rainfall is averaged from 10°W to 10°E and from 12°N to 20°N . The black curve denotes the seasonal mean, the red curve the 11-yr running mean.*

contrast occurs between the periods before and after 1950 (Nicholson 1983, Nicholson 1986). Earlier, marked changes occurred from year to year, with dry years rapidly alternating with wet years, but on the whole, rainfall conditions were relatively good. Droughts occurred in the 1910s and 1940s. After

1950, the year to year fluctuations were more moderate (Nicholson 1989). The Sahel index reveals a period of wetness through the 1950s, followed by an extended dry period since the 1970s. Annual rainfall during the last 30 years has been, on average, some 20 to 40% lower than the 30-year "normal" for 1931-1960 (Nicholson et al. 2000). The increase in persistence after 1950 may be an indication of a shift from a regime dominated by interannual variability to one characterized by decadal-scale variability (Hulme 2001). The decreasing rainfall during the last three decades of the 20th century is among the largest recent climate changes recognized. The extremely dry years had devastating environmental and socio-economic impacts. About 250,000 people died in the Sahel drought of 1968-1973 (UNCOD 1977 in ICPP 2001). The vulnerability of West African societies to climate variability is likely to increase in the next decades because of increasing demands on resources and a rapidly growing population. These pressures could be exacerbated by regional climate change (IPCC, 2001). Thus, there is a strong societal need to develop strategies that reduce the socio-economic impacts of rainfall variability. Better rainfall predictions, which could improve decision making and benefit the local population, require a better scientific understanding of the rainfall variability. The source of the pronounced decadal variability in these regions (Sahel and Morocco) is one of the most pressing questions in climate dynamics today (Ward et al. 1999).

1.1.1 What are the mechanisms which govern the sub-Saharan West African rainfall variability?

Different hypothesis have been put forward to explain the drought in the Sahel. One focuses on anthropogenic factors such as overgrazing and conversion of woodland to agriculture (e. g. , Charney et al. 1975, 1977). Deforestation and overgrazing tend to increase surface albedo and reduce the moisture supply to the atmosphere. Less sunlight is absorbed at the surface due to a larger reflexion of incoming sunlight. The heating of the atmosphere by the ground is reduced, rendering the atmosphere less conducive to the development of convective disturbances. This leads to less precipitation and even less favorable conditions for vegetation. General circulation model sensitiv-

ity studies have concluded that anthropogenic land-cover change in the Sahel could cause a significant drought in the region (e.g., Xue and Shukla 1993). But it is important to note that these studies used idealized and highly unrealistic scenarios of land-cover change that greatly exaggerated the degree of land degradation in the Sahel region (Taylor et al. 2002). Taylor et al. (2002) test the hypothesis that recent changes in land use have been large enough to cause the observed drought. Their results suggest that while the climate of the region is rather sensitive to small changes in albedo and leaf area index, recent historical land use changes are not large enough to have been the principal cause of the Sahel drought. However, the climatic impacts of land use change in the region are likely to increase rapidly in the coming years.

Rainfall variability of the West African monsoon (WAM) has been linked to sea surface temperature (SST) anomaly patterns on a wide range of space- and time-scales. It was originally proposed by Lamb (1978a,b) that fluctuations of summer Sahel rainfall are associated with sea surface temperature variability in the tropical Atlantic (see Rowell et al. 1995). This was confirmed by other studies (Hastenrath 1984; Semazzi 1988; Hastenrath 1990; Lamb and Peppler 1992). The interannual variability of the West African monsoon (WAM) summer rainfall exhibits distinct spatial large-scale rainfall anomaly patterns. WAM seasonal rainfall anomalies tend to be of either opposite sign between the Sahel region and along the coast of Guinea (i.e., a "dipole"; e.g., Lamb 1978a; Nicholson and Grist 2001) or the same sign across all of the sub-saharan West Africa region (e.g., Nicholson and Grist 2001). The dipole rainfall behavior has been linked to the interannual variability of tropical Atlantic SST anomaly patterns (e.g., Rowell et al. 1995, Ward, 1998). In dipole years, there is a strong regional-scale climate variability, with higher SST and lower sea level pressure in the equatorial and tropical South Atlantic accompanying wetter conditions on the Guinea Coast and drier conditions in the Sahel region (Ward 1998). The interannual variability of sub-Saharan West African rainfall has been shown to be also associated with ENSO (e.g., Rowell et al. 1995, Janicot et al. 1996, Rowell 2001). The El Niño phase increases the likelihood of Sahel drought (Rowell 2001). Folland et al. (1986) show – from statistically-based analyses of

observations – that contrasting wet and dry periods in the Sahel region are strongly related to contrasting patterns of sea surface temperature (SST) anomalies on a near global scale. The anomalies include relative changes in SST between the hemispheres, on timescales of years to tens of years, which are most pronounced in the Atlantic. Their experiments with a global general atmospheric circulation model (AGCM) support the idea that the worldwide SST anomalies modulate summer Sahel rainfall through changes in tropical atmospheric circulation. Also Ward (1998) shows that the substantial multi-decadal rainfall variability experienced in the Sahel during the 20th century has been associated with a global interhemispheric SST anomaly difference.

Zeng et al.(1999) analyzed the role of naturally varying vegetation in influencing the climate variability in the West African Sahel in a coupled atmosphere-land-vegetation model. They found that the Sahel rainfall variability is influenced by sea surface temperature variations in the oceans. Land-surface feedback increases this variability both on interannual and interdecadal time scales. Interactive vegetation enhances the interdecadal variation substantially but can reduce year-to-year variability because of a phase lag introduced by the relatively slow vegetation adjustment time. Variations in vegetation accompany the changes in rainfall, in particular the multi-decadal drying trend from the 1950s to the 1980s. The involved feedbacks through albedo and evaporation changes are similar to those proposed in the land use change mechanism.

Anthropogenic aerosols are intricately linked to the climate system and to the hydrologic cycle. The net effect of aerosols is to cool the climate system by reflecting sunlight. Depending on their composition, aerosols can also absorb sunlight in the atmosphere, further cooling the surface but warming the atmosphere in the process. These effects of aerosols on the temperature profile, along with the role of aerosols as cloud condensation nuclei, impact the hydrologic cycle, through changes in cloud cover, cloud properties and precipitation. Unravelling these feedbacks is particularly difficult because aerosols take a multitude of shapes and forms, ranging from desert dust to urban pollution, and because aerosol concentrations vary strongly over time

and space. Increases in aerosol concentration and changes in their composition, driven by industrialization and an expanding population, may adversely affect the Earth's climate and water supply (Kaufmann et al. 2002).

Rotstayn and Lohmann (2002) ran an atmospheric global climate model coupled to a mixed layer ocean model to study changes in tropical rainfall due to the indirect effects of anthropogenic sulfate aerosol. The model included interactions between sulphur dioxide emissions and cloud formation. Two likely effects of anthropogenic aerosols on liquid water clouds have been identified. The first indirect effect refers to the radiative impact of a decrease in cloud droplet effective radius that results from increases in aerosols. The second indirect effect refers to the radiative impact of a decrease in precipitation efficiency that results from increases in aerosols (Rotstayn and Lohmann 2002). Acting as cloud condensation nuclei, thereby modifying cloud albedo, precipitation formation, and lifetime of warm clouds, aerosols lead to surface cooling.

The model was run for present-day and preindustrial sulfur emission scenarios. When the present-day sulphur emissions were included in their model, a southward shift of tropical rainfall was simulated causing drought in the Sahel. This was largely due to a hemispheric asymmetry in the reduction of sea surface temperature (SST) induced by the perturbation of cloud albedo and lifetime (Rotstayn and Lohmann 2002).

The impact of internal atmospheric variability on Sahelian rainfall has been tested by Rowell et al. (1992) and Palmer et al. (1992). They performed atmospheric general circulation model (AGCM) sensitivity experiments in which they changed the initial atmospheric conditions, but keeping the SST forcing constant. They found little difference between the seasonal Sahel rainfall totals, suggesting that although some internal atmospheric variability exists, it is dominated by the oceanic forcing (Rowell et al. 1995).

1.2 The North Atlantic Oscillation

The North Atlantic Oscillation is the dominant mode of climate variability in the North Atlantic region ranging from central North America to Europe

and much into Northern Asia. It is most pronounced during winter. The NAO is a large-scale seesaw in atmospheric mass between the subtropical Atlantic and the Arctic. It is usually defined through changes in surface pressure in the centers of action near Iceland and the Azores. The positive phase of the NAO is characterized by a large meridional pressure gradient over the North Atlantic, because of a deeper than normal Icelandic Low and a stronger Subtropical High (Figure 1.2a). Both centers are weakened during its "negative" phase (Figure 1.2b). The changes in pressure gradient from one

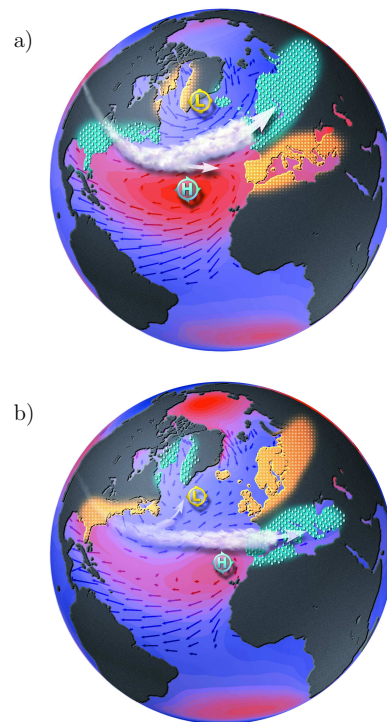


Figure 1.2: *Illustration of the two extreme phases of the North Atlantic Oscillation (NAO) with some climatic impacts. Figure a) shows the positive and b) the negative NAO phase. Figures are available at <http://www.ldeo.columbia.edu/~visbeck/misc>.*

phase to another produce large changes in the mean wind speed and direction over the North Atlantic. Heat and moisture transport between the Atlantic and the surrounding continents also vary markedly, as do the intensity and number of winter storms, their paths, and the weather associated with them

(Hurrell et al. 2001).

In the positive phase of the NAO the enhanced pressure difference results in stronger westerlies across middle latitudes, and in more and stronger winter storms crossing the Atlantic Ocean on a more northerly track (see Figure 1.2b). This phase of the NAO is associated with cold and dry winters over the northwest Atlantic and warm and wet winters in Northern Europe as well as dry conditions over Southern Europe. The negative NAO index phase shows a weak subtropical high and a weak Icelandic low. The reduced pressure gradient results in fewer and weaker winter storms crossing on a more west-east pathway. They bring moist air into the Mediterranean and cold air to Northern Europe (see Figure 1.2b). The NAO is associated e.g., with changes in the wind field in the troposphere (Thompson and Wallace, 2000) and with changes in SST and salinity: The NAO induces changes in surface wind patterns over the Atlantic Ocean, thereby altering the ocean surface heat and freshwater flux. These changes affect the strength and character of the Atlantic thermohaline circulation (THC) and the horizontal flow of the upper ocean (Hurrell et al. 2001). The NAO is associated with precipitation changes (Lamb, 1978; Folland et al. 1986; Hurrell and van Loon, 1997), changes in the storm tracks and intensity over the Atlantic (Rogers, 1990, 1997; see Figures 1.2a and 1.2b), and it has a wide range of effects on marine and terrestrial ecosystems, including the large-scale distribution and population of fish and shellfish, the production of zooplankton, the flowering dates of plants, and the growth, reproduction, and demography of many land animals (Hurrell et al. 2001). A remarkable feature of the NAO that has motivated much recent study is its trend toward a more positive phase over the past 30 years (see Figure 1.3). The positive trend in the NAO accounts for several remarkable changes recently in the climate and weather over the middle and high latitudes of the Northern Hemisphere, as well as in marine and terrestrial ecosystems:

- milder winters in Europe and Asia; colder winters over eastern Canada and the northwest Atlantic (Hurrell, 1996),
- stronger westerlies in the lower stratosphere (Thompson et al. 2000),
- regional changes in precipitation (Hurrell, 1995b; Hurrell and van Loon,

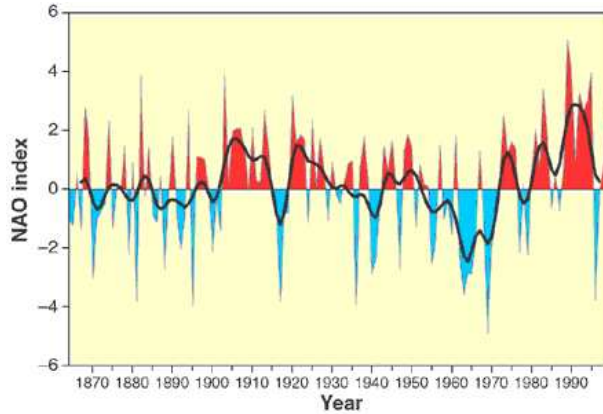


Figure 1.3: Winter (December to March) index of the NAO based on the difference of normalized pressures between Lisbon, Portugal, and Stykkishólmur/Reykjavik, Iceland from 1864 through 2000. The heavy solid line represents the meridional pressure gradient smoothed to remove fluctuations with periods less than 4 years. From Hurrell et al. (2001).

1997),

- decrease in mean sea level pressure (SLP) over the Arctic (Walsh et al. 1996),
- convection intensity changes in the Labrador and the Greenland-Iceland Seas (Dickson et al. 1996) which influence the strength and character of the Atlantic meridional overturning circulation,
- changes in storm activity and the shifts in the Atlantic storm track (Hurrell, 1995a), changes in the blocking frequencies (Nakamura, 1996).

Thus, understanding the physical mechanisms that govern the NAO variability on intraseasonal-to-interdecadal timescales, and how the NAO may be influenced by anthropogenic climate change is of high importance.

1.2.1 What are the mechanisms which govern the NAO variability?

There is no consensus on the processes that are responsible for the observed low-frequency variations in the NAO. There is evidence that much of the atmospheric circulation variability in the form of the NAO arises from internal atmospheric processes. Atmospheric general circulation models (AGCMs) forced by climatological sea surface temperature, and fixed atmospheric trace-gas concentrations, display NAO-like fluctuations (e.g., Saravanan 1998). The governing dynamical mechanisms are eddy mean flow interaction at the exit region of the Atlantic storm track and eddy-eddy interaction between baroclinic transients and low-frequency variability (Hurrell 1995b). On the other hand, it has long been recognized that fluctuations in SST and the strength of the NAO are related (Bjerknes, 1964), and there are clear indications that the North Atlantic Ocean varies significantly with the overlying atmosphere. The leading mode of SST variability over the North Atlantic during winter consists of a tri-polar pattern with a cold anomaly in the subpolar region, a warm anomaly in the middle latitudes centered off Cape Hatteras, and a cold subtropical anomaly between the equator and 30N (e.g., Deser and Blackmon 1993; Rodwell et al. 1999). The strength of the correlation increases when the NAO index leads the SST, which indicates that SST is responding to atmospheric forcing on monthly time scales (e.g., Battisti et al. 1995). But SST observations also display interannual and decadal responses (Sutton and Allen 1997; Visbeck et al. 1998), which may indicate that decadal/multi-decadal variations of the ocean surface have an impact on the atmosphere. Rodwell et al. (1999) forced their AGCM by the observed, global SSTs and sea ice concentration over the past 50 years (see also Latif et al. 2000; Mehta et al. 2000). They captured much of the multi-annual to multi-decadal variability in the observed NAO index since 1947, including about 50% of the observed strong upward trend over the past 30 years. To confirm that North Atlantic SSTs force the NAO they drove their AGCM with a North Atlantic SST pattern similar to the observed SST tripole. They found that the atmospheric response in mean sea level pressure between model simulations with positive and negative versions of the SST

tripole is similar to the classical NAO pattern. They concluded that much of the multiannual to multidecadal variability of the winter NAO over the past half century may be reconstructed from a knowledge of North Atlantic sea surface temperatures.

A recent study concludes that NAO variability is closely tied to SSTs over the tropical Ocean. Hoerling et al. (2001) presented evidence that North Atlantic Climate change since 1950s is linked to a progressive warming of tropical SSTs. They argue that the ocean changes alter the pattern and magnitude of tropical rainfall and atmospheric heating, the atmospheric response to which includes the spatial structure of the NAO.

Watanabe and Nitta (1999) have suggested that land processes are responsible for decadal changes in the NAO. They find that the change toward a more positive wintertime NAO index in 1989 was accompanied by large changes in snow cover over Eurasia and North America. Moreover, the relationship between snow cover and the NAO was even more coherent when the preceding fall snow cover was analyzed, suggesting that the atmosphere may have been forced by surface conditions over the upstream land mass. Watanabe and Nitta (1998) reproduce a considerable part of the atmospheric circulation changes by prescribing the observed snow cover anomalies in an AGCM.

Several recent studies suggest that both the oceanic wind forced gyre circulation and the thermohaline circulation can actively interact with atmospheric flow to produce coupled decadal and interdecadal climate variability. In the paper of Grötzner et al. (1998) a decadal climate cycle in the North Atlantic that was derived from an integration with a coupled ocean-atmosphere general circulation model is described. The decadal mode shares many features with the observed decadal variability in the North Atlantic. The decadal mode is based on unstable air-sea interactions and must be therefore regarded as an inherently coupled mode. It involves the subtropical gyre and the North Atlantic Oscillation. The memory of the coupled system, however, resides in the ocean and is related to horizontal advection and to the oceanic adjustment to low-frequency wind stress curl variations. Although differing in details, the North Atlantic decadal mode and the North Pacific mode described by Latif and Barnett (1996) are based on the same fundamental mechanism: a feedback loop between the wind driven subtropical gyre and

the extratropical atmospheric circulation.

Other studies have suggested a coupled mode of variability involving the thermohaline circulation. Modeling results of Timmermann et al. (1998) suggested that an anomalous strong thermohaline circulation produces positive SST anomalies over the North Atlantic. The atmospheric response is a strengthened NAO. The stronger NAO produces anomalous fresh water fluxes, and Ekman transport off Newfoundland and the Greenland Sea. This results in a reduced sea surface salinity which is advected by the subpolar gyre. This finally reduces the convective activity south of Greenland, thereby weakening the strength of the thermohaline circulation. This results in a reduced poleward oceanic heat transport and the formation of negative SST anomalies, which completes the phase reversal and results in multi-decadal variability.

1.3 Scientific Objectives

The aim of this Ph.D. thesis is to elucidate further the impact of sea surface temperature (SST) anomalies on the rainfall variability over north West Africa on interannual to decadal timescales and on the North Atlantic Oscillation (NAO) on decadal timescales. In addition to the investigation of rainfall variability over the West Sahel, I will also analyze the rainfall variability along Guinea Coast and over Morocco. Several experiments have been performed with the atmospheric general circulation model ECHAM4.5 – run in stand-alone mode – and with the global ocean-atmosphere-sea ice model MPI-OM/ECHAM5 to investigate the following specific questions:

- The review of the literature leads to the conclusion that Sahelian dry conditions in the late twentieth century were most probably driven by changes in ocean surface temperatures, which led to changes in atmospheric circulation (e.g., Ward et al. 1998; Zeng et al. 1999). Interactions between the Sahelian land surface and the regional atmosphere via vegetation dynamics appear to have played a role in modulating interannual and decadal scale variations in rainfall (e.g., Zeng et al. 1999; Taylor et al. 2002).

I would like to answer the following questions: Is the drying trend over the West Sahel in particular driven by changes in only one ocean basin? Is it possible to restrict the region of SST anomalies to the tropical Atlantic, Pacific or Indian Oceans? What kind of SST pattern in the individual ocean basins is the most important? What is/are the basic physical atmospheric process(es) which lead(s) to the rainfall change over the West Sahel?

- The review about the NAO shows that the evolution of global sea surface temperatures (SSTs) has exerted an important controlling effect on the North Atlantic Oscillation. Key evidence is the reproducibility of the observed low-frequency changes of the NAO, across different climate models forced with prescribed, global SSTs (Rodwell et al. 1999, Latif et al. 2000, and Mehta et al. 2000). A key piece of evidence that changes in tropical SSTs are the principal source for the trend of the NAO comes from Hoerling et al. (2001). Forcing their AGCM only with the observed SSTs in the Tropics (30°S-30°N) the model reproduced the observed trend pattern of North Atlantic climate change.

The questions I would like to answer are basically the same as in case of the Sahelian drought. Which ocean basin is the most important for the trend of the NAO? What is the mechanism responsible for the change of the NAO, since a clear mechanism of how the tropical SSTs impact the NAO was not given by Hoerling et al. (2001)?

To answer these questions – concerning the NAO and the Sahel trend – the same experiments can be used.

- Sub-Saharan summer rainfall anomalies are mainly characterized by two distinctive patterns: A "dipole" and a "monopole" rainfall anomaly pattern between Sahel and Guinea Coast rainfall anomalies (see review). The identification of key ocean areas for driving these two basic rainfall anomaly patterns over sub-Saharan West Africa in summer is another major aim of this thesis. This could improve the ability to predict sub-Saharan West African rainfall variability on interannual to decadal timescales.

1.4 Contents of my Ph. D. thesis

My thesis is based on three papers/manuscripts which are listed below.

- Chapter 2: Bader J. , and M.Latif, 2003: The impact of decadal-scale Indian Ocean SST anomalies on Sahelian rainfall and the North Atlantic Oscillation, *Geophysical Research Letters*, **30**, DOI 10.1029/2003GL018426.
- Chapter 3: Bader J. , and M.Latif, 2004: Combined Tropical Oceans Drive Anomalous Sub-Saharan West African Rainfall, *Journal of Climate*, submitted.
- Chapter 4: Bader J. , and M.Latif, 2004: North Atlantic Oscillation response to anomalous Indian Ocean SST in a coupled GCM, *Journal of Climate*, submitted.

The thesis is concluded with a Summary/Outlook.

1.5 References

- Battisti, D. S., U. S. Bhatt, and M. A. Alexander, 1995: A modeling study of the interannual variability in the wintertime North Atlantic Ocean, *Journal of Climate*, **8**, 3067-3083.
- Bjerknes, J., 1964: Atlantic air-sea interaction, *Adv. Geophys.*, **10**, 1-82.
- Charney, J., Stone, P. H. and Quirk, W. J. 1975. Drought in the Sahara: a biogeophysical feedback mechanism, *Science*, **187**, 434-435.
- Charney, J., Quirk, W. J., Chow, S. H. and Kornfield, J. 1977. A comparative study of the effects of albedo change on drought in semi-arid regions, *Journal of the Atmospheric Sciences*, **34**, 1366-1386.
- Deser, C., and M. L. Blackmon, 1993: Surface climate variations over the North Atlantic Ocean during winter: 1900-1993, *Journal of Climate*, **6**, 1743-1753.
- Dickson, R. R., J. Lazier, J. Meincke, P. Rhines, and J. Swift, 1996: Long-term co-ordinated changes in the convective activity of the North Atlantic, *Progress in Oceanography*, **38**, 241-295.
- Folland, C.K., T.N. Palmer, D.E. Parker, 1986: Sahel rainfall and worldwide sea temperatures, 1901-85, *Nature*, **320**, 602-607.
- Grötzner, A., M. Latif, and T. P. Barnett, 1998: A decadal climate cycle in the North Atlantic Ocean as simulated by the ECHO coupled GCM, *Journal of Climate*, **11**, 831-847.
- Hastenrath S. 1984: Interannual variability and annual cycle – mechanisms and climate in the tropical Atlantic sector, *Monthly Weather Review*, **112**, 1097-1107.
- Hastenrath S. 1990: Decadal-scale changes of the circulation in the tropical Atlantic sector associated with Sahel drought, *International Journal of Climatology*, **10**, 459-472.

- Hoerling, M.P., J.W. Hurrell, T.Y. Xu, 2001: Tropical origins for recent North Atlantic climate change, *Science*, **292**, 90-92.
- Hulme, M., 1992: Rainfall changes in Africa 1931-1960 to 1961-1990, *International Journal of Climatology*, **12**, 685-699.
- Hulme, M., 2001: Climatic perspectives on Sahelian desiccation: 1973-1998, *Global Environmental Change*, **11**, 19-29.
- Hulme, M., Doherty, R., Ngara, T., New, M. and Lister, D. 2001: African climate change: 1900-2100. *Climate Research*, **17**, 145-168.
- Hurrell, J. W., 1995a: Decadal trends in the North Atlantic Oscillation regional temperatures and precipitation, *Science*, **269**, 676-679.
- Hurrell, J. W., 1995b: Transient eddy forcing of the rotational flow during northern winter, *Journal of Atmospheric Science*, **52**, 2286-2301.
- Hurrell, J. W., 1996: Influence of variations in extratropical wintertime teleconnections on Northern Hemisphere temperatures, *Geophysical Research Letters*, **23**, 665-668.
- Hurrell, J. W., and H. van Loon, 1997: Decadal variations in climate associated with the North Atlantic Oscillation, *Climatic Change*, **36**, 301-326.
- Hurrell, J. W., Y. Kushnir, and M. Visbeck 2001: The North Atlantic Oscillation, *Science*, **291**, 603-605.
- IPCC, Climate Change 2001: Impacts, adaptation and vulnerability – contribution of working group II to the third assessment report of the Intergovernmental Panel on Climate Change (IPCC), James J. McCarthy, Osvaldo F. Canziani, Neil A. Leary, David J. Dokken and Kasey S. White, Eds., Cambridge University Press, pp 1000, (available at http://www.grida.no/climate/ipcc_tar/wg2/index.htm).
- Janicot S, V. Moron, B. Fontaine, 1996: Sahel droughts and ENSO dynamics, *Geophysical Research Letters*, **23**, 515-518.

- Kaufmann Y. J. , D. Tanre, and O. Boucher, 2002: A satellite view of aerosols in the climate system, *Nature*, **419**, 215-223.
- Lamb, P.J., 1978a: Case studies of tropical Atlantic surface circulation patterns during recent sub-Saharan weather anomalies: 1967 and 1968, *Monthly Weather Review*, **106**, 482-491.
- Lamb, P.J., 1978b: Large-scale tropical Atlantic surface circulation patterns associated with sub-Saharan weather anomalies, *Tellus*, **A30**, 240-251.
- Lamb, P.J., 1986: Waiting for rain – A new theory links drought in West Africa to temperatures in the Atlantic, *Sciences*, **26**, 30-36.
- Lamb, P. J. and R. A. Pepler, 1991: West Africa, *Teleconnections linking worldwide climate anomalies*, M. Glantz, R. Katz and N. Nicholls, Eds. , Cambridge University Press, 121-189.
- Lamb, P.J., and R.A. Pepler, 1992: Further case studies of tropical Atlantic surface circulation patterns associated with sub-Saharan drought, *Journal of Climate*, **5**, 476-488.
- Latif, M., and T. Barnett, 1996: Decadal climate variability over the North Pacific and North America-dynamics and predictability, *Journal of Climate*, **9**, 2407-2423.
- Latif, M., K. Arpe, and E. Roeckner, 2000: Oceanic control of North Atlantic sea level pressure variability in Winter, *Geophysical Research Letters*, **27**, 727-730.
- Mehta V.M., M. J. Suarez, J. V. Manganello, and T. L. Delworth, 2000: Oceanic influence on the North Atlantic Oscillation and associated Northern Hemisphere climate variations: 1959-1993, *Geophysical Research Letters*, **27**, 121-124.
- Nakamura, H., 1996: Year-to-year and interdecadal variability in the activity of intraseasonal fluctuations in the Northern Hemisphere wintertime circulation, *Theor. Appl. Climatol.* , **55**, 19-32.

- Nicholson, S. E. 1978: Climatic variations in the Sahel and other African regions during the past five centuries, *Journal of Arid Environments*, **1**, 3-24.
- Nicholson, S. E. 1983: Sub-Saharan Rainfall in the Years 1976-1980: Evidence of Continued Drought, *Monthly Weather Review*, **111**, 1646-1654.
- Nicholson, S.E., 1986: The spatial coherence of African rainfall anomalies: inter-hemispheric teleconnections, *Journal of Climate and Applied Meteorology*, **25**, 1365-1381.
- Nicholson, S.E., 1989: African drought: characteristics, causal theories and global teleconnections. *Understanding Climate Change*, A. Berger, R. E. Dickinson, J. W. Kidson, Eds. , American Geophysical Union, 79-100.
- Nicholson, S.E., 1995: Sahel, West Africa, *Encyclopedia of Environmental Biology*, **V3**, 261-275.
- Nicholson S.E, 2000: The nature of rainfall variability over Africa on time scales of decades to millenia, *Global and Planetary Change*, **26**, 137-158.
- Nicholson S.E., J.P. Grist, 2001: A conceptual model for understanding rainfall variability in the West African Sahel on interannual and interdecadal timescales, *International Journal of Climatology*, **21**, 1733-1757.
- Palmer T. J. ,C. Brankovic, P. Viterbo, M. J. Miller, 1992: Modeling inter-annual variations of summer monsoons, *Journal of Climate*, **5**, 399-417.
- Rodwell, M. J. , D. P. Rowell, and C. K. Folland, 1999: Oceanic forcing of the wintertime North Atlantic Oscillation and European climate, *Nature*, **398**, 320-323.
- Rogers, J. C. , 1990: Patterns of low-frequency monthly sea level pressure variability (1899-1986) and associated wave cyclone frequencies, *Journal of Climate*, **3**, 1364-1379.

- Rogers, J. C. , 1997: North Atlantic storm track variability and its association to the North Atlantic Oscillation and climate variability of Northern Europe, *Journal of Climate*, **10**, 1635-1647.
- Rotstayn, L. D. , and U.Lohmann, 2002: Tropical rainfall trends and the indirect aerosol effect, *Journal of Climate*, **15**, 2103-2115.
- Rowell, D. P. C. K. Folland K. Maskell, J. A. Owen and M. N. Ward, 1992: Modeling the impact of global sea surface temperatures on the variability and predictability of seasonal Sahel rainfall, *Geophysical Research Letters*, **19**, 905-908.
- Rowell, D. P. and J. R. Milford 1993: On the generation of African squall lines, *Journal of Climate* **6**, 1181-1193.
- Rowell, D. P. , C. K. Folland, K. Maskell, and M. N. Ward, 1995: Variability of summer rainfall over tropical north Africa (1906-92): Observations and modeling, *Q. J. Meteorol. Soc.* , **121**, 669-704.
- Rowell, D. P., 2001: Teleconnections between the tropical Pacific and the Sahel, *Quart. J. Roy. Meteor. Soc.*, **127**, 1683-1706.
- Saravanan, R., 1998: Atmospheric low frequency variability and its relationship to midlatitude SST variability: studies using the NCAR Climate System Model, *Journal of Climate*, **11**, 1386-1404.
- Semazzi F. H. M. , V. Mehta, and Y. C. Sud, 1988: An investigation of the relationship between sub-Saharan rainfall and global sea-surface temperatures, *Atmosphere-Ocean*, **26**, 118-138.
- Sutton, R. T., and M. R. Allen, 1997: Decadal predictability of North Atlantic sea surface temperature and climate, *Nature*, **388**, 563-567.
- Taylor C. M. , E. F. Lambin, N. Stephenne, R. J. Harding, R. L. H. Essery, 2002: The influence of land use change on climate in the Sahel, *Journal of Climate*, **15**, 3615-3629.

- Thompson, D. W. J., and J. M. Wallace, 2000: Annual modes in the extratropical circulation: Part I month-to-month variability, *Journal of Climate*, **13**, 1000-1016.
- Thompson, D. W. J., J. M. Wallace, and G. C. Hegerl, 2000: Annual modes in the extratropical circulation: Part II. Trends, *Journal of Climate*, **13**, 1018-1036.
- Timmermann, A., M. Latif, R. Voss, and A. Grötzner, 1998: Northern Hemisphere interdecadal variability: a coupled air-sea mode, *Journal of Climate*, **11**, 1906-1931.
- Visbeck, M., H. Cullen, G. Krahnemann, N. Naik, 1998: An ocean model's response to North Atlantic Oscillation-like wind forcing, *Geophysical Research Letters*, **25**, 4521-4524.
- Walsh, J. E., W. L. Chapman, and T. L. Shy, 1996: Recent decrease of sea level pressure in the central Arctic, *Journal of Climate*, **9**, 480-486.
- Watanabe, M. and T. Nitta, 1998: Relative impact of snow and sea surface temperature anomalies on an extreme phase in the winter atmospheric circulation, *Journal of Climate*, **11**, 2837-2857.
- Watanabe, M. and T. Nitta, 1999: Decadal changes in the atmospheric circulation and associated surface climate variations in the Northern Hemisphere winter, *Journal of Climate*, **12**, 494-510.
- Ward, M.N., 1998: Diagnosis and short-lead time prediction of summer rainfall in tropical North Africa at interannual and multi-decadal time scales, *Journal of Climate*, **11**, 3167-3191.
- Ward, M.N., P. J. Lamb, D. H. Portis, M. el Hamly, and R. Sebbari, 1999: Climate variability in northern Africa. Understanding droughts in the Sahel and the Maghreb. *Beyond el Niño: Decadal and interdecadal climate variability*, A. Navarra, Ed., Springer-Verlag, 119-140.
- Zeng, N., J. D. Neelin, K. M. Lau, C. J. Tucker, 1999: Enhancement of interdecadal climate variability in the Sahel, *Science*, **286**, 1537-1540.

- Xue, Y. , and J. Shukla, 1993: The influence of land-surface properties on Sahel climate. 1. Desertification, *Journal of Climate*, **6**, 2232-2245.

Chapter 2

The Impact of Decadal-Scale Indian Ocean Sea Surface Temperature Anomalies on Sahelian Rainfall and the North Atlantic Oscillation

Jürgen Bader^{1,2,*} and Mojib Latif³

¹Institute of Geophysics and Meteorology, University of Cologne, Cologne, Germany

²Max-Planck-Institute for Meteorology, Hamburg, Germany

³Institute for Marine Research at the University of Kiel, Kiel, Germany

*Corresponding author address: Jürgen Bader, Max-Planck-Institute for Meteorology, Bundesstraße 53, 20146 Hamburg, Germany. E-mail: bader@dkrz.de

Abstract

The sea surface temperatures (SSTs) of the tropical Indian Ocean show a pronounced warming since the 1950s. We have analyzed the impact of this warming on Sahelian rainfall and on the North Atlantic Oscillation (NAO) by conducting ensemble experiments with an atmospheric general circulation model. Additionally, we investigate the impact of the other two tropical oceans on these two climate parameters. Our results suggest that the warming trend in the Indian Ocean played a crucial role for the drying trend over the West Sahel from the 1950s to 1990s and may also have contributed to the strengthening of the NAO during the most recent decades.

2.1 Introduction

The climate of the 20th century exhibited some rather strong decadal-scale changes. One example is the drying trend in the Sahelian region from the 1950s to the 1990s (Fig. 2.1a). Another is the strengthening of the North Atlantic Oscillation (NAO, Hurrell 1995), the leading mode of North Atlantic climate variability, from the 1970s onward (Fig. 2.1b). Both phenomena are the subject of many observational and modelling papers (e.g., Folland et al. 1986, Hurrell 2003 and articles therein), but it remains controversial which processes lead to the decadal climate fluctuations. We address in this paper the role of the tropical Indian Ocean SST in driving these changes, since the tropical Indian Ocean SST exhibits a remarkable warming trend during the last 50 years (Figure 2.1c).

The regions north and south of the Sahara desert are regions with climates that are among the most variable in the world (Ward et al. 1999). The Sahelian region is located south of the Sahara desert, defined here as the latitudinal band spanning the African continent from 12°N to 20°N . The rainy season is from June to September (JJAS) and associated with the seasonal movement of the intertropical convergence zone (ITCZ). The West Sahel JJAS rainfall index (defined from 10°W to 10°E and from 12°N to 20°N – indicated by the box in Figures 2.2b, and 2.3a-c) shows a strong decadal trend. There was anomalously strong rainfall in the 1950s and early

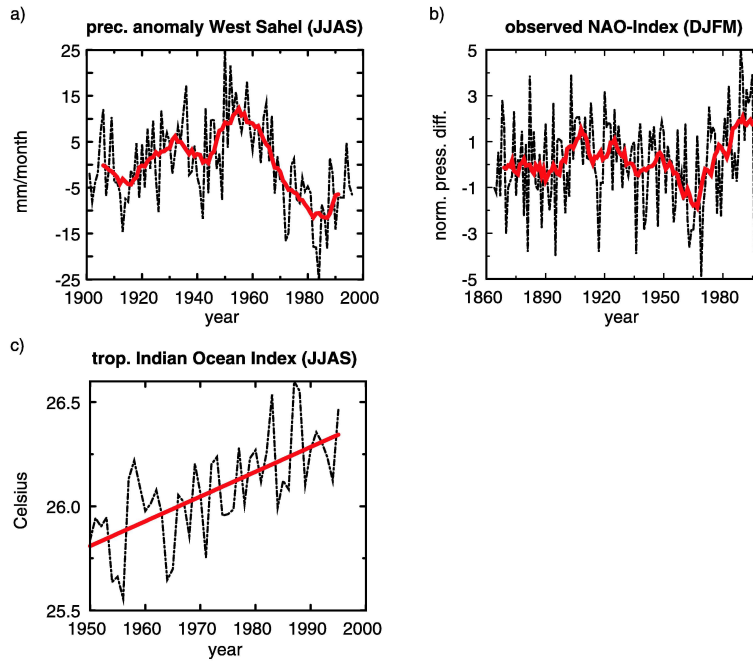


Figure 2.1: a) Observed JJAS rainfall anomaly over the West Sahel, based on the Climate Research Unit dataset (mm/month), b) observed winter (DJFM) NAO index defined by Hurrell (1995), c) observed tropical Indian Ocean SST Index for the JJAS season (in Celsius), based on the Reynolds SSTs; averaged from the east coast of Africa to 120°E and from 30°S to 30°N . The black curves denote the seasonal means, the red curves the 11-yr running mean or the linear trend.

1960s (wet mode), followed by an extended anomalously dry period since the 1970s (dry mode) (see Figure 2.1a) that had and continues to have important economic and social impacts. Observational and model studies show that Sahelian rainfall variability is associated with regional and global SST anomaly patterns. These include changes in the tropical Atlantic (e.g., Lamb 1978a, b; Hastenrath 1984; Lamb and Pepler 1992; Ward 1998; Vizzy and Cook 2001, 2002), in the Pacific (e.g., Janicot 1996; Rowell 2001), in the Indian Ocean (Palmer 1986, Shinoda and Kawamura 1994), and in the Mediterranean (Rowell 2003). Folland et al. (1986) linked near global changes in sea surface temperatures to Sahelian rainfall variability. In the first part of this paper, we investigate the impact of tropical SSTAs on the low-frequency variability of sub Saharan rainfall by conducting a series of experiments with an atmospheric general circulation model (AGCM). We investigate the role of the different tropical ocean basins and their combinations in forcing decadal Sahelian rainfall anomalies.

In the second part of our study, the model experiments with our atmospheric general circulation model are analyzed with regard to the impact of tropical SSTs on the extratropical climate, specifically the NAO. The NAO shows strong interannual and decadal variabilities during the last century (Figure 2.1b). Different hypotheses were put forward to explain the low-frequency changes of the NAO. Internal atmospheric dynamics were suggested by James and James (1989). Saravanan and McWilliams (1997) linked the low-frequency variability to a stochastic forcing of the atmosphere driving low-frequency changes in the ocean which feed back on the atmosphere. In AGCM experiments, Rodwell et al. (1999) and Latif et al. (2000) found an oceanic control of decadal North Atlantic sea level pressure variability in winter. Hoerling et al. (2001) linked the recent trend of the NAO to a warming of the tropical oceans. Our study investigates not only whether the recent decadal change of the NAO is of tropical origin, but also which tropical ocean basin contributed most to the change. We focus on the role of the tropical Indian Ocean, since it exhibits a rather gradual warming trend during the recent decades (Figure 2.1c).

2.2 Model and experiments

We use the atmospheric general circulation model ECHAM4.5 (Roeckner et al. 1996). The model forced by the observed SSTs from 1951 to 1994 reproduces the decadal trend of Sahelian rainfall (Schnitzler et al. 2001) and simulates the observed low-frequency NAO index variations reasonably well (Latif et al. 2000). As described above, rainfall over the West Sahel shows a multidecadal drying trend from the 1950s (wet mode) to the beginning of the 1990s (dry mode). The wet and dry modes are defined here as the periods from January 1951 to December 1960 and from January 1979 to February 1996, respectively. We examine the decadal-scale response of ECHAM4.5 to the observed tropical SST anomaly field representing the difference between the dry and wet mode. The model's response to the total SST forcing, its individual components in the different ocean basins and combinations of these are analyzed. Figure 2.2a shows the tropical (30°S - 30°N) SST difference field (here for the June to September (JJAS) season) contrasting the situations between the dry and wet mode in the Sahel. In the 1950s, the tropical SSTs were considerably colder relative to the 1980s and 1990s, and we address the impact of these anomalously cold tropical SSTs on Sahelian rainfall and the NAO. Please note that the strongest cold anomaly is found in the tropical Indian Ocean, and we are here mostly concerned with the impact of this anomaly on the tropical and Northern Hemisphere climate. In the dry mode experiment, the climatological AMIP2-SST (Taylor et al. 2000) is used, while in the wet mode experiment, the climatological monthly means are computed from the Reynolds SSTs (Reynolds SST data provided by the NOAA-CIRES Climate Diagnostics Center, Boulder, Colorado, USA, from their Web site at <http://www.cdc.noaa.gov/>). Results are obtained from a set of 21-year long SST sensitivity experiments. The results are averaged over the last twenty years and only the mean response (sensitivity run minus control integration) is shown here.

The integrations are as follows: The control integration is driven with the climatological AMIP2-SST (dry mode). In the integration "Global Tropics", the full SST anomaly field of Figure 2.2a is added to these values. In the integrations "Atlantic", "Pacific", and "Indic" only the SST anomalies in

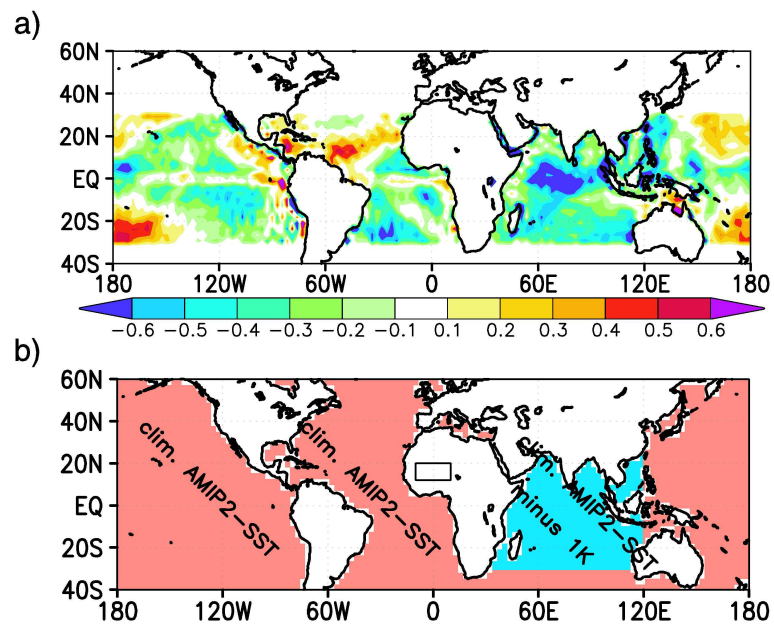


Figure 2.2: a) SST difference field: JJAS SST anomaly in the tropics (Wet-Mode (1951-1960) minus Dry-Mode (1979-1995)) (in Kelvin) and b) SST anomaly for the "Indian Ocean minus 1K" experiment (in Kelvin)

Figure 2.2a from the respective ocean basins are added to the climatological AMIP SSTs of the control run.

2.3 Results

In the experiment "Global Tropics", the tropical SSTs are changed according to Fig. 2.2a in order to simulate the situation in the 1950s. Consistent with the observations, the tropical SST anomalies produce a precipitation increase in the whole sub-Saharan Sahel region (Figure 2.3a). In particular, the response is significant according to a two-sided t-test at the 95%-confidence-level over the West Sahel (indicated by the box). Over the tropical Atlantic, the model simulates a northward shift of the intertropical convergence zone (ITCZ), with more rainfall in the north and less in the south.

Next we investigate the rainfall response to the SST anomalies in the individual tropical ocean basins. In the "Atlantic" integration, the rainfall response is primarily characterized by a rainfall decrease over southern West Africa and the eastern tropical Atlantic. Over the West Sahel significant less rainfall is simulated (not shown). In the "Pacific" experiment, a positive rainfall anomaly is simulated over the eastern Sahel but not over the western Sahel, and the maximum rainfall anomaly is located close to the Red Sea (not shown). In the "Indic" experiment, the rainfall is enhanced over West Africa, the ITCZ is intensified over the tropical Atlantic Ocean, and the rainfall is reduced over East Africa (Figure 2.3b). Please note that the rainfall enhancement over West Africa is associated with an intensification of the ITCZ and not with a meridional shift. Thus, the Indian Ocean SST anomalies appear to be most important forcing in driving the decadal drying trend in the West Sahel. The results of considering the SST forcing in two ocean basins together (not shown) confirm the importance of the tropical Indian Ocean for the decadal rainfall change over the West Sahel. Tropical Atlantic SST anomalies with either the tropical Pacific or Indian Ocean SST anomalies produces nearly the same rainfall anomalies over North Africa as the Pacific or Indian Oceans alone. The main influence of the tropical Atlantic Ocean is on the Atlantic coastal regions and over the Atlantic Ocean itself. The "Pacific/Indic" experiment produces a similar rainfall response as

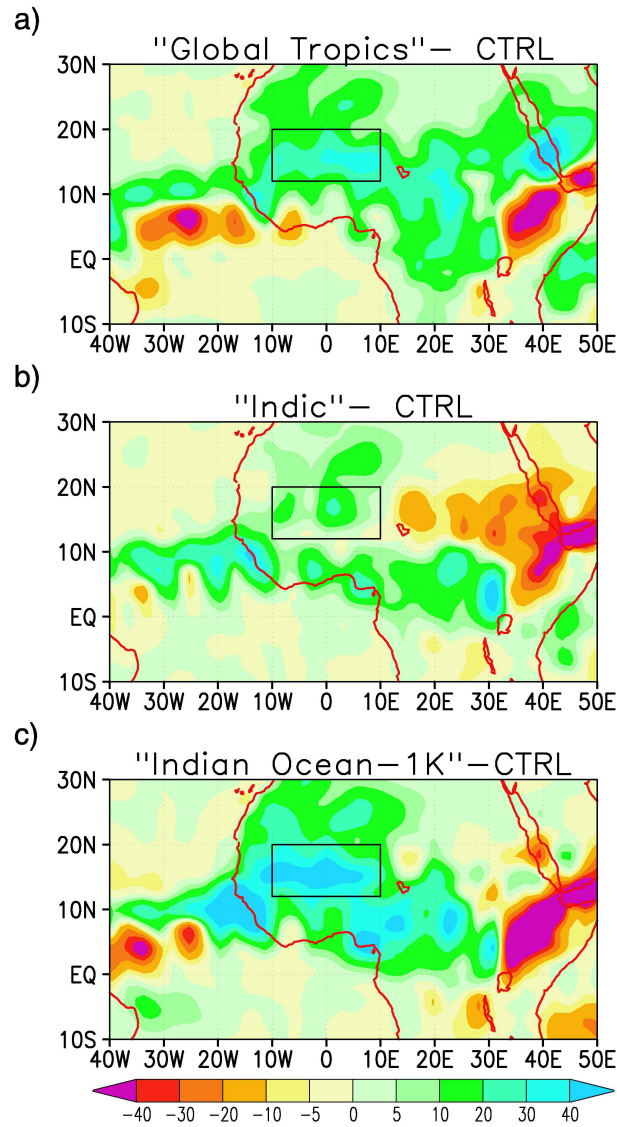


Figure 2.3: a) Simulated JJAS rainfall anomaly (relative to control integration) for the experiments with: Full SST anomaly of Figure 2.2a ("Global Tropics"); b) Indian Ocean portion of Figure 2.2a ("Indic"); c) SST anomaly of Figure 2.2b ("Indian Ocean minus 1K"); units: mm/month; the box indicates the West Sahel.

the "Global Tropics" experiment over the Sahel.

Thus, our SST sensitivity experiments indicate that the Pacific Ocean is the most important agent in producing the decadal rainfall reduction over the East Sahel while the tropical Indian Ocean drives the anomalies over the West Sahel. As described above, the SST of the Indian Ocean shows a pronounced warming since the 1950s. In order to further investigate the role of the Indian Ocean SST, the tropical Indian Ocean SST of the control integration is reduced by one Kelvin (see Figure 2.2b) in an additional sensitivity experiment to "mimic" the 1950s. Again, significant JJAS rainfall enhancement over West Africa is obtained (Figure 2.3c) confirming our hypothesis that the tropical Indian Ocean plays an important role in forcing Sahelian rainfall anomalies. Further analyses of the experiments provide the following picture: The reduced SSTs in the tropical Indian Ocean lead to less convection/precipitation over most of the tropical Indian Ocean. This results in an anomalous downward motion, reduced latent heat release, and upper tropospheric convergence. The anomalous inflow results in anomalous westerly winds over Africa. This anomalous east-west circulation in the upper atmosphere links the region of anomalous convergence over the Indian Ocean to the region of anomalous divergence centered over West Africa. The latter is connected with upward motion over West Africa, and the enhanced convection is amplified by enhanced moisture convergence and convective heating. Next, the experiments are analyzed with regard to the impact of tropical sea surface temperatures on the Northern Hemisphere winter (December to February (DJF)) climate, specifically the changes of the North Atlantic Oscillation. The NAO exhibits a strong upward trend since the 1970s and a reverse trend in the 1950s and 1960s (Hurrell 1995). In the "Global Tropics" experiment, a weakening of both the Icelandic low and the Azorian high is simulated (Figure 2.4a), which results in a weakening of the NAO and is in agreement with the observations. Thus, our experiment indicates that the decadal trend of the NAO in the recent decades contains a tropical SST forced component, a result that is consistent with findings of Hoerling et al. (2001). Hoerling (2001), however, did not consider the impact of the individual tropical ocean basins on the NAO. The results of our experiments with the SST forcing restricted to individual ocean basins and combinations

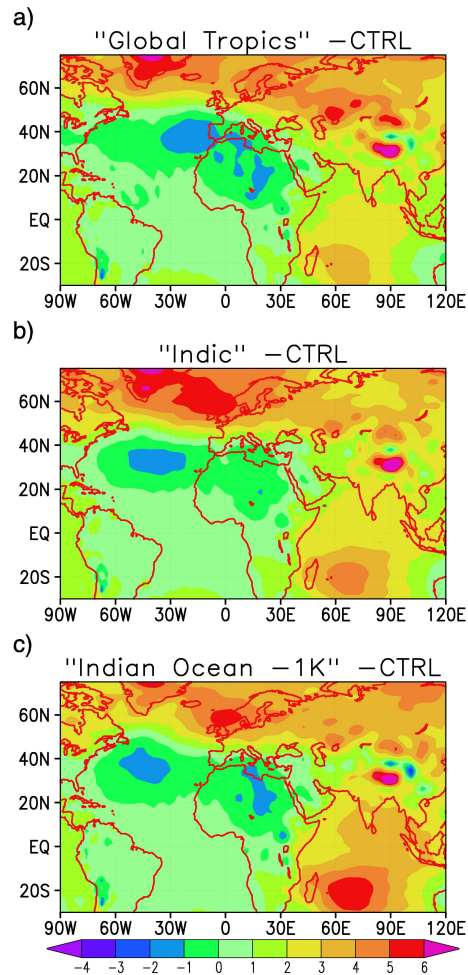


Figure 2.4: a) Simulated DJF sea level pressure (SLP) anomaly (relative to control integration) for the experiments with: Full SST anomaly of Figure 2.2a ("Global Tropics"); b) Indian Ocean portion of Figure 2.2a ("Indic"); c) SST anomaly of Figure 2.2b ("Indian Ocean minus 1K"); units: hPa.

of these show the strongest impact on the NAO from the Indian Ocean (Figure 2.4b). The sensitivity experiment, in which the tropical Indian Ocean is simply reduced by one Kelvin (Figure 2.2b) shows a similar NAO response as the "Global Tropics" and "Indian Ocean" experiments (Figure 2.4c). A t-test indicated that the results are significant at the 95%-confidence-level in all three experiments, at least in the centers of action. These experiments indicate that the warming of the Indian Ocean during the last decades seems to be of large importance for the strengthening of the NAO.

2.4 Summary

In summary, we find by conducting a set of numerical experiments with an atmospheric general circulation model that the warming of the Indian Ocean in the last decades is of paramount importance in driving the observed decadal drying trend over the West Sahel. We find additionally that the warming of the tropical Indian Ocean may have also contributed to the strengthening of the NAO observed during the recent decades.

The role of the tropical Indian Ocean SST in driving Sahelian rainfall anomalies is supported by relatively high anti-correlations between the observed low-pass-filtered rainfall over the West Sahel and tropical Indian Ocean SSTs and by an observational study of Shinoda and Kawamura (1994). According to our experiments, the tropical Pacific's influence is predominantly over the East Sahel. The tropical Atlantic impacts rainfall only over the Atlantic itself and along its coasts, e.g., the Guinea Coast. Furthermore, our experiments confirm the hypothesis that the recent decade-long strengthening of the NAO is at least partly of tropical origin. We conclude that the Indian Ocean SSTs play an important role not only in forcing regional climate anomalies (e.g., Latif et al. 1999) but also in driving extra-tropical climate anomalies.

Acknowledgments

The authors would like to thank Dr. Noel Keenlyside, Dr. Christian Reick, and Dr. Reiner Schnur for their useful comments. This work was supported

by the Federal German Ministry of Education and Research (BMBF) under grant No. 01 LW 0301A (Glowa), and under grant No. 01 LD 0030 (DEKLIM), the Ministry of Science and Research (MWF) of the state of Northrhine-Westfalia under grant No. 223 - 212 00 200, and by the European Union's PROMISE project.

2.5 References

- Folland, C.K., T.N. Palmer, D.E. Parker, 1986: Sahel rainfall and worldwide sea temperatures, 1901-85, *Nature*, **320**, 602-607.
- Hastenrath, S., 1984: Interannual variability and annual cycle: Mechanism of circulation and climate in the tropical Atlantic sector, *Monthly Weather Review*, **112**, 1097-1107.
- Hoerling, M.P., J.W. Hurrell, T.Y. Xu, 2001: Tropical origins for recent North Atlantic climate change, *Science*, **292**, 90-92.
- Hurrell, J.W., 1995: Decadal trends in the North Atlantic Oscillation: Regional temperatures and precipitation, *Science*, **269**, 676-679.
- Hurrell, J.W., Y. Kushnir, G. Ottersen and Martin Visbeck (Eds.), *The North Atlantic Oscillation: Climatic significance and environmental impact*, 279 pp., American Geophysical Union, Washington DC, 2003.
- James I.N., and P.M. James, 1989: Ultra-low-frequency variability in a simple atmospheric model. *Nature*, **342**, 53-55.
- Janicot S, V. Moron, B. Fontaine, 1996: Sahel droughts and ENSO dynamics, *Geophysical Research Letters*, **23**, 515-518.
- Lamb, P.J., 1978a: Case studies of tropical Atlantic surface circulation patterns during recent sub-Saharan weather anomalies: 1967 and 1968, *Monthly Weather Review*, **106**, 482-491.
- Lamb, P.J., 1978b: Large-scale tropical Atlantic surface circulation patterns associated with sub-Saharan weather anomalies, *Tellus*, **A30**, 240-251.
- Lamb, P.J., and R.A. Pepler, 1992: Further case studies of tropical Atlantic surface circulation patterns associated with sub-Saharan drought, *Journal of Climate*, **5**, 476-488.
- Latif, M., D. Dommenges, M. Dima, and A. Grotzner, 1999: The role of Indian Ocean sea surface temperature in forcing east African rainfall

- anomalies during December-January 1997/98, *Journal of Climate*, **12**, 3497-3504.
- Latif, M., K. Arpe, and E. Roeckner, 2000: Oceanic Control of North Atlantic Sea Level Pressure Variability in Winter, *Geophysical Research Letters*, **27**, 727-730.
- Palmer, T.N., 1986: Influence of the Atlantic, Pacific and Indian Oceans on Sahel rainfall, *Nature*, **322**, 251-253.
- Roeckner, E., K. Arpe, L. Bengtsson, M. Christoph, M. Claussen, L. Dümenil, M. Esch, M. Giorgetta, U. Schlese, and U. Schulzweida, 1996: The atmospheric general circulation model ECHAM-4: Model description and simulation of present-day climate, *MPI Report*, **218**.
- Rodwell, M. J., D. P. Rowell, and C. K. Folland, 1999: Oceanic forcing of the wintertime North Atlantic Oscillation and European climate, *Nature*, **398**, 320-323.
- Rowell, D.P., 2001: Teleconnections between the tropical Pacific and the Sahel, *Quart. J. Roy. Meteor. Soc.*, **127**, 1683-1706.
- Rowell, D.P., 2003: The impact of Mediterranean SSTs on the Sahelian rainfall season, *Journal of Climate*, **16**, 849-862.
- Saravanan, R., and J.C. McWilliams, 1997: Stochasticity and spatial resonance in interdecadal climate fluctuations, *Journal of Climate*, **10**, 2299-2320.
- Shinoda, M. and R. Kawamura, 1994: Tropical rainbelt, circulation, and sea surface temperatures associated with the Sahelian rainfall trend. *Journal of the Meteorological Society of Japan*, **72**, 341-357.
- Schnitzler, K. G., W. Knorr, M. Latif, J. Bader, and N. Zeng, 2001: Vegetation feedback on Sahelian rainfall variability in a coupled climate land-vegetation model. *MPI Report*, **329**.

- Taylor, K. E., D. Williamson, and F. Zwiers, 2000: The sea surface temperature and sea ice concentration boundary conditions for AMIP II simulations, *PCMDI Report*, **60**.
- Vizy, E.K. and K.H. Cook, 2001: Mechanisms by which Gulf of Guinea and eastern North Atlantic sea surface temperature anomalies can influence African rainfall, *Journal of Climate*, **14**, 795-821.
- Vizy, E.K. and K.H. Cook, 2002: Development and application of a mesoscale climate model for the tropics: Influence of sea surface temperature anomalies on the West African monsoon, *J. Geophysical Research - Atmosphere*, **107**, 4023, doi:10.1029/2001JD000686.
- Ward, M.N., 1998: Diagnosis and short-lead time prediction of summer rainfall in tropical North Africa at interannual and multidecadal timescales, *Journal of Climate*, **11**, 3167-3191.
- Ward, M.N., P.J. Lamb, D.H. Portis, M. el Hamly, and R. Sebbari, Climate variability in northern Africa: Understanding droughts in the Sahel and the Maghreb, in *Beyond el Nino: Decadal and interdecadal climate variability*, edited by A. Navarra, pp. 119-140, Springer-Verlag, Berlin Heidelberg, 1999.

Chapter 3

Combined Tropical Oceans Drive Anomalous Sub-Saharan West African Rainfall

Jürgen Bader^{1,2,*} and Mojib Latif³

¹Institute of Geophysics and Meteorology, University of Cologne, Cologne,
Germany

²Max-Planck-Institute for Meteorology, Hamburg, Germany

³Leibniz-Institute for Marine Sciences at the University of Kiel, Kiel,
Germany

*Corresponding author address: Jürgen Bader, Max-Planck-Institute for Meteorology,
Bundesstraße 53, 20146 Hamburg, Germany. E-mail: bader@dkrz.de

Abstract

Two large-scale rainfall anomaly patterns describe most of the summer rainfall variability over sub-Saharan West Africa. One is an out-of-phase distribution between Sahel and Guinea Coast summer rainfall anomalies and the second one is characterized by anomalies of the same sign over these two areas. The impact of sea surface temperature anomalies (SSTAs) in forcing these two rainfall anomaly patterns is investigated by analyzing observations and conducting ensemble experiments with an atmospheric general circulation model. Observations and experiments show that these patterns can be induced by simultaneous SSTAs in the tropical Indian Ocean and in the eastern tropical Atlantic. According to the model experiments, simultaneous rainfall intensity changes caused by contemporaneous SST changes in the tropical Indian Ocean and eastern Atlantic can "mimic" a shift of the intertropical convergence zone (ITCZ) over West Africa in summer.

3.1 Introduction

Many studies have shown that there exists marked interannual to decadal rainfall variability over sub-Saharan West Africa (e.g. Ward et al. 1999). Since the early seventies sub-Saharan West-Africa has suffered from a prolonged drought that had and continues to have large effects on farming, industrial development, health, and electricity (hydro-power) and caused migration problems. Better predictions of the West African monsoon will have large social and economic benefits. Improved predictions require a better understanding of the mechanisms behind West African rainfall variations.

Two large-scale rainfall anomaly patterns describe most of the rainfall variability over sub-Saharan West Africa (e.g. Nicholson 1980, Janowiak 1988, Janicot 1992, Nicholson and Palao 1993, Ward 1998, and Nicholson and Grist 2001): One of these patterns is characterized by anomalies of opposite signs along Guinea Coast and over the Sahel. This pattern is often referred as a "dipole" in the literature. The node of this dipole is centered around 10°N (e.g. Nicholson and Grist 2001, see also Figures 3.1a and 3.2 in this paper). It has been suggested that this dipole can be explained by an anoma-

lous latitudinal location of the ITCZ. The second rainfall anomaly pattern is characterized by anomalies of the same sign over entire sub-Saharan West Africa and cannot be explained by a displacement of the ITCZ. Thus, two causes for the precipitation anomaly patterns over sub-Saharan West Africa are given: One results from a rainfall intensity change, the other from a displacement of the ITCZ.

Observational and model studies show that sub-Saharan West African rainfall variability is associated with regional and global SST anomaly patterns. These include changes in the Atlantic (e.g. Lamb 1978a, b; Hastenrath 1984; Lamb and Pepler 1992; Ward 1998; Vizzy and Cook 2001, 2002), in the Pacific (e.g. Janicot 1996; Rowell 2001), in the Indian Ocean (Palmer 1986, Shinoda and Kawamura 1994, Bader and Latif 2003), and in the Mediterranean (Rowell 2003). Folland et al. (1986) linked near global changes in sea surface temperatures to Sahelian rainfall variability.

Here we show by analyzing observations and conducting ensemble experiments with the atmospheric general circulation model ECHAM4.5 that the two basic rainfall anomaly patterns (described above) can be induced by simultaneous SSTAs in the tropical Indian Ocean and in the eastern tropical Atlantic (ETA).

3.2 Observations

Figures 3.1a and 3.1b show the first two leading Empirical Orthogonal Functions (EOF)-patterns of the observed July to September (JAS) rainfall over sub-Saharan West Africa. The rainfall data are from the Climate Research Unit dataset (New et al. 2000) and cover the time period from 1901 to 1996. The first EOF-pattern (Figure 3.1a) shows an out-of-phase rainfall variability along Guinea Coast and the West Sahel. This type of rainfall variability is often believed to be associated with changes in the latitudinal location of the ITCZ (e.g. Janicot 1992). Figure 3.2 shows the correlation coefficients between the observed JAS rainfall averaged over the box centered near 15°N with the observed JAS rainfall over West Africa. One finds positive correlation coefficients between the JAS rainfall over the West Sahel and over West Africa approximately north of 10°N and negative south of this latitude. The

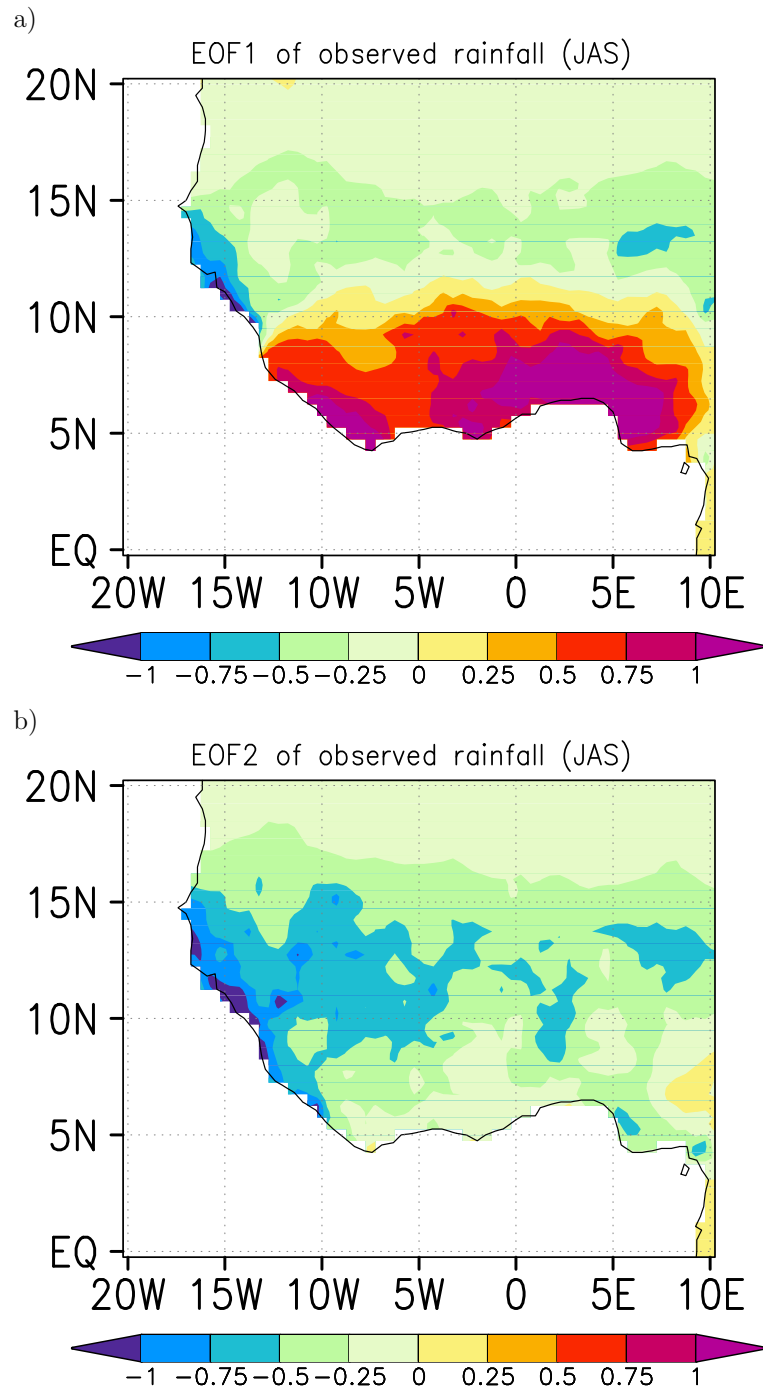


Figure 3.1: Empirical Orthogonal Function (EOF) analysis loading patterns of the observed July to September rainfall; (a) EOF1, (b) EOF2.

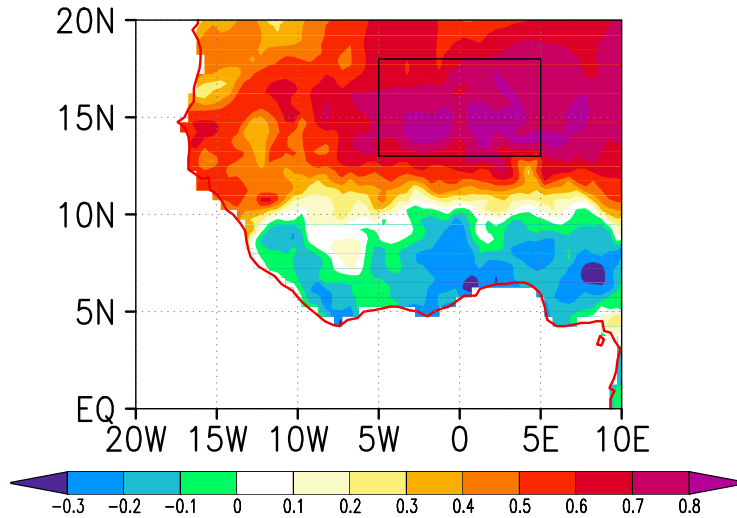


Figure 3.2: *Correlation coefficients between the observed JAS rainfall averaged over the box with the observed JAS rainfall over West Africa.*

anti-correlations between the rainfall over the West Sahel and large parts along Guinea Coast are significant at the 95% confidence level (according to two-tailed t-test), albeit weak ($r \approx [-0.3, -0.2]$). The correlation analysis seems to support the existence of a "dipole" mode between the West Sahel and Guinea Coast. The second EOF-pattern (Figure 3.1b) is characterized by anomalies of the same sign over West Africa. This type of variability is often believed to be associated with intensity changes of the ITCZ.

We address the following question: What are the causal factors governing these two basic/fundamental types of rainfall variability. Explaining the mechanisms behind the two types of rainfall patterns could also help to better predict rainfall variability over sub-Saharan West Africa.

We concentrate on the role of SST variations driving these two types of rainfall variability. To find the ocean areas most important to the rainfall variability, we correlated two observed rainfall indices with the observed SSTs considering the JAS season. The West Sahel index is defined from 10°W to 10°E and from 12°N to 20°N, the Guinea Coast index from 10°W to 10°E and from the South Coast to 9°N. These two boxes are indicated in Figures 3.3a and 3.3b, respectively. The SST data are of the Hadley Centre for Climate Prediction and Research (Rayner et al. 2003) and the rainfall data of the Cli-

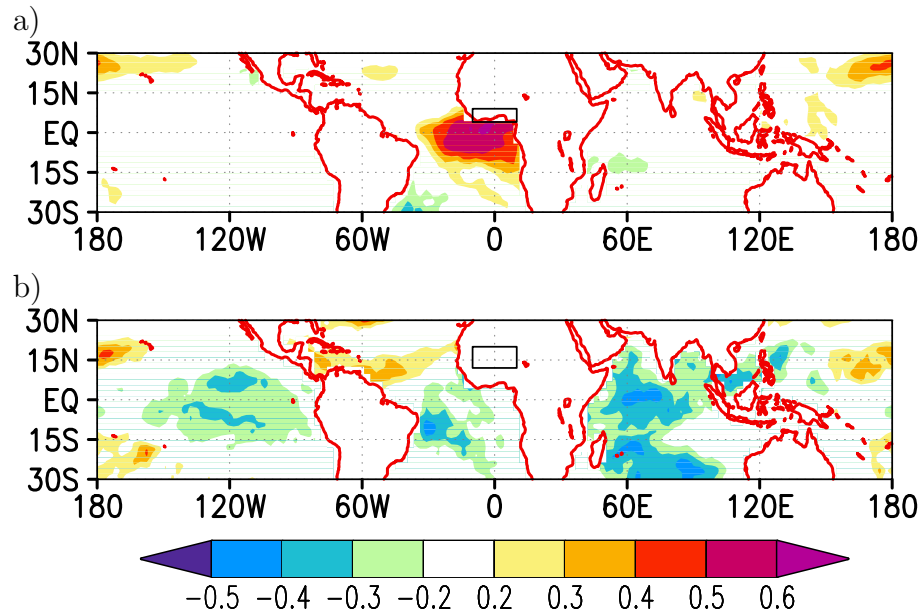


Figure 3.3: *Correlation between the observed JAS SST and the observed JAS rainfall averaged over: a) the Guinea Coast area (indicated by the box) ; b) the West Sahel region (indicated by the box).*

mate Research Unit dataset (New et al. 2000). All time series were linearly detrended before computing the correlations. The time period considered extends from 1901 to 1996. The strongest correlations between Guinea Coast rainfall and SST is in the eastern tropical Atlantic (ETA) ($r \approx 0.6$; Figure 3.3a). The SST anomaly pattern is that of the equatorial Atlantic oscillation, an El Niño-like mode in the eastern equatorial Atlantic (e.g., Zebiak 1993, Latif and Grötzner 2000).

The correlation pattern between Sahelian rainfall and tropical Atlantic SSTs is mainly characterized by positive correlation coefficients in the North and negative in the South Atlantic. Lamb and Pepler (1992) linked in an observational study Sahelian drought years to a distinctive basin wide SST anomaly pattern: Positive SST anomalies south of 10°N and negative anomalies between $10^\circ - 25^\circ\text{N}$. Unfortunately the results were not characteristic of the extremely deficient sub-Saharan rainy season 1983. These findings may indicate that SST's from other ocean areas are important in forcing Sahelian rainfall. This seems to be confirmed by our correlation analysis. The

strongest correlation between West Sahel rainfall and global SST is in the Indian Ocean, with negative correlations amounting to -0.5 (Figures 3.3b). This link is confirmed by model studies. Bader and Latif (2003) showed that Indian Ocean SST anomalies produce significant rainfall anomalies over the West Sahel in atmospheric general circulation model (AGCM) experiments. There are also some anti-correlations between Sahel rainfall and the SSTs in the ENSO region. In spite of this we shall focus on the Indian Ocean, because first, the anti-correlation with the Indian Ocean is highest and second, no apparent relationship between ENSO and the dipole rainfall anomaly pattern was found by Janowiak (1988). At least parts of the anti-correlation between Sahel rainfall and the SSTs in the ENSO region might be explained by the impact of ENSO on the Indian Ocean. The results of Nicholson (1997) strongly indicate that the ENSO signal in rainfall is manifested via ENSO's influence on SSTs in the Atlantic and Indian Ocean, which in turn modulate the interannual rainfall variability over Africa. If the tropical Indian and eastern tropical Atlantic Oceans are the key areas driving rainfall anomalies over the sub-Saharan West Africa region, then the two basic patterns of rainfall variability should be reproducible in atmospheric general circulation model (AGCM) experiments by changing the SSTs in these two ocean areas. This idea is tested by ensemble SST-sensitivity-experiments with an AGCM, described next.

3.3 Model and experiments

In this study, the atmospheric general circulation model ECHAM4.5 (Roeckner et al. 1996) is used. The horizontal resolution is T42 ($2.8^\circ \times 2.8^\circ$). The control integration is forced by the climatological AMIP2-SST (Taylor et al. 2000). The climatological AMIP2-SST covers the period from January 1979 to February 1996 and consists of a seasonal cycle of twelve monthly values. Figures 5.3a and 5.3b show the annual cycle of observed and simulated precipitation along Guinea Coast and over the West Sahel. The solid lines show the observations (CRU) and the dotted-dashed lines the simulated rainfall of the control integration. The main features along Guinea Coast are two rainfall maxima, one in June and one in September. The ECHAM4.5

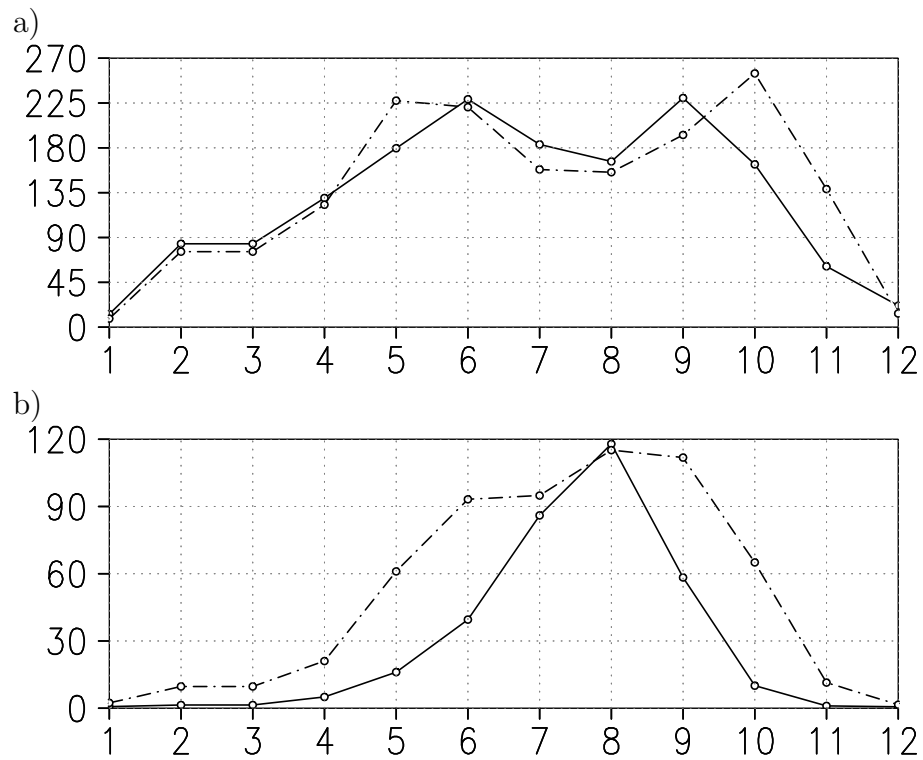


Figure 3.4: Annual cycle of the precipitation averaged over a) the Guinea Coast region and b) the West Sahel; solid line: observation (CRU); dot dashed line: simulated rainfall of the CTRL integration; units: mm/month.

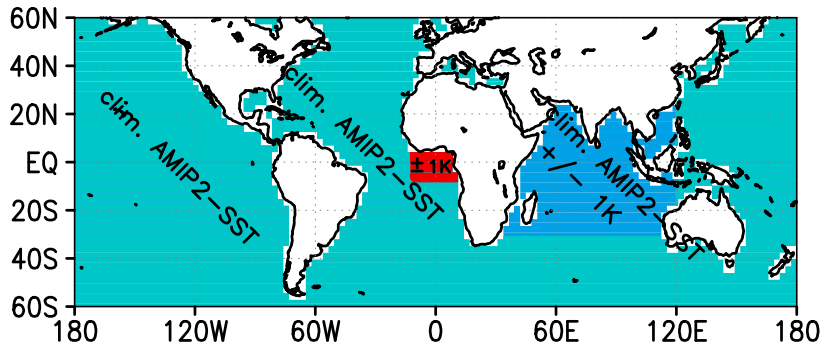


Figure 3.5: *Illustration of the SST anomaly in the individual experiments.*

simulation shows the spring maxima one month earlier and the fall maximum one month later than observed. The strength of the simulated rainfall along Guinea Coast is in good agreement with the observations.

The rainfall over the West Sahel is strongly seasonally concentrated. Approximately eighty percent of the annual rainfall occurs during July-September (Figure 5.3b). Small amounts of rain fall in the adjacent months May, June and October. The model reproduces the observed rainfall maximum in August, but it overestimates the rainfall in spring and autumn. Concerning the main rainy season July-September the model reproduces the observed rainfall amounts in July-August in good agreement with the observations.

In the SST-sensitivity-experiments, the climatological SST of the control integration (Taylor et al. 2000) is changed by plus and minus one Kelvin in either the ETA (from 14°W to the west coast of Africa and from 7°S to the south coast of West Africa) or the tropical Indian Ocean (from the east coast of Africa to 120°E and from 30°S to 30°N) or in both (Figure 3.5). The model's response to these eight SSTA patterns on the sub-Saharan West African rainfall is analyzed in detail. Results are obtained from a set of 21-year long SST-sensitivity-experiments. The results are averaged over the last twenty years and only the JAS mean response (sensitivity run minus control integration) is shown here.

3.4 Results

First, we test whether the two observed basic rainfall anomaly patterns are due to internal variability of the atmosphere or if other feedbacks – e.g. SST variations – are essential in causing these patterns. Figures 3.6a and 3.6b show the two leading EOFs of the JAS rainfall occurring in our atmospheric model driven with climatological SSTs (our CTRL simulation). The first EOF-pattern is mainly characterized by variability concentrated over the central West Sahel. The second EOF-pattern shows an east-west like dipole pattern. Since the observed large-scale rainfall anomaly patterns do not emerge as the leading rainfall anomaly patterns in our atmospheric model simulation forced by climatological SSTs other external factors must be essential in producing these patterns.

Now the results of considering the SST forcing of only one ocean region (eastern tropical Atlantic (ETA) or Indian Ocean) at a time on the sub-Saharan West African rainfall are presented. Reducing/enhancing the SST by one Kelvin in the ETA reduces/amplifies significantly the rainfall along Guinea Coast and over the Atlantic. No clear impact of the ETA-SST on the rainfall over large parts of the West Sahel is obtained (Figures 3.7a and 3.7b). In particular, no "dipole" distribution of the rainfall between Guinea Coast and the West Sahel is simulated in the "ETA minus one Kelvin"-experiment. Also in the second experiment, no clear out-of-phase rainfall anomaly pattern is simulated. The rainfall anomalies are only significant to approximately 10°N and the anomalies show a tripole like pattern over the West Sahel (negative anomalies over the west, positive over the central and negative over the east). The dominant impact of the ETA on sub-Saharan West African rainfall is confined to the coastal regions, and the rainfall response is almost linear. The reduced/enhanced SSTs in the eastern tropical Atlantic lead to reduced/enhanced evaporation. This leads to a significant reduction/enhancement of the water vapor content of the lower troposphere over the eastern tropical Atlantic and the surrounding coastal regions (Figure 3.8) and therefore to a reduction/enhancement of precipitable water. The simulated rainfall response along Guinea Coast is consistent with the positive correlation computed from the observations.

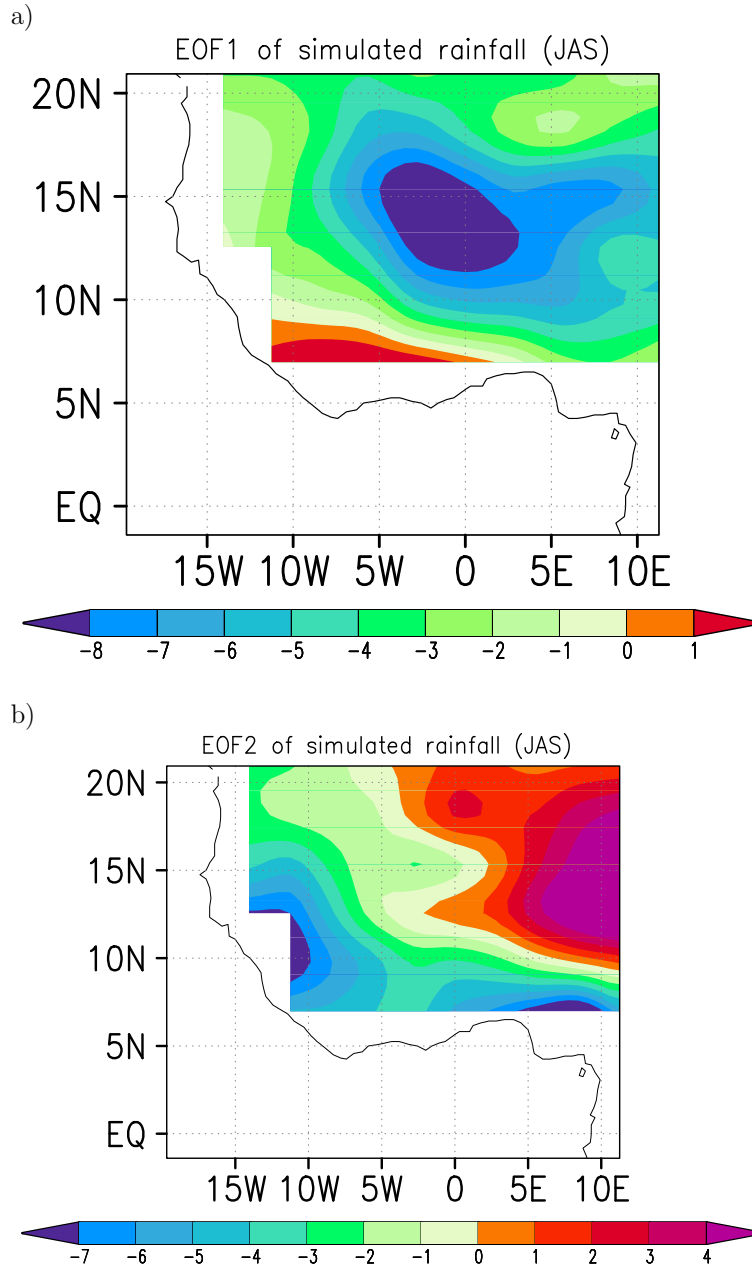


Figure 3.6: Empirical Orthogonal Function (EOF) analysis loading patterns of the simulated July to September rainfall in an atmospheric model driven with climatological SSTs; (a) EOF1, (b) EOF2.

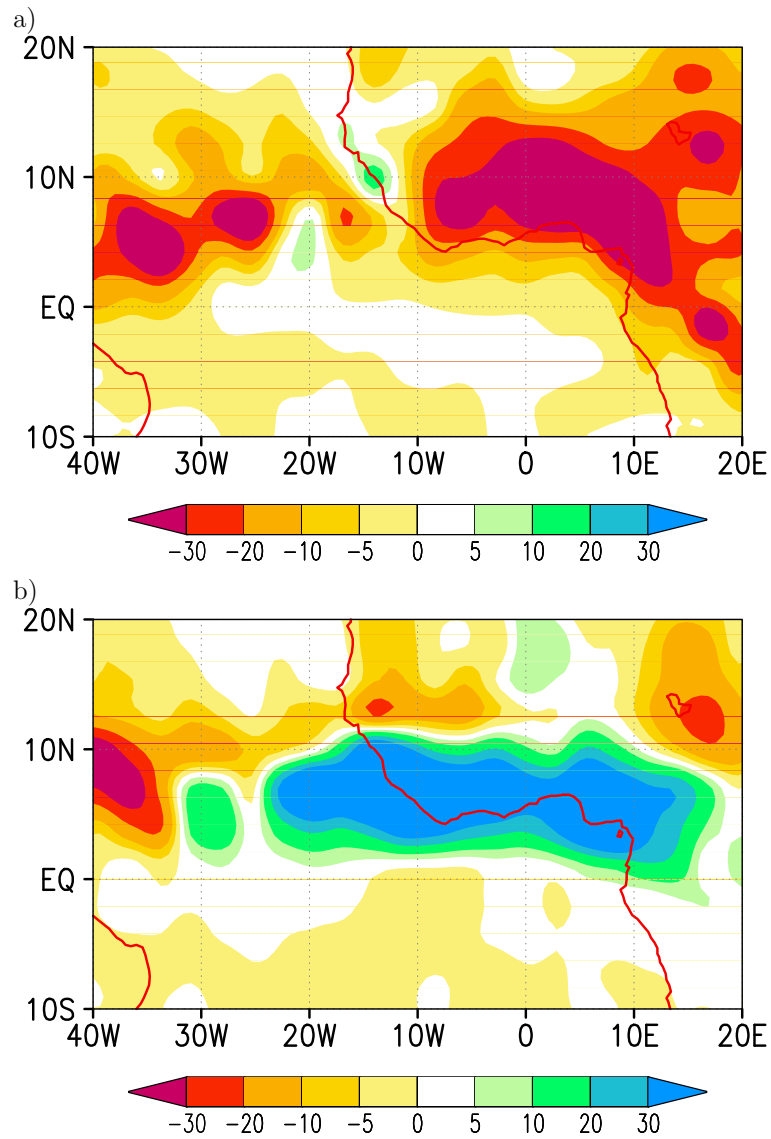


Figure 3.7: Simulated JAS rainfall anomaly (relative to control integration) for the experiments with: a) eastern tropical Atlantic reduced by one Kelvin; b) eastern tropical Atlantic enhanced by one Kelvin; units: mm/month.

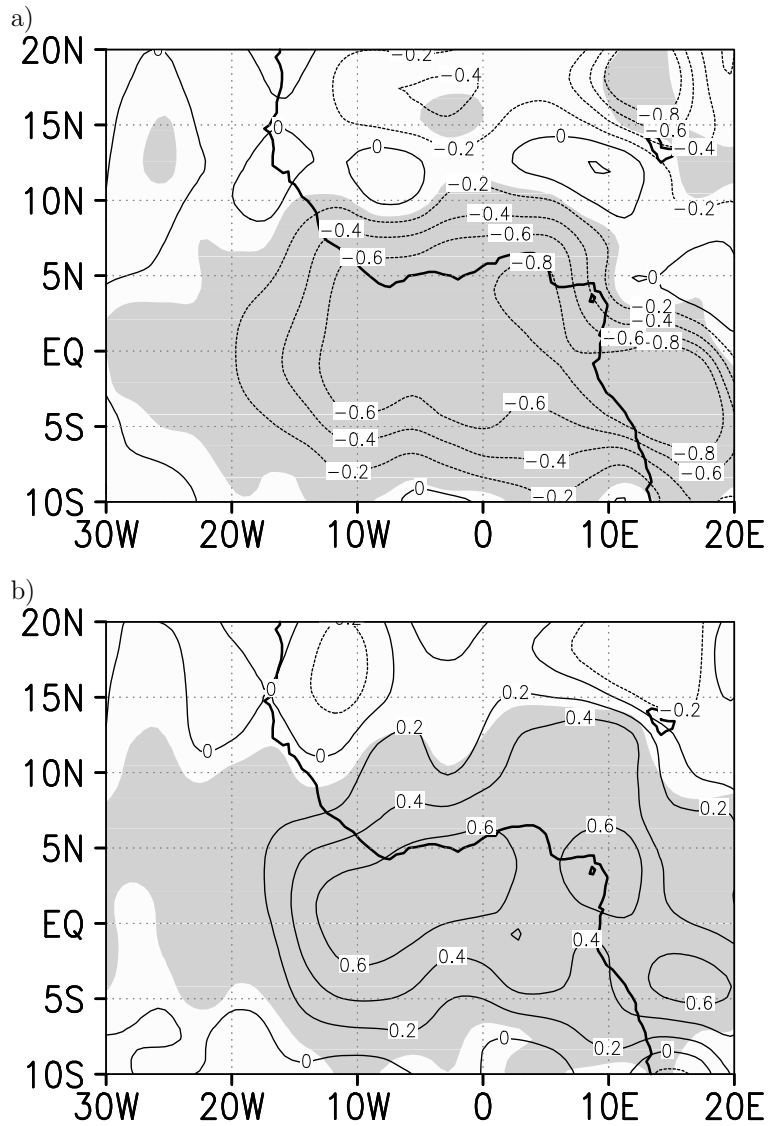


Figure 3.8: Simulated 1000hPa JAS humidity anomaly (relative to control integration) for the experiments with: a) eastern tropical Atlantic reduced by one Kelvin; b) eastern tropical Atlantic enhanced by one Kelvin; units: g/kg; shading indicates significant changes at the 95% confidence level according to a two-tailed *t*-test.

In contrast to the ETA SSTs, reducing/enhancing tropical Indian Ocean SST leads to a significant rainfall enhancement/reduction over the Sahelian region and over the tropical Atlantic Ocean (Figures 3.9a and 3.9b). No out-of-phase rainfall distribution between Guinea Coast and the West Sahel is simulated. The simulated rainfall response over the West Sahel is also consistent with the anti-correlation computed from the observations. The reduction/enhancement of precipitation is due to large-scale subsidence/ascent over sub-Saharan West Africa (Figure 3.10). Note that the unit of the vertical velocity ω is in Pa/s – negative values indicate upward motion, positive values downward motion. The anomalous descending/ascending motion suppresses/enhances convective activity.

Further analyses of these two Indian Ocean only experiments provides the following mechanism by which these circulation changes are induced by the Indian Ocean SST anomalies: Reduced/enhanced SSTs in the tropical Indian Ocean lead to less/enhanced convection over the west and central tropical Indian Ocean. This results in an anomalous downward/upward motion, reduced/enhanced latent heat release in the western and central Indian Ocean. This induces an anomalous zonal overturning circulation (Figure 3.11 – note the vertical velocity is multiplied by $(-1) \times 10^2$). Over the West Sahel, upward/downward motion is simulated in the middle and upper troposphere enhancing/suppressing convection. Interestingly, a reduced/enhanced 200hPa Tropical Easterly Jet (TEJ) over West Africa is associated with enhanced/reduced convection. Although there is less agreement as to the role that the TEJ plays in rainfall variability (Nicholson and Grist 2003), observational studies show that wet/dry years in the Sahel are associated with a stronger/weaker TEJ (Newell and Kidson 1984; Fontaine et. al. 1995 and Nicholson and Grist 2001). Forcing our model with the tropical SST pattern associated with the wet and dry mode in the Sahel (see Bader and Latif 2003) the model is able to produce the observed connection between TEJ and Sahel rainfall. These experiments may indicate that a change of the TEJ is not an essential forcing of Sahelian rainfall, but rather a consequence of the changed zonal overturning circulation induced by SST anomalies.

Next, the SST is changed simultaneously in both the tropical Indian Ocean and the ETA. The response to a negative SSTA in both ocean areas is a signif-

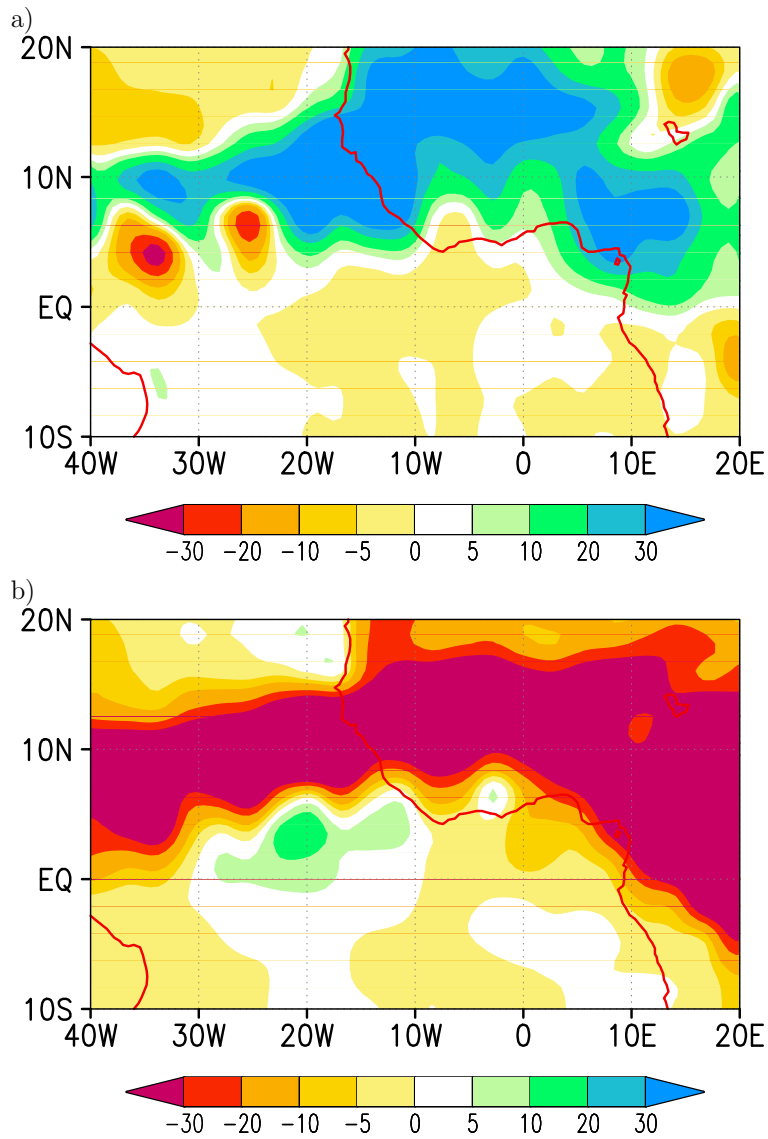


Figure 3.9: Simulated JAS rainfall anomaly (relative to control integration) for the experiments with: a) Indian Ocean reduced by one Kelvin; b) Indian Ocean enhanced by one Kelvin; units: mm/month.

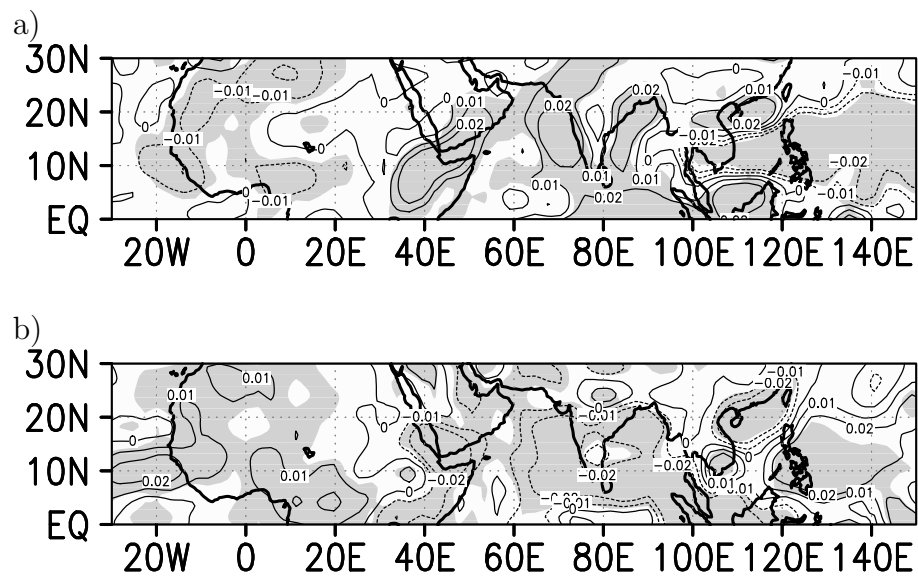


Figure 3.10: Simulated 500 hPa JAS vertical velocity (ω) anomaly (relative to control integration) for the experiments with: a) Indian Ocean reduced by one Kelvin; b) Indian Ocean enhanced by one Kelvin; units: Pa/s; shading indicates significant changes at the 95% confidence level according to a two-tailed *t*-test).

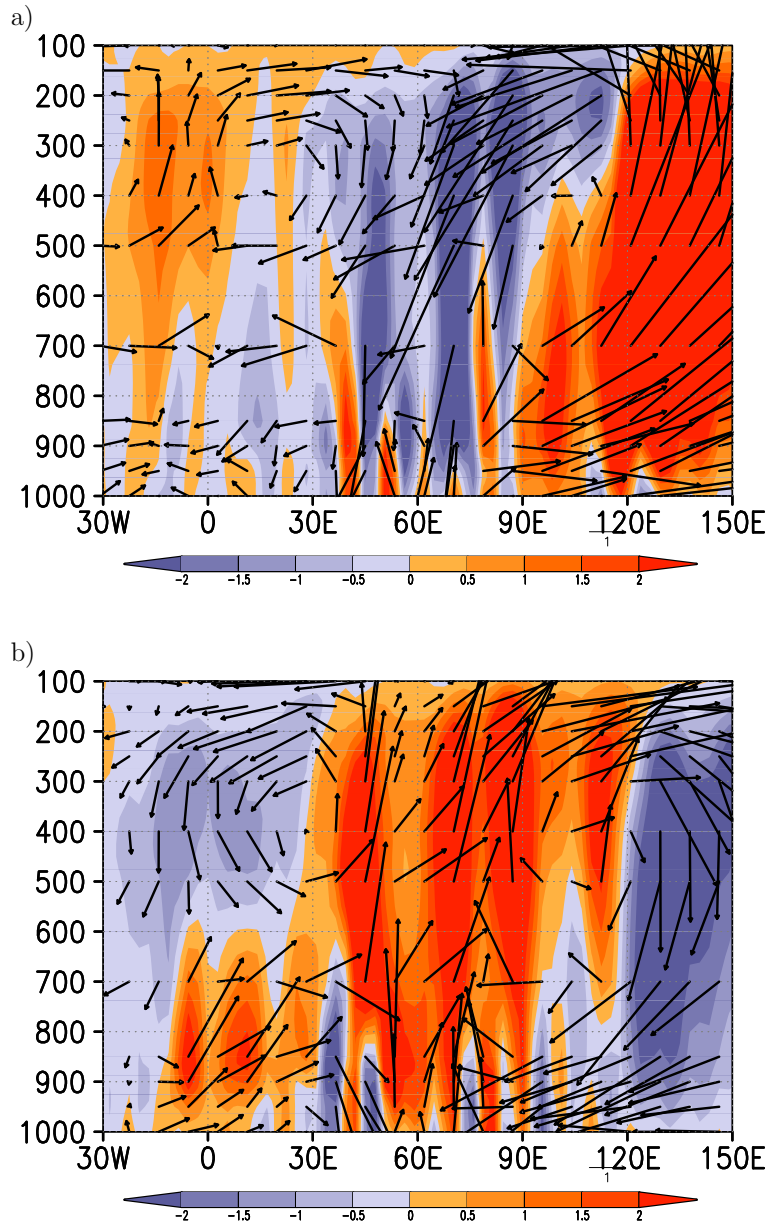


Figure 3.11: Coloring shows vertical velocity anomaly (in Pa/s; multiplied by $(-1) \times 10^2$) and vectors the zonal and vertical wind anomaly (u -component in m/s; z -component in Pa/s but multiplied by $(-1) \times 10^2$) for the experiments with: a) Indian Ocean reduced by one Kelvin; b) Indian Ocean enhanced by one Kelvin; u - and z -component averaged from $12^\circ N$ to $20^\circ N$.

icant rainfall enhancement over the West Sahel and a reduction along Guinea Coast (Figure 3.12a). Enhancing the SST in these two ocean areas produces also a clear out-of-phase precipitation anomaly pattern over sub-Saharan West Africa, but with reversed sign: less rainfall over the West Sahel and increased precipitation along Guinea Coast (Figure 3.12b). Apparently, the rainfall response is almost linear with a clear out-of-phase rainfall anomaly pattern simulated in both experiments. The dividing line is centered in both experiments near $10^{\circ}N$. This is in agreement with observational findings of Nicholson and Grist (2001) and with our correlation analysis of the observed rainfall variability (Figure 3.2).

The two experiments show that SSTAs of the same sign in the ETA and the Indian Ocean are able to produce the out-of-phase rainfall anomaly pattern. This out-of-phase rainfall anomaly pattern looks like a shift of the intertropical convergence zone (ITCZ) over West Africa. This "shift" of the ITCZ, however, is caused by different SST forcings dominating the response in the north and south. In the north, the remote SST forcing of the Indian Ocean leads to the rainfall change. Over the south of West Africa (to $\approx 10^{\circ}N$), the more local SSTs from the ETA region are the controlling forcing. Hence, we explain the anti-correlation of West Sahel and Guinea Coast rainfall by the precipitation response in these two regions being dominated by the two different ocean areas, mutually exclusively. Taking into account the two experiments in which only the SSTs in the ETA are changed, it can be concluded that the ETA is a dominant SST forcing for the rainfall along the Guinea Coast. This dominant SST forcing for the rainfall along Guinea Coast is maintained in the ETA/Indian Ocean experiments to approximately $10^{\circ}N$. Over the West Sahel, the Indian Ocean SSTs play the crucial role for the precipitation in this region.

In the literature two main causes for rainfall changes over West Africa are given: intensity changes and location changes of the ITCZ. According to our experiments simultaneous rainfall intensity changes caused by a forcing of the two different oceanic regions can "mimic" a shift of the ITCZ over West Africa. Thus, at least in some cases, location changes of the ITCZ can be caused by intensity changes originating in different ocean basins.

Figure 3.13 shows the correlation coefficients between the observed JAS east-

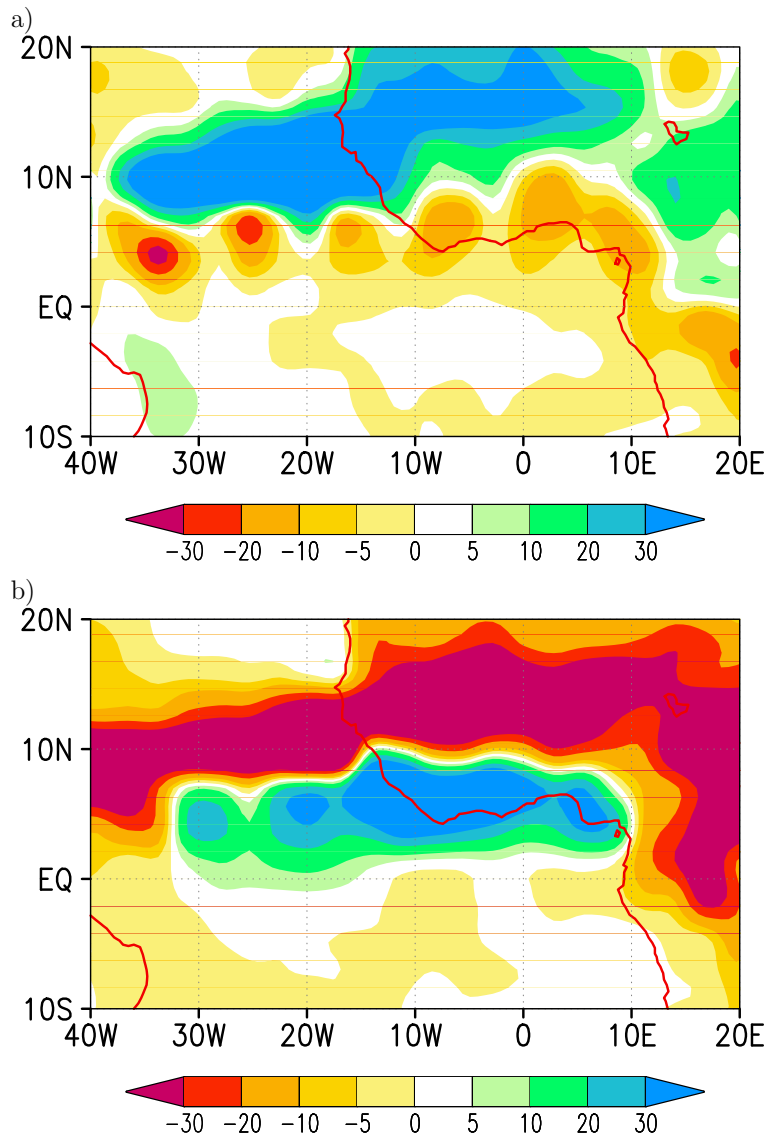


Figure 3.12: Simulated JAS rainfall anomaly (relative to control integration) for the experiments with: a) Indian Ocean and eastern tropical Atlantic reduced by one Kelvin; b) Indian Ocean and eastern tropical Atlantic enhanced by one Kelvin; units: mm/month.

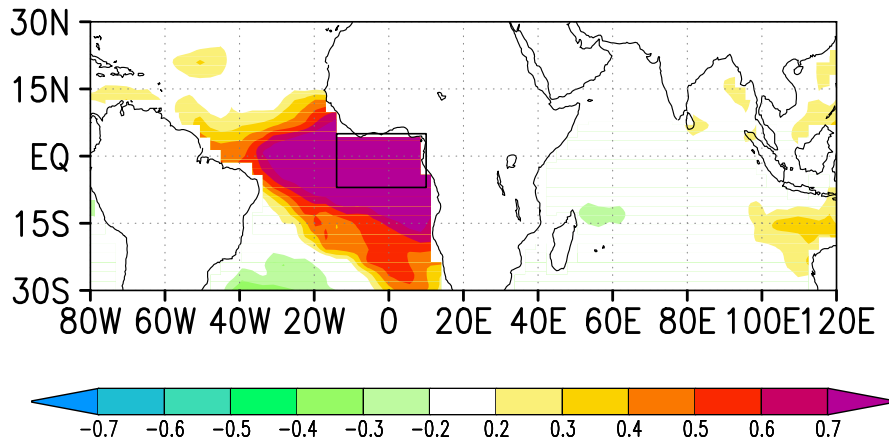


Figure 3.13: *Correlation between the observed JAS SST averaged over the eastern tropical Atlantic area (indicated by the box) and the observed JAS SST.*

ern tropical Atlantic SSTs (indicated by the box) and the observed JAS Indian Ocean SSTs. No significant relationship of the ETA and the Indian Ocean SSTs is found over most of the tropical Indian Ocean. This may indicate that the SSTs in the eastern tropical Atlantic and the Indian Ocean develop more or less independently. However, further analysis is needed: Can, for example, an Indian Ocean warming drive through an "atmospheric bridge" an Atlantic SST response that in turn engages an African rainfall response? Possible interactions between Indian and Atlantic Oceans SSTs and the cause of the SST anomalies will be subject of a forthcoming paper and is beyond the scope of this paper. This study concentrates on the impact of SST anomalies on sub-Saharan West African rainfall and not on the origin of the SST anomalies. Provided that the SSTs in the ETA and in the Indian Ocean develop more or less independently, our experiments indicate that the out-of-phase rainfall distribution is not necessarily a physical mode.

An important implication is also that the rainfall enhancement/reduction over the West Sahel is not necessarily associated with a supply of unusually wet/dry air to West Africa from the tropical Atlantic. In the experiment, in which the SSTs in the Indian Ocean and the ETA are enhanced by one Kelvin simultaneously, a significant enhancement of the low level specific humidity is simulated in the source region, the tropical Atlantic (Figure 3.14). In spite

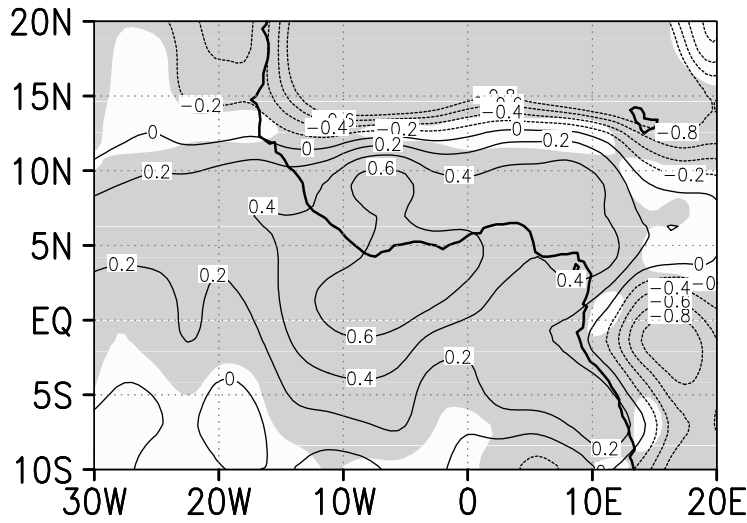


Figure 3.14: *Simulated 1000hPa JAS humidity anomaly (relative to control integration) for the experiment with Indian Ocean and eastern tropical Atlantic enhanced by one Kelvin; units: g/kg; shading indicates significant changes at the 95% confidence level according to a two-tailed t-test.*

of this humidity increase the rainfall over the West Sahel is reduced (Figure 3.12b). Observational findings of Lamb and Pepler (1992) support our result: In the year 1983, the rainfall was extremely deficient in the Sahel but the SST departures were positive over much of the tropical Atlantic. Please note that the SSTs in the Indian Ocean were much higher than normal in the year 1983 (Figure 3.15b).

The out-of-phase rainfall anomaly pattern is also evident on decadal timescales (Nicholson and Grist 2001). Figures 3.15a and 3.15b show the observed area-averaged SST indices of the ETA and the tropical Indian Ocean. A clear warming trend is observed since the 1950s in both the ETA and the tropical Indian Ocean (Figure 3.15). This simultaneous decadal warming trend may be responsible for the out-of-phase rainfall anomaly pattern that is also observed on decadal timescales, as suggested by our model experiments.

Finally, two additional experiments are performed in which the imposed SSTAs in the Indian Ocean and in the ETA are of opposite signs. The two experiments show significant rainfall reduction/enhancement over the whole sub-Saharan West African region (Figures 3.16a and 3.16b), i.e. the

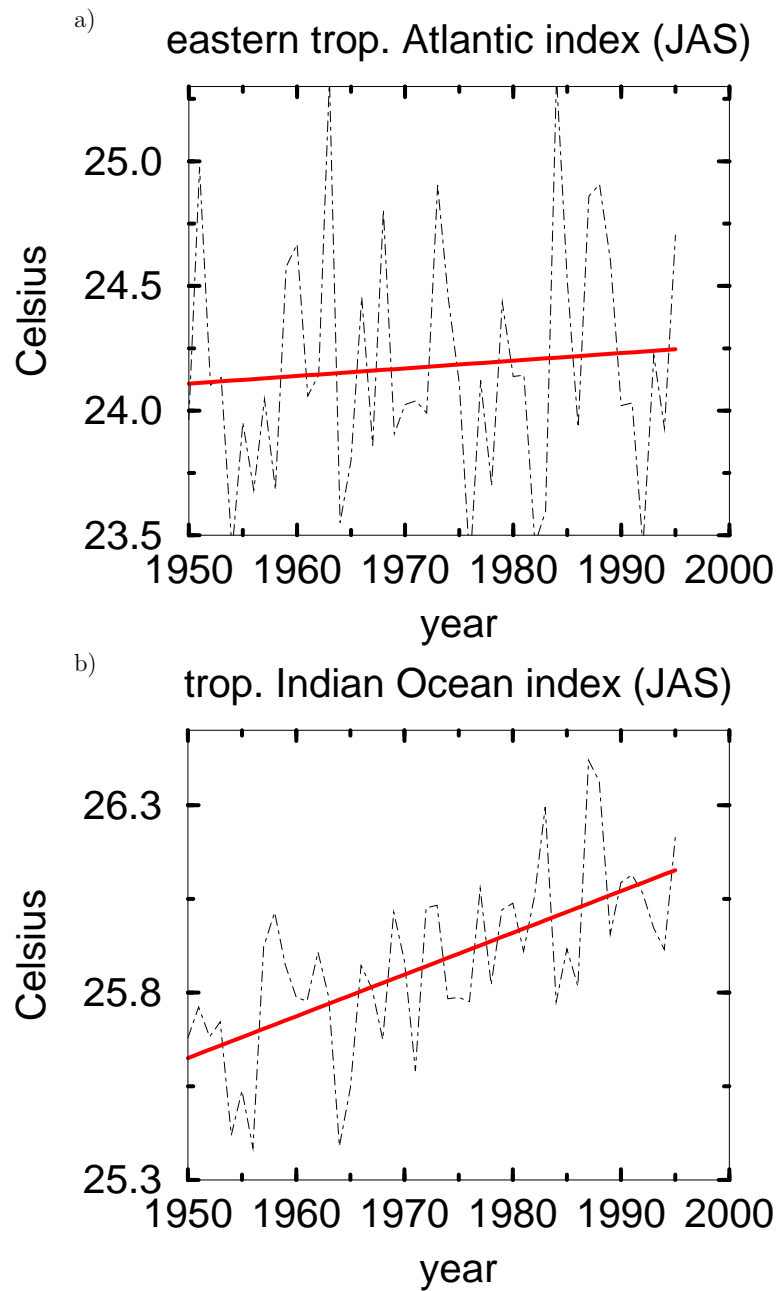


Figure 3.15: Observed area-averaged SST Index for: a) eastern tropical Atlantic; b) tropical Indian Ocean; both for the JAS season (in Celsius), based on the Reynolds SSTs; the black curves denote the JAS means; the red curves the linear trend.

monopolar pattern shown in Figure 3.1b. Thus, both leading rainfall variability patterns can be driven by combinations of anomalous SSTs in the Indian Ocean and the ETA.

The correlation analysis shows also a relationship between Sahelian rainfall and Atlantic and Pacific SSTs. Therefore, some additional experiments are performed in which the SST is changed in the tropical North and South Atlantic and in the NINO3 ($150^{\circ}W - 90^{\circ}W; 5^{\circ}S - 5^{\circ}N$) area. These experiments are especially performed in order to investigate the role of the inter-hemispheric Atlantic SST gradient and ENSO on Sahelian rainfall via the atmosphere. The results of the experiments are discussed only briefly here. The focus is on the impact of eastern tropical Atlantic and Indian Ocean SST anomalies on Sahelian and Guinea Coast rainfall. When changing the SST in the North and South Atlantic our model simulates significant rainfall reductions over the Sahelian area (not shown). No significant rainfall enhancement over the Sahel is simulated by changing only Atlantic SSTs – except along the Sahelian West Coast (not shown). Further, an SST-sensitivity-experiment in which we changed the SSTs in the NINO3 ($150^{\circ}W - 90^{\circ}W; 5^{\circ}S - 5^{\circ}N$) area simulates no significant impact on the West Sahelian summer rainfall (not shown). The "ENSO"-experiment indicates that there is no significant direct impact of SSTs in the ENSO region on West Sahelian rainfall. This might confirm the findings of Nicholson (1997) that the ENSO signal in rainfall is due to ENSO's impact on Atlantic and Indian Oceans SSTs. The Atlantic experiments as well as the findings of Lamb and Pepler (1992) confirm that other mechanisms (e.g. teleconnections from other ocean areas) may play an important role in Sahelian rainfall.

3.5 Conclusions

We have identified the Indian and eastern tropical Atlantic Oceans as two key ocean areas for driving the two basic rainfall anomaly patterns over sub-Saharan West Africa in summer. By changing the SSTs in these two ocean areas simultaneously in atmosphere model experiments we are able to simulate the observed two basic patterns of the boreal summer rainfall variability over sub-Saharan West Africa. The dominant SST forcing along

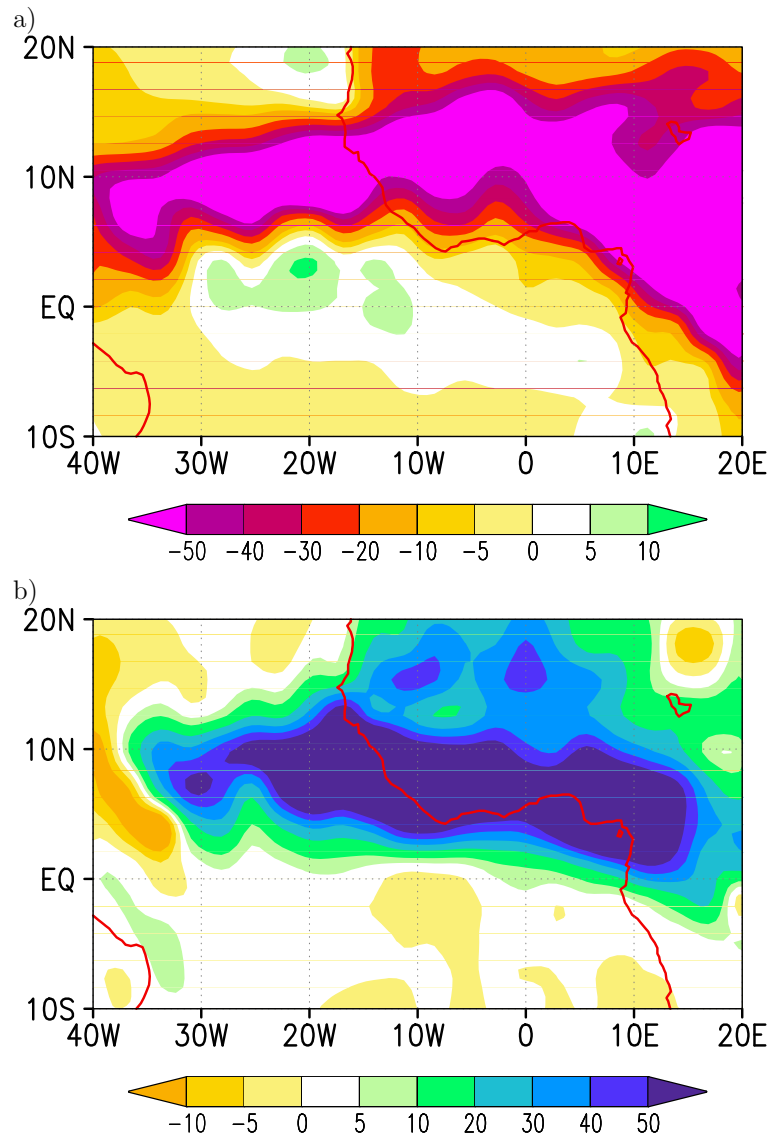


Figure 3.16: Simulated JAS rainfall anomaly (relative to control integration) for the experiments with: a) Indian Ocean enhanced and eastern tropical Atlantic reduced by one Kelvin; b) Indian Ocean reduced and eastern tropical Atlantic enhanced by one Kelvin; units: mm/month.

Guinea Coast are the SST anomalies of the eastern tropical Atlantic and the associated anomalous water vapor content of the lower troposphere. The impact of these SST anomalies in the eastern tropical Atlantic on the boreal summer rainfall over sub-Saharan West Africa is confined to approximately 10°N . The rainfall north of this latitude (e.g., over the West Sahel) is linked via changes in the large-scale atmospheric circulation to changes of the Indian Ocean SST. These findings are confirmed by our correlation analysis between the observed July to September rainfall indices of our two regions and the observed July to September sea surface temperatures. The out-of-phase rainfall anomaly pattern is associated with SST anomalies of the same sign in the eastern tropical Atlantic and the Indian Ocean. Opposite SST changes in these two ocean areas lead to a monopolar rainfall change over the whole west sub-Saharan region.

Intensity and position changes of the ITCZ are referred to as the main causes for rainfall changes over West Africa in the literature. Our analysis shows that rainfall intensity changes – originating in different ocean basins – can “mimic” a shift of the ITCZ in summer. Hence, position changes of the ITCZ over sub-Saharan West Africa can partly be deduced from intensity changes caused by SST anomalies in different oceans.

Our simulations indicate that a rainfall enhancement/reduction over the West Sahel is not necessarily linked to a supply of exceptionally wet/dry air to West Africa from the tropical Atlantic.

Since tropical SSTs appear to be predictable at least one season ahead, our results imply a great deal of predictability in sub-Saharan West African rainfall.

Acknowledgments

The authors would like to thank Dr. Noel Keenlyside, Dr. Christian Reick, Holger Pohlmann, Daniela Matei, and Katja Lohmann for their useful comments. This work was supported by the Federal German Ministry of Education and Research (BMBF) under grant 01 LW 0301A (Glowa) and under grant 01 LD 0030 (DEKLIM), the Ministry of Science and Research (MWF) of the state of Northrhine-Westfalia under grant 223 - 212 00 200.

3.6 References

- Bader, J., and M. Latif, 2003: The impact of decadal-scale Indian Ocean sea surface temperature anomalies on Sahelian rainfall and the North Atlantic Oscillation, *Geophysical Research Letters*, **30(22)**, 2169, doi: 10.1029/2003GL018426.
- Folland, C.K., T.N. Palmer, D.E. Parker, 1986: Sahel rainfall and worldwide sea temperatures, 1901-85, *Nature*, **320**, 602-607.
- Fontaine B., S. Janicot and V. Moron, 1995: Rainfall anomaly patterns and wind field signals over West Africa in August (1958-1989), *Journal of Climate*, **8**, 1503-1510.
- Hastenrath, S., 1984: Interannual variability and annual cycle: Mechanism of circulation and climate in the tropical Atlantic sector, *Monthly Weather Review*, **112**, 1097-1107.
- Janicot, S., 1992: Spatiotemporal variability of West African rainfall. Part I: Regionalizations and typings, *Journal of Climate*, **5**, 489-497.
- Janicot, S., V. Moron, B. Fontaine, 1996: Sahel droughts and ENSO dynamics, *Geophysical Research Letters*, **23**, 515-518.
- Janowiak, J.E., 1988: An investigation of interannual rainfall variability in Africa, *Journal of Climate*, **1**, 240-255.
- Lamb, P.J., 1978a: Case studies of tropical Atlantic surface circulation patterns during recent sub-Saharan weather anomalies: 1967 and 1968, *Monthly Weather Review*, **106**, 482-491.
- Lamb, P.J., 1978b: Large-scale tropical Atlantic surface circulation patterns associated with sub-Saharan weather anomalies, *Tellus*, **A30**, 240-251.
- Lamb, P.J., and R.A. Pepler, 1992: Further case studies of tropical Atlantic surface circulation patterns associated with sub-Saharan drought, *Journal of Climate*, **5**, 476-488.

- Latif, M., and A. Grötzner, 2000: The equatorial Atlantic oscillation and its response to ENSO, *Climate Dynamics*, **2-3**, 213-218.
- New, M. G., M. Hulme, and P. D. Jones, 2000: Representing twentieth-century space-time climate variability, Part II: Development of 1901-1996 monthly grids of terrestrial surface climate, *Journal of Climate*, **13**, 2217-2238.
- Newell, R.E. and J.W. Kidson, 1984: African mean wind changes between Sahelian wet and dry periods, *Journal of Climatology*, **4**, 27-33.
- Nicholson S.E., 1980: The nature of rainfall fluctuations in subtropical West Africa, *Monthly Weather Review*, **108**, 473-487.
- Nicholson S.E., and Palao, 1993: A re-evaluation of rainfall variability in the Sahel Part I. Characteristics of rainfall fluctuations, *International Journal of Climatology*, **13**, 371-389.
- Nicholson S.E., 1997: An analysis of the ENSO signal in the tropical Atlantic and western Indian oceans, *International Journal of Climatology*, **17**, 345-375.
- Nicholson S.E., J.P. Grist, 2001: A conceptual model for understanding rainfall variability in the West African Sahel on interannual and inter-decadal timescales, *Journal of Climatology*, **21**, 1733-1757.
- Nicholson S.E., J.P. Grist, 2003: The seasonal evolution of the atmospheric circulation over West Africa and Equatorial Africa, *Journal of Climate*, **16**, 1013-1030.
- Palmer, T.N., 1986: Influence of the Atlantic, Pacific and Indian Oceans on Sahel rainfall, *Nature*, **322**, 251-253.
- Rayner, N. A., D. E. Parker, E. B. Horton, C. K. Folland, L. V. Alexander, D. P. Rowell, E. C. Kent, and A. Kaplan, 2003: Global analyses of sea surface temperature, sea ice, and night marine air temperature since the late nineteenth century, *J. Geophys. Res.-Atmospheres*, **108** (D14), 4407, doi: 10.1029/2002JD002670.

- Roeckner, E., K. Arpe, L. Bengtsson, M. Christoph, M. Claussen, L. Dümenil, M. Esch, M. Giorgetta, U. Schlese, and U. Schulzweida: The atmospheric general circulation model ECHAM-4: Model description and simulation of present-day climate, 1996, *MPI Report*, **218**.
- Rowell, D.P., 2001: Teleconnections between the tropical Pacific and the Sahel, *Quart. J. Roy. Meteor. Soc.*, **127**, 1683-1706.
- Rowell, D.P., 2003: The impact of Mediterranean SSTs on the Sahelian rainfall season, *Journal of Climate*, **16**, 849-862.
- Shinoda, M. and R. Kawamura, 1994: Tropical rainbelt, circulation, and sea surface temperatures associated with the Sahelian rainfall trend, *Journal of the Meteorological Society of Japan*, **72**, 341-357.
- Taylor, K.E., D. Williamson, and F. Zwiers, 2000: The sea surface temperature and sea ice concentration boundary conditions for AMIP II simulations, *PCMDI Report*, **60**.
- Vizy, E. K. and K. H. Cook, 2001: Mechanisms by which Gulf of Guinea and eastern North Atlantic sea surface temperature anomalies can influence African rainfall, *Journal of Climate*, **14**, 795-821.
- Vizy, E. K. and K. H. Cook, 2002: Development and application of a mesoscale climate model for the tropics: Influence of sea surface temperature anomalies on the West African monsoon, *J. Geophysical Research - Atmosphere*, **107**, 4023, doi:10.1029/2001JD000686.
- Ward, M.N., 1998: Diagnosis and short-lead time prediction of summer rainfall in tropical North Africa at interannual and multidecadal timescales, *Journal of Climate*, **11**, 3167-3191.
- Ward, M.N., P. J. Lamb, D. H. Portis, M. el Hamly, and R. Sebbari, 1999. Climate variability in northern Africa. Understanding droughts in the Sahel and the Maghreb. *Beyond el Niño: Decadal and interdecadal climate variability*, A. Navarra, Ed., Springer-Verlag, 119-140.

- Zebiak, S.E., 1993: Air-sea interactions in the equatorial Atlantic region, *Journal of Climate*, **6**, 1567-1586.

Chapter 4

North Atlantic Oscillation response to anomalous Indian Ocean SST in a coupled GCM

Jürgen Bader^{1,2,*} and Mojib Latif³

¹Institute of Geophysics and Meteorology, University of Cologne, Cologne,
Germany

²Max-Planck-Institute for Meteorology, Hamburg, Germany

³Leibniz-Institute for Marine Sciences at the University of Kiel, Kiel,
Germany

*Corresponding author address: Jürgen Bader, Max-Planck-Institute for Meteorology,
Bundesstraße 53, 20146 Hamburg, Germany. E-mail: bader@dkrz.de

Abstract

The dominant pattern of atmospheric variability in the North Atlantic sector is the North Atlantic Oscillation (NAO). Since the 1970s the NAO is well characterized by a trend towards its positive phase. Recent atmospheric general circulation model studies have linked this trend to a progressive warming of the Indian Ocean. Unfortunately, a clear mechanism – responsible for the change of the NAO – could not be given. This study provides further details of the NAO response to Indian Ocean sea surface temperature (SST) anomalies. We do this by conducting experiments with a coupled ocean-atmosphere general circulation model (OAGCM). We develop a hypothesis of how the Indian Ocean impacts the NAO.

4.1 Introduction

The NAO is a large-scale alternation of atmospheric mass with centers of action near the Icelandic Low and the Azorian High. It is the dominant pattern of atmospheric variability in the North Atlantic sector throughout the year, although it is most pronounced during the winter and accounts for more than one-third of the total variance in sea level pressure (Cayan 1992, Hurrell 2003 and references therein). The NAO shows strong interannual and decadal variabilities during the last century (Figure 4.1). The NAO exhibits a strong upward trend since the 1970s and a reverse trend in the 1950s and 1960s (Hurrell 1995). Different hypotheses were put forward to explain the low-frequency changes of the NAO. Internal atmospheric dynamics were suggested by James and James (1989). Saravanan and McWilliams (1997) linked the low-frequency variability to a stochastic forcing of the atmosphere driving low-frequency changes in the ocean which feed back on the atmosphere. In atmospheric general circulation model (AGCM) experiments, Rodwell et al. (1999) and Latif et al. (2000) found an oceanic control of decadal North Atlantic sea level pressure variability in winter. Using atmospheric general circulation models Hoerling et al. (2001, 2004), Bader and Latif (2003), and Hurrell et al. (2004) recently showed that the progressive warming of the Indian Ocean (see Figure 4.2) may be a principal contributor to the recent

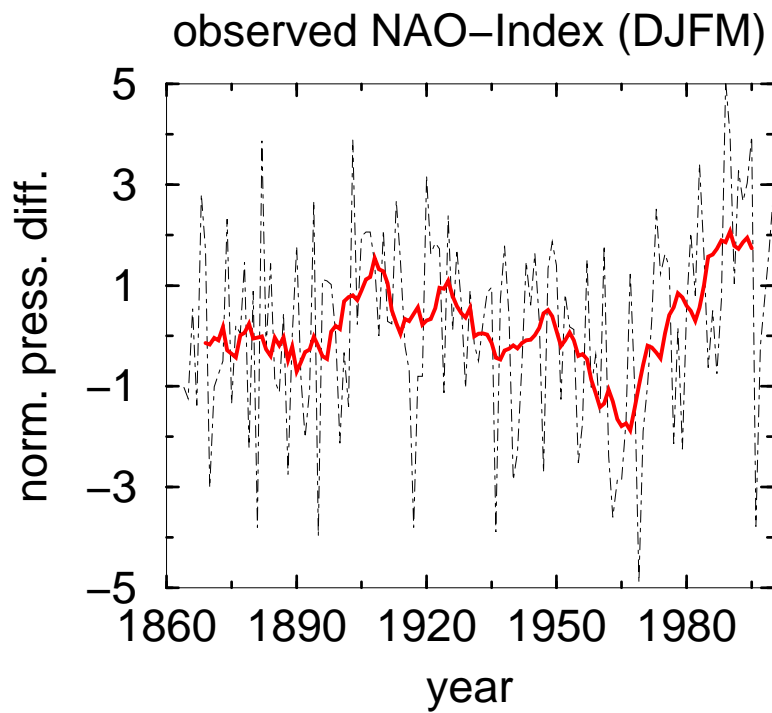


Figure 4.1: *Observed winter (DJFM) NAO index defined by Hurrell (1995). The black curve denotes the seasonal mean, the red curve the 11-yr running mean.*

change of the North Atlantic Oscillation. This study puts forward a hypothesis of how the Indian Ocean sea surface temperature anomalies may affect the North Atlantic Oscillation. Since we are using a coupled ocean-atmosphere model in which the SSTs are interactively calculated in the Atlantic sector we are able to account for ocean-atmosphere feedbacks in this sector.

4.2 Model and Experiments

The model used in this study is the global ocean-atmosphere-sea ice model MPI-OM/ECHAM5. A detailed description of the atmosphere model ECHAM5 is given in a technical report (Roeckner et al. 2003). The ocean model is described in Marsland et al. (2003). First applications of the coupled model are studies of Latif et al. (2003) and Pohlmann et al. (2004). The atmospheric model is run at T31 ($\approx 3.75^\circ \times 3.75^\circ$) horizontal resolution with 19 vertical levels. The ocean model MPI-OM is run at a horizontal resolution of $\approx 3^\circ \times 3^\circ$ with 40 vertical levels. The model does not employ flux corrections. A 200-year-long control simulation is performed – initialized at year 140 of another control integration to get rid of the spin up. Additionally, two sensitivity experiments are performed. In these experiments the ocean temperature of the first layer in the tropical Indian Ocean (see Figure 4.3) is prescribed using climatological SST of the control integration and a trend is superimposed. In the first 75 years, the climatological values are enhanced/reduced by 1.5 Kelvin in the tropical Indian Ocean. Thereafter the SST in the Indian Ocean is kept constant (Figure 4.4). Please note that the trend is much stronger than the interannually produced variability in the control integration. In all other ocean areas than the tropical Indian Ocean the SST is calculated interactively.

Figure 4.5 shows the leading empirical orthogonal function (EOF) pattern of the winter – December to February (DJF) – sea level pressure in the Atlantic area of the control integration. The model simulates realistically the North Atlantic Oscillation pattern. The model is able to capture the essential feature of the observed NAO, the mass exchange between the high latitudes and midlatitudes.

Additionally, sensitivity experiments are performed with the atmospheric

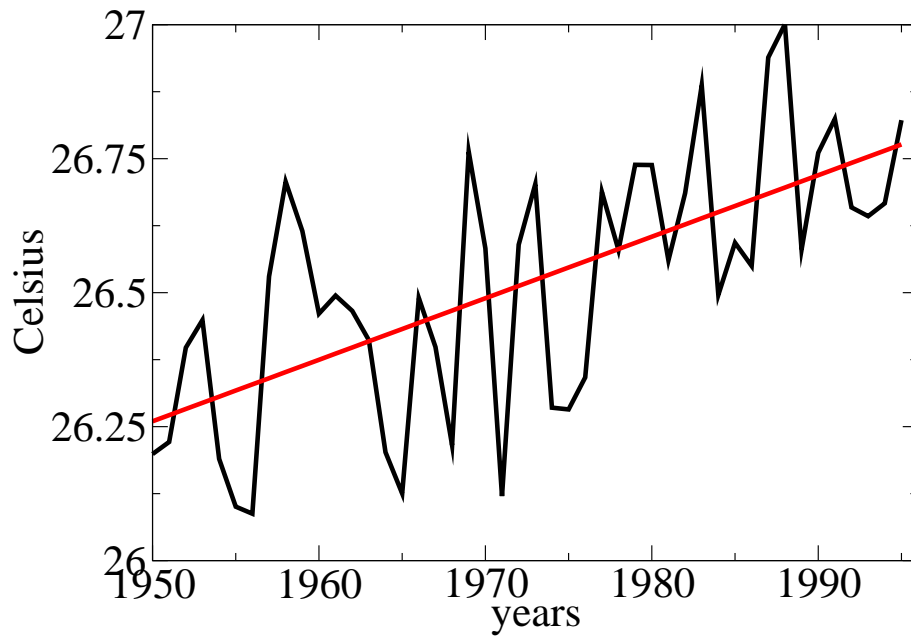


Figure 4.2: *Observed annual tropical Indian Ocean SST Index (in Celsius), based on the Reynolds SSTs; averaged from the east coast of Africa to 120°E and from 30°S to 30°N. The black curve denotes the annual means, the red curve the linear trend.*

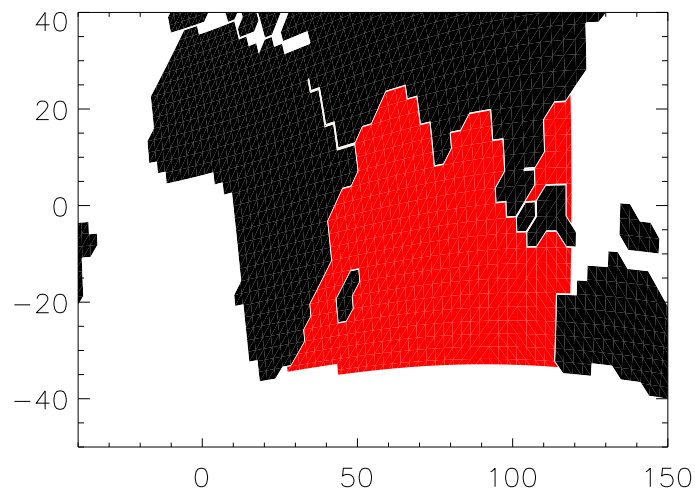


Figure 4.3: Red coloring shows the area of the tropical Indian Ocean in which the sea surface temperatures are prescribed for the individual OAGCM SST-sensitivity experiments.

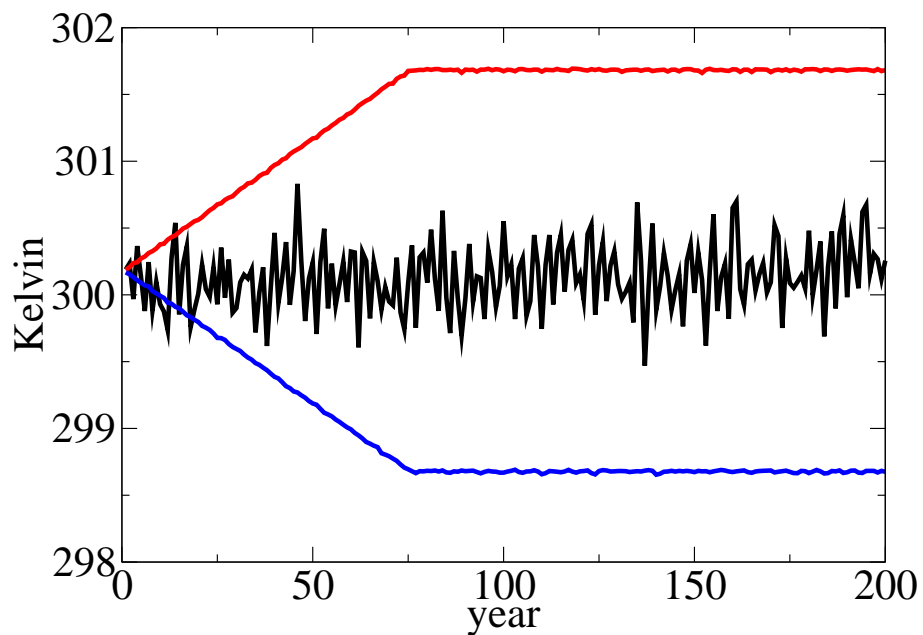


Figure 4.4: Annual sea surface temperatures averaged over the tropical Indian Ocean: for the control integration (black curve); for the SST-sensitivity experiment "warm Indian Ocean" (red curve); for the SST-sensitivity experiment "cold Indian Ocean" (blue curve); units [Kelvin].

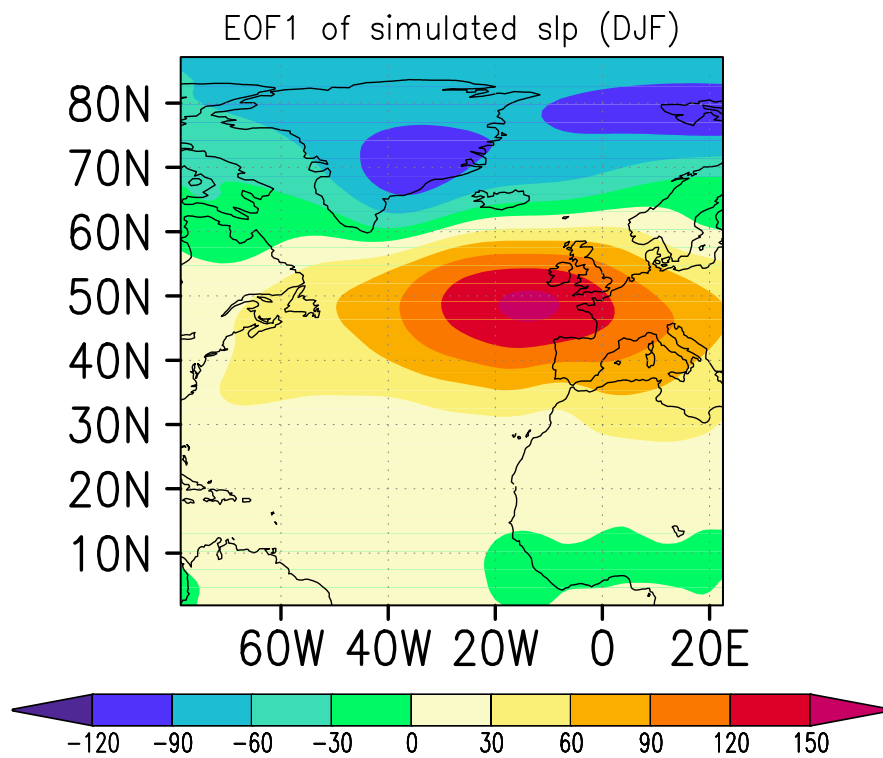


Figure 4.5: *First Empirical Orthogonal Function (EOF) loading pattern of the simulated winter (DJF) sea level pressure of the OAGCM control integration.*

general circulation model ECHAM4.5 (Roeckner et al. 1996) run in stand-alone mode. The model forced by the observed SSTs from 1951 to 1994 simulates the observed low-frequency NAO index variations reasonably well (Latif et al. 2000). The climatological AMIP2-SSTs (Taylor et al. 2000) are used for the control experiment. Two sensitivity experiments are performed. In the first sensitivity experiment the climatological SSTs in the whole tropical Indian Ocean are reduced by one Kelvin (Figure 4.6a). In the second

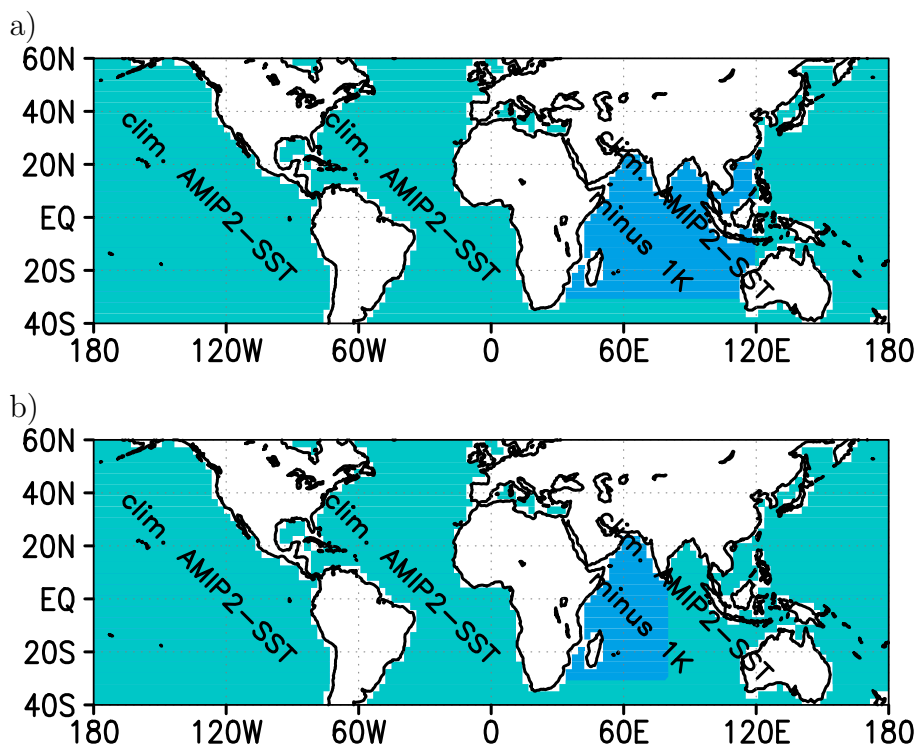


Figure 4.6: *SST anomaly for a) the Indian Ocean minus 1K AGCM experiment; b) the western Indian Ocean minus 1K AGCM experiment.*

sensitivity experiment the SST anomalies are restricted to the western tropical Indian Ocean (Figure 4.6b). Results for the AGCM experiments are obtained from a set of 21-year long SST sensitivity experiments. The results are averaged over the last nineteen years and only the mean December to February (DJF) response (sensitivity run minus control integration) is shown here.

4.3 Results

Figures 4.7a and 4.7b show the mean December to February (DJF) sea level pressure response for the two individual OAGCM sensitivity simulations (mean of the sensitivity experiment minus mean of the control integration; the means are computed over the whole integration length). The sea level pressure response to a warm/cold Indian Ocean shows a meridional seesaw pattern, with low/high SLP anomalies north of approximately 55°N and high/low SLP south of this latitude. A warm Indian Ocean produces a stronger (Figure 4.7a) and a cold Indian Ocean a weaker NAO (Figure 4.7b). To first order the response is almost linear. The response patterns are very similar to the first EOF loading pattern of the simulated winter sea level pressure of the control integration. These coupled atmosphere-ocean experiments confirm the findings that slow changes in the state of the ocean force the NAO on longer time scales (e.g. Rodwell et al. 1999 and Latif et al. 2000) and especially show a clear Indian Ocean impact on the NAO. This is in agreement with the findings of e.g. Hoerling et al. (2001, 2004), Bader and Latif (2003) and Hurrell et al. (2004) who analyzed AGCM experiments. Key questions concern the mechanisms by which changes in the tropical Indian Ocean SSTs can influence the NAO. It is well established that tropical SST anomalies impact tropical rainfall and, thus, latent heating, which in turn drives changes in atmospheric circulation at higher latitudes (Hoerling et al. (2001)). A prominent example is El Niño (see e.g. Trenberth et al. 1998). How does the Indian Ocean affect the North Atlantic sector? The study by Branstator (2002) shows that disturbances in the vicinity of the mean jets, especially the South Asian Jet, lead to covariability between widely separated points. He shows that the NAO is likely to include contributions from the circumglobal waveguide pattern. Based on this study we would like to show that the circumglobal teleconnection associated with the South Asian Jet Stream may be the link between the Indian Ocean warming and the recent trend of the North Atlantic Oscillation, which was also suggested by Lu et al. (2004) as a topic for future study.

First, we show that this type of circumglobal wave is simulated in our model. We begin our analysis by considering the 300hPa meridional wind in our con-

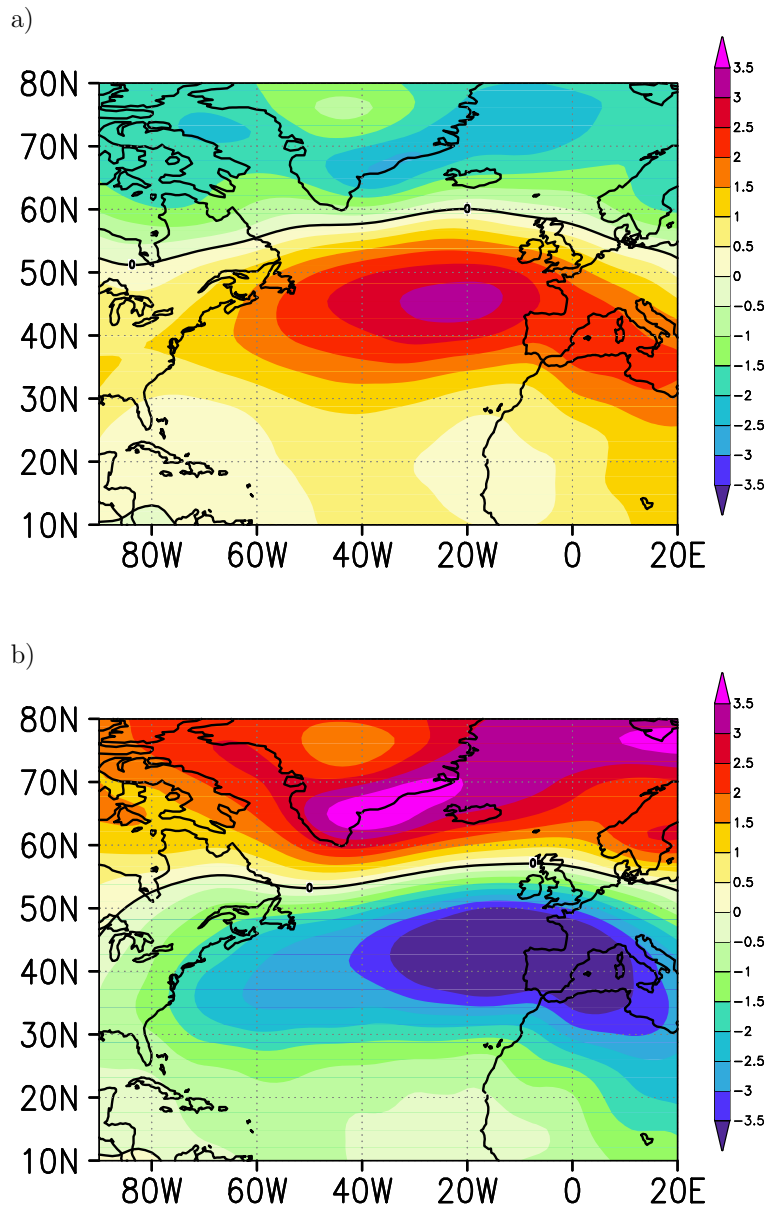


Figure 4.7: Mean DJF sea level pressure anomaly (relative to control integration): a) for the SST-sensitivity experiment "warm Indian Ocean"; b) for the SST-sensitivity experiment "cold Indian Ocean"; units [hPa].

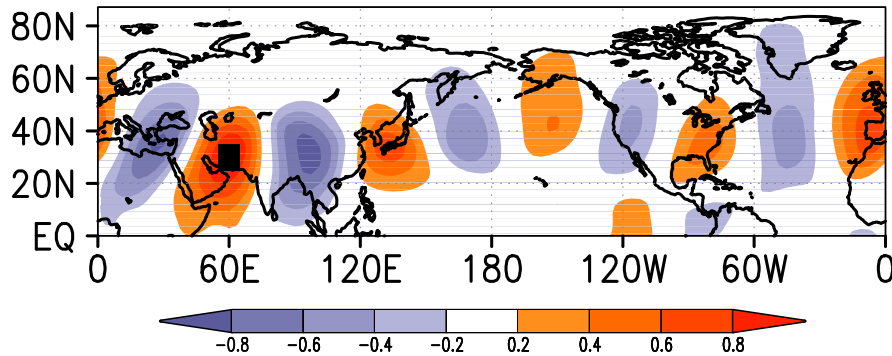


Figure 4.8: *Correlation of winter (DJF) 300hPa meridional wind averaged over the black box and winter 300hPa meridional wind in the Northern Hemisphere.*

trol integration of the coupled model. To show covariability between points in the South Asian Jet and distant regions, the correlation between the winter (DJF) 300hPa meridional wind averaged over the area from 55°E to 65°E and from 25°N to 35°N – indicated by the black box in Figure 4.8 – and the DJF meridional wind in the Northern Hemisphere in our control integration is calculated. Figure 4.8 reveals an anomaly pattern with alternating signs which is meridionally confined to the vicinity of the jets and consists of anomalies which are zonally oriented extending over the whole Northern Hemisphere. This circumglobal covariability is confirmed by the first EOF of the winter 300hPa meridional wind in the control run (Figure 4.9). Our findings are in agreement with the more comprehensive analysis of Branstator (2002) who found the largest teleconnectivity in the jet stream waveguide both in simulations and observations. In the following we test whether there is any connection between the NAO and this circumglobal pattern in our control simulation. Figure 4.10 shows the correlation between the NAO index – the first principal component (PC1) of winter sea level pressure in the Atlantic sector (region displayed in Figure 4.5) – and the winter 300hPa meridional wind. To show the similarity in the correlation and in the circumglobal pattern of Figure 4.9 the crosses in Figure 4.10 mark the centers of the ten lobes of the circumglobal pattern. In agreement to Branstator (2002) we find that the NAO is likely to have contributions from the circumglobal pattern.

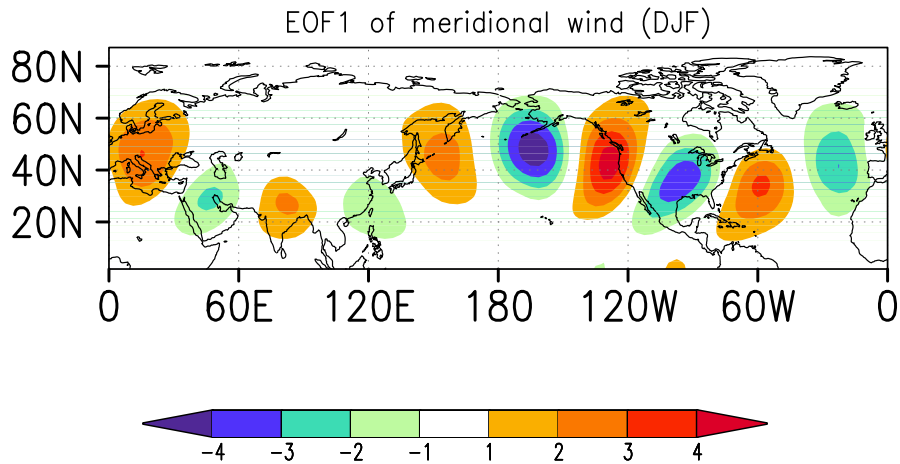


Figure 4.9: *The leading EOF of Northern Hemisphere 300hPa winter (DJF) meridional wind [m/s per standard deviation].*

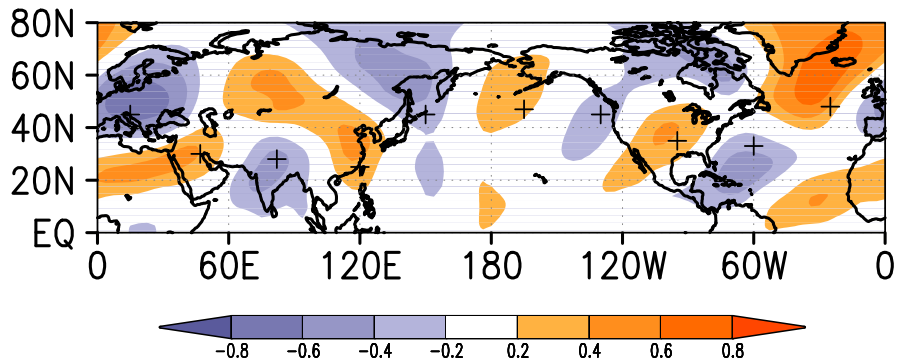


Figure 4.10: *Correlation of winter (DJF) 300hPa meridional wind with the first principal component of winter (DJF) sea level pressure over the North Atlantic sector (NAO index) in the control integration. The crosses mark the centers of the ten lobes in the EOF1 plot of the meridional wind in Figure 4.9.*

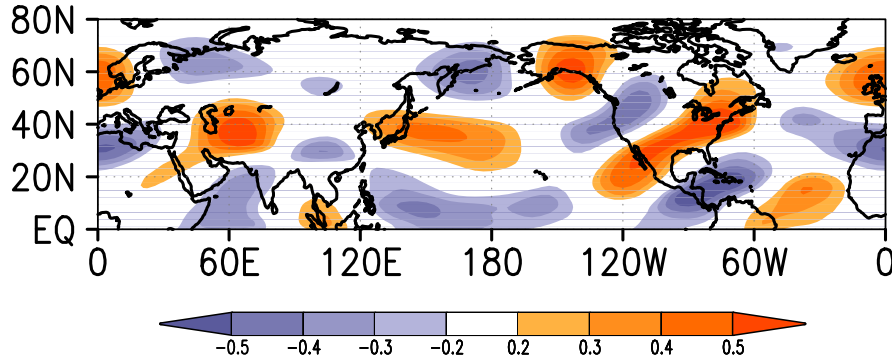


Figure 4.11: *Correlation of winter (DJF) 300hPa zonal wind with the first principal component of winter (DJF) meridional wind in the control integration.*

Next, we investigate whether the circumglobal pattern of Figure 4.9 is associated with zonal wind anomalies. Figure 4.11 shows the correlation coefficients between the circumglobal pattern index – PC1 of the winter 300hPa meridional wind – and the zonal wind in the control integration. We find a wave-like pattern spanning the whole Northern Hemisphere, and the circumglobal pattern is associated with zonal wind anomalies in the area of the South Asian Jet (Figure 4.11). The pattern in the South Asian region (from the equator and 45°N and eastward from 0° to 120°E) is characterized by positive correlation coefficients in the western part of the South Asian Jet and negative ones over the north western Indian Ocean. Additionally, we show the relationship between the NAO and the zonal wind anomalies. Figure 4.12 shows the correlation between the NAO index – the first principal component (PC1) of winter sea level pressure in the Atlantic sector (region displayed in Figure 4.5) – and the winter 300hPa zonal wind in the control simulation. We find the typical NAO wind anomalies in the Atlantic sector and a similar correlation pattern in the South Asian Jet region as that in Figure 4.11.

We have shown that changes in the NAO are associated with changes in the South Asian Jet via the circumglobal pattern. An amplified/reduced NAO is connected with a stronger/weaker South Asian Jet especially in the area around 60°E. Hence, we shall test next if similar changes of the South

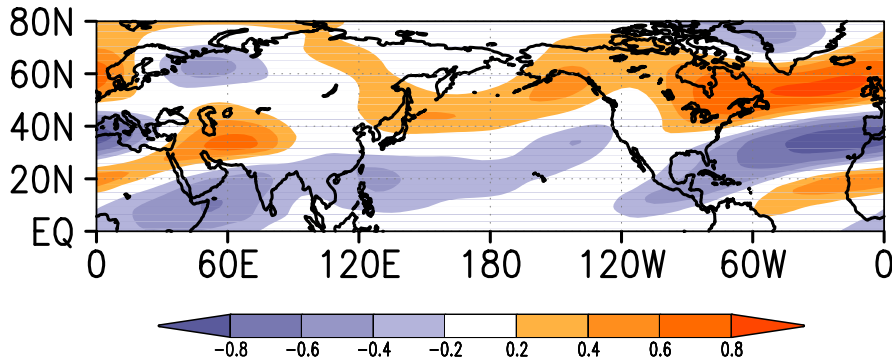


Figure 4.12: *Correlation of winter (DJF) 300hPa zonal wind with the first principal component of winter (DJF) sea level pressure over the North Atlantic sector (NAO index) in the control integration.*

Asian Jet as those in Figures 4.11 and 4.12 are produced in our sensitivity experiments.

Figures 4.13a and 4.13b show the simulated winter zonal wind response of the warm and cold Indian Ocean experiments. The warm Indian Ocean experiment (strong NAO) is characterized by positive anomalies in the area of the Asian jet and negative over the north western Indian Ocean (Figure 4.13a) and vice versa for the cold experiment (weak NAO; Figure 4.13b). The cause for the intensity change of the South Asian Jet could be the thermal wind balance due to a change of the horizontal temperature gradient. Figure 4.14 shows the winter precipitation response for the two OAGCM sensitivity experiments. The precipitation response especially near the south equatorial Indian Ocean is characterized by an increase/reduction in rainfall due to higher/lower SSTs. The enhancement/decrease in latent heat release increases/reduces the meridional temperature gradient up to the mid-troposphere which then intensifies/weakenes the South Asian Jet. Figure 4.15a shows the timeseries of the simulated South Asian Jet index – zonal wind in 300hPa averaged from 40°E to 80°E and from 30°N to 45°N – for the individual OAGCM simulations. Additionally, the NAO indices for the individual experiments are shown in 4.15b. The NAO index here is defined by the difference in box-averaged normalized DJF sea level pressure between a southern and a northern box in the North Atlantic sector. The northern

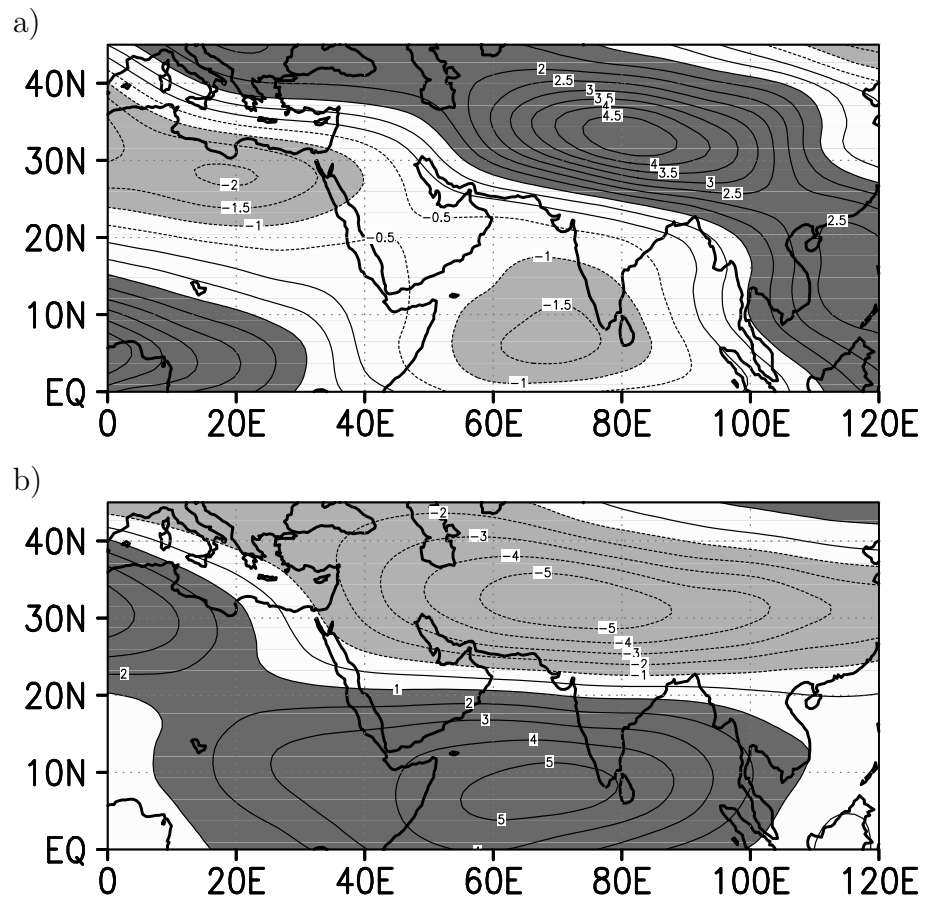


Figure 4.13: Mean simulated winter (DJF) zonal wind anomaly (relative to control integration): a) for the SST-sensitivity experiment "warm Indian Ocean"; b) for the SST-sensitivity experiment "cold Indian Ocean"; [m/s].

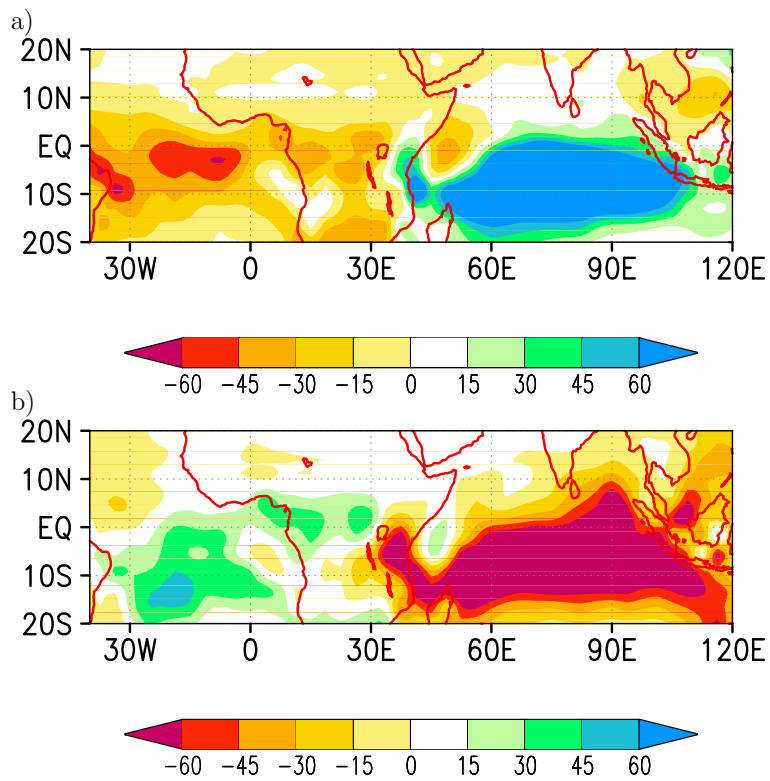


Figure 4.14: Mean simulated winter (DJF) precipitation anomaly (relative to control integration): a) for the SST-sensitivity experiment "warm Indian Ocean"; b) for the SST-sensitivity experiment "cold Indian Ocean"; units [mm/month].

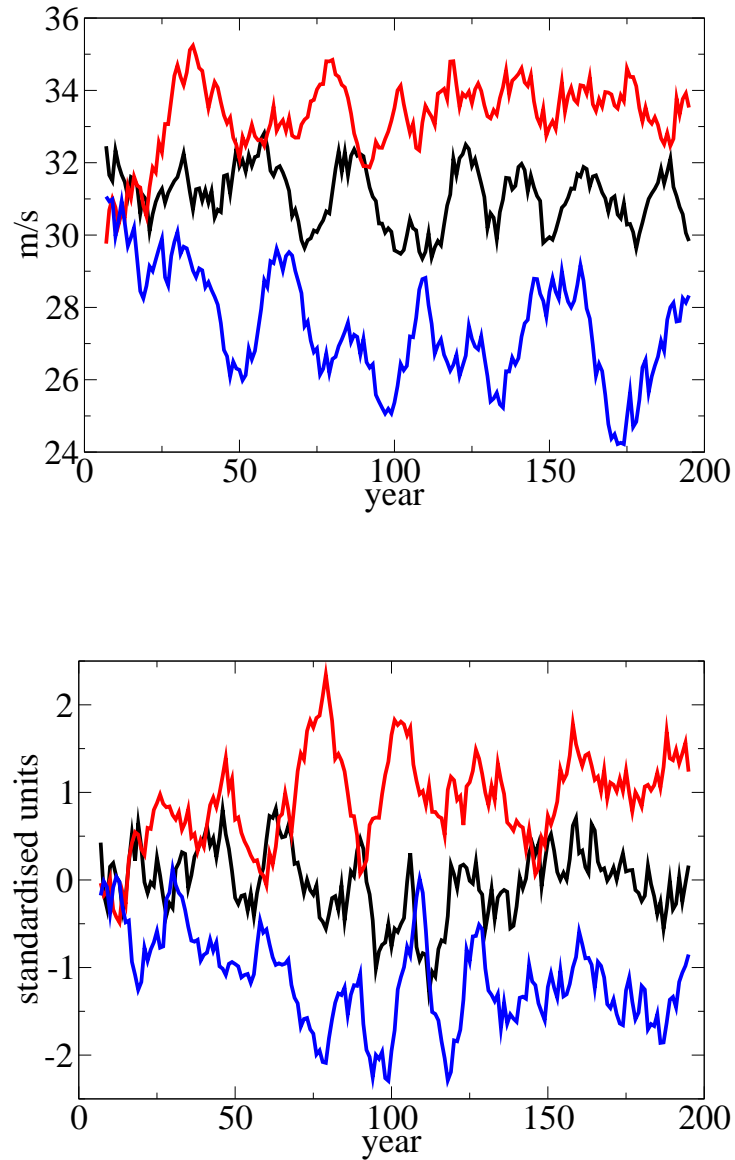


Figure 4.15: Simulated 11-yr running mean timeseries of the winter (DJF) a) zonal wind anomaly index in the South Asian Jet region and b) NAO index (relative to the mean of the control integration) for the control integration (black curve); for the SST-sensitivity experiment "warm Indian Ocean" (red curve); for the SST-sensitivity experiment "cold Indian Ocean" (blue curve).

box is defined from 60°W to 0° and from 60°N to 80°N and the southern box from 60°W to 0° and from 30°N to 50°N . Figure 4.15b shows the three NAO indices relative to the mean of the control integration. Figures 4.15a and 4.15b show clearly that a positive NAO index is connected with a stronger South Asian Jet and vice versa. The response of the jet appears to be somewhat stronger in the cold Indian Ocean experiment.

The observed warming trend in the Indian Ocean (Figure 4.2) should also be associated with a trend in the observed South Asian Jet. Figure 4.16 shows the timeseries of the observed South Asian Jet – DJF zonal wind in 300hPa averaged from 40°E to 80°E and from 30°N to 45°N –, based on the NCEP reanalysis data. There is a clear trend towards a stronger South Asian Jet, which confirms our findings. Figure 4.17 shows the observed (NCEP reanalysis data) winter 300hPa meridional wind anomaly between the mean of the years ((1982-1993) minus (1949-1960)). The wave-like anomaly pattern is similar to the circumglobal pattern. Together figures 4.17 and 4.16 indicate that the recent NAO trend is also in reality associated with the circumglobal pattern.

Figure 4.12 shows the strongest correlation between NAO and winter zonal 300hPa wind in the South Asian Jet region between approximately 55°E to 65°E . Since the change of the South Asian Jet is likely due to changes in the horizontal meridional temperature gradient it is likely that the west Indian Ocean may be the principal contributor for the change in the western South Asian Jet and therefore in the NAO. This is tested by two simple AGCM experiments. In the first experiment the whole Indian Ocean climatological SSTs are reduced by one Kelvin. In the second sensitivity experiment with the AGCM, the SST anomalies are restricted to the western tropical Indian Ocean (Figure 4.6b). Figure 4.18 shows the sea level pressure response for the two individual experiments. Both experiments produce a NAO-like sea level pressure response. A weakening of both the Icelandic low and the Azorian high is simulated. A two-tailed t-test indicates that the results are significant at the 95%-confidence-level in both experiments, at least in the centers of action. Apparently, west Indian Ocean SST anomalies are sufficient to force the NAO. Figure 4.19 shows the mean DJF 300hPa meridional wind response for the "western Indian Ocean minus 1K" experiment (sensitivity

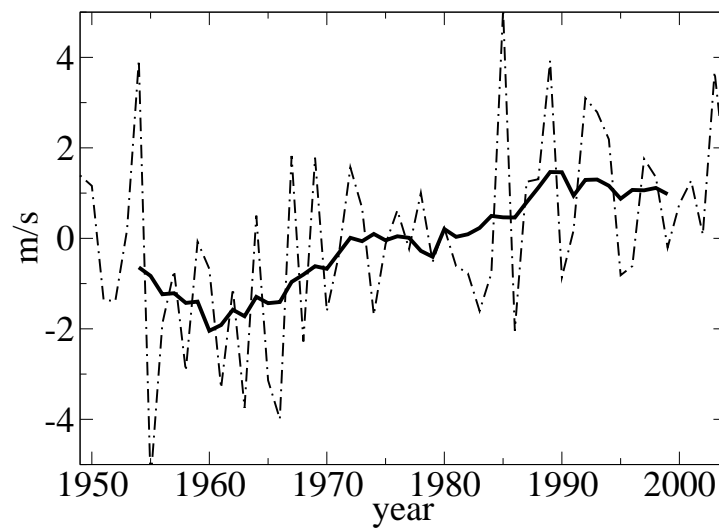


Figure 4.16: *Observed winter (DJF) zonal wind anomaly index (see text for details) in the South Asian Jet region, based on the NCEP reanalysis data. The dotted-dashed curve denotes the seasonal means, the thick solid black curve the 11-yr running mean.*

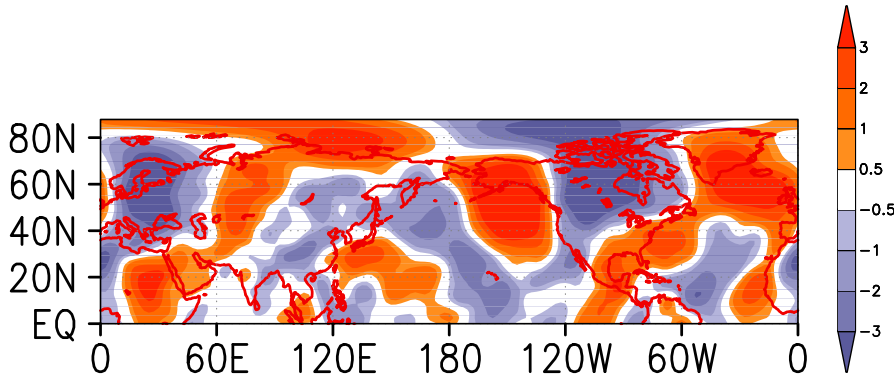


Figure 4.17: Observed meridional 300hPa winter (DJF) wind anomaly between the mean of the years ((1982-1993) minus (1949-1960)), based on the NCEP reanalysis data; [m/s].

experiment minus control integration). It reveals a wavy response in the Northern Hemisphere closely resembling the circumglobal pattern. A clear reduction in the western South Asian Jet is simulated (not shown). These atmospheric experiments confirm that Indian Ocean SST anomalies force changes in the South Asian Jet. The South Asian Jet produces a variability pattern that comprises the whole Northern Hemisphere. This circumglobal pattern then can lead to changes in the NAO.

4.4 Conclusions

By analyzing model simulations we found that the South Asian Jet can act as a waveguide with circumglobal teleconnection in the Northern Hemisphere. The meridional wind pattern – associated with this circumglobal teleconnection – is connected with the North Atlantic Oscillation. A warming/cooling in the Indian Ocean, especially in the western Indian Ocean, produces anomalies in the South Asian Jet. The waveguiding effect of the South Asian Jet carries the perturbation into the North Atlantic sector and leads to a NAO-like response.

The observed recent positive trend in the NAO has likely contributions from the observed warming in the Indian Ocean. Our analysis – confirmed by the observed trend in the western South Asian Jet and the anomaly pattern of

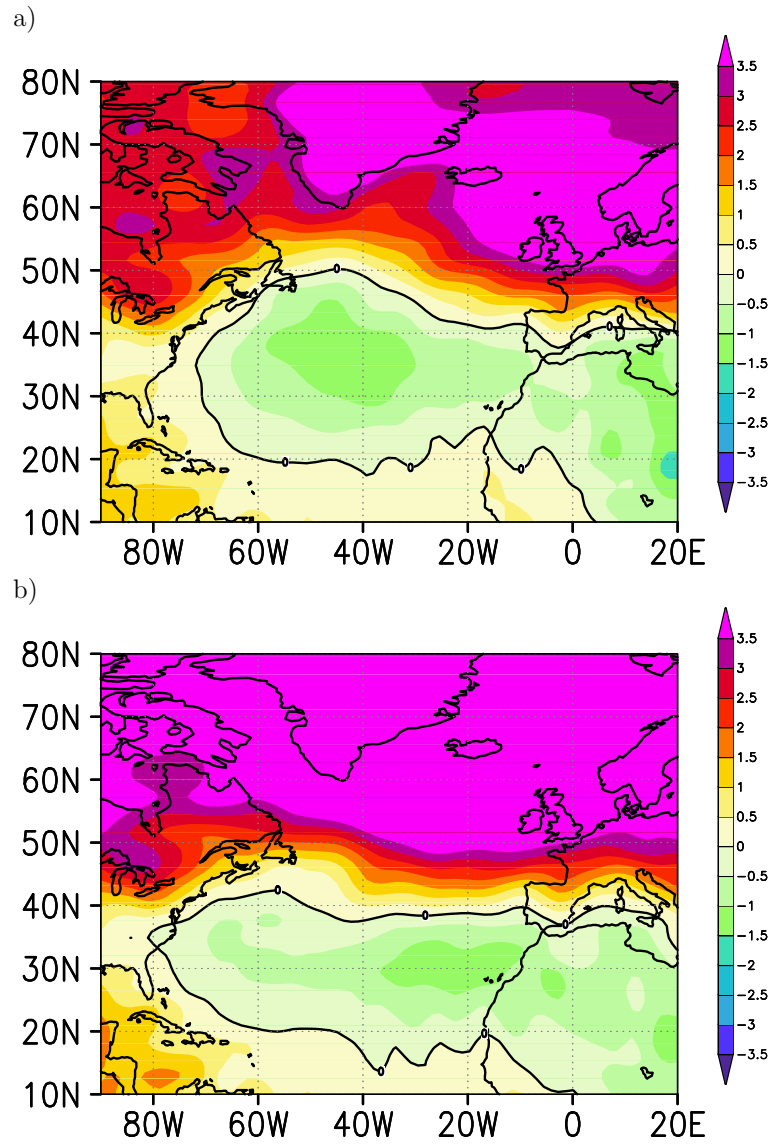


Figure 4.18: Mean DJF sea level pressure anomaly (relative to control integration): a) for the SST-sensitivity experiment "Indian Ocean minus 1K"; b) for the SST-sensitivity experiment "western Indian Ocean minus 1K experiment"; [hPa].

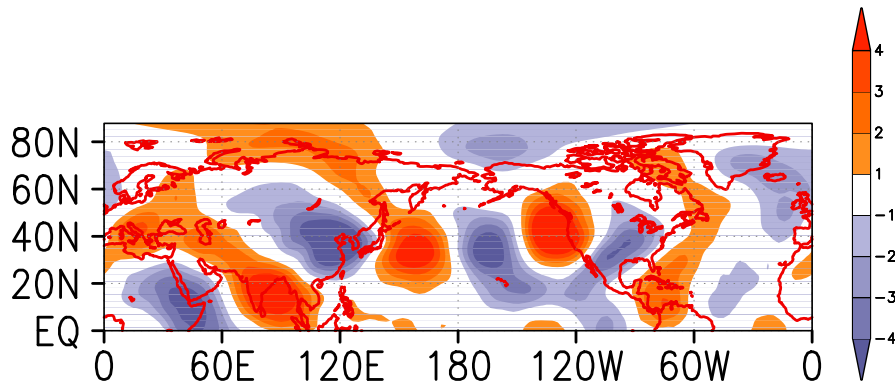


Figure 4.19: Meridional 300hPa winter (DJF) wind response for the "western Indian Ocean minus 1K" experiment; [m/s].

the 300hPa winter meridional wind – indicates that the change of the NAO may be via the circumglobal pattern.

Acknowledgments

The authors would like to thank Dr. Johann Jungclaus for the help with the coupled model, Daniela Matei for her useful comments and Katja Lohmann for the IDL help. This work was supported by the Federal German Ministry of Education and Research (BMBF) under grant No. 01 LW 0301A (Glowa) and under grant No. 01 LD 0030 (DEKLIM), the Ministry of Science and Research (MWF) of the state of Northrhine-Westfalia under grant No. 223 - 212 00 200. The model runs were performed at the German Climate Computing Center (DKRZ).

4.5 References

- Bader, J., and M. Latif, The impact of decadal-scale Indian Ocean sea surface temperature anomalies on Sahelian rainfall and the North Atlantic Oscillation, *Geophysical Research Letters*, **30(22)**, 2169, doi:10.1029/2003GL018426, 2003.
- Branstator, G., Circumglobal teleconnections, the jet stream waveguide, and the North Atlantic Oscillation, *Journal of Climate*, **15**, 1893-1910, 2002.
- Cayan D. R. , Latent and sensible heat-flux anomalies over the northern oceans - the connection to monthly atmospheric circulation, *Journal of Climate*, **17**, 1992.
- Hoerling, M.P., J.W. Hurrell, T.Y. Xu, Tropical origins for recent North Atlantic climate change, *Science*, **292**, 90-92, 2001.
- Hoerling, M. P., J. W. Hurrell, T. Xu, G. T. Bates, and A. Phillips (2004), Twentieth century North Atlantic climate change. Part II: Understanding the effect of Indian Ocean warming, *Climate Dynamics*, **23**, 391-405.
- Hurrell, J.W., Decadal trends in the North Atlantic Oscillation: Regional temperatures and precipitation, *Science*, **269**, 676-679, 1995.
- Hurrell, J.W., Y. Kushnir, G. Ottersen and Martin Visbeck (Eds.), *The North Atlantic Oscillation: Climatic significance and environmental impact*, 279 pp., American Geophysical Union, Washington DC, 2003.
- Hurrell, J. W., M. P. Hoerling, A. Phillips, and T. Xu, Twentieth century North Atlantic climate change. Part I: Assessing determinism, *Climate Dynamics*, **23**, 371-389, 2004.
- James I.N., and P.M. James, Ultra-low-frequency variability in a simple atmospheric model, *Nature*, **342**, 53-55, 1989.

- Latif, M., K. Arpe, and E. Roeckner, 2000: Oceanic Control of North Atlantic Sea Level Pressure Variability in Winter, *Geophysical Research Letters*, **27**, 727-730.
- Latif, M., E. Roeckner, M. Botzet, M. Esch, H. Haak, S. Hagemann, J. Jungclaus, S. Legutke, S. Marsland, U. Mikolajewicz, and J. Mitchell, 2004: Reconstructing, monitoring, and predicting multidecadal-scale changes in the North Atlantic Thermohaline Circulation with sea surface temperature, *Journal of Climate*, **17**, 1605-1614
- Lu, J., R. J. Greatbatch, and A. Peterson, Trend in Northern Hemisphere winter atmospheric circulation during the last half of the twentieth century, *Journal of Climate*, **17**, 3745-3760, 2004.
- Marsland, S. J., H. Haak, J. H. Jungclaus, M. Latif, and F. Röske, 2003: The Max-Planck-Institute global ocean/sea ice model with orthogonal curvilinear coordinates, *Ocean Modell.*, **5**, 91-127
- Pohlmann, H., M. Botzet, M. Latif, A. Roesch, M. Wild, and P. Tschuck, Estimating the decadal predictability of a coupled OAGCM, *Journal of Climate*, **17**, 4463-4472, 2004.
- Roeckner, E., K. Arpe, L. Bengtsson, M. Christoph, M. Claussen, L. Dümenil, M. Esch, M. Giorgetta, U. Schlese, and U. Schulzweida, The atmospheric general circulation model ECHAM-4: Model description and simulation of present-day climate, *MPI Report*, **218**, 1996.
- E. Roeckner, G. Bäuml, L. Bonaventura, R. Brokopf, M. Esch, M. Giorgetta, S. Hagemann, I. Kirchner, L. Kornblüeh, E. Manzini, A. Rhodin, U. Schlese, U. Schulzweida, A. Tompkins (2003): The atmospheric general circulation model ECHAM 5, *MPI Report*, **349**, 2003.
- Rodwell, M. J., D. P. Rowell, and C. K. Folland, Oceanic forcing of the wintertime North Atlantic Oscillation and European climate, *Nature*, **398**, 320 - 323, 1999.

- Saravanan, R., and J.C. McWilliams, Stochasticity and spatial resonance in interdecadal climate fluctuations, *Journal of Climate*, **10**, 2299-2320, 1997.
- Taylor, K. E., D. Williamson, and F. Zwiers, The sea surface temperature and sea ice concentration boundary conditions for AMIP II simulations, *PCMDI Report*, **60**, 2000.
- Trenberth K. E., G. W. Branstator, D. Karoly, A. Kumar, N. C. Lau, C. Ropelewski, Progress during TOGA in understanding and modeling global teleconnections associated with tropical sea surface temperatures, *J. Geophysical Research-Oceans*, **103 C7**, 14291-14324, 1998.

Chapter 5

Summary

5.1 Conclusions

This study explored the role of the tropical oceans in driving the recent trends of the NAO and the Sahelian rainfall. A focus was placed on the role of tropical Indian Ocean sea surface temperatures which have strongly increased in the past 50 years (e. g. , Kumar et al. 2004).

The basis for this attribution research is ensemble climate simulations with an atmospheric general circulation model (AGCM) and a coupled ocean-atmosphere general circulation model (OAGCM). These experiments provide evidence that the recent trends of the NAO and of West Sahelian rainfall have been strongly determined by the 20th Century trajectory of tropical SSTs, with the Indian Ocean warming trend being especially relevant.

The aim of this Ph. D. thesis was to obtain a better understanding of the the impact of sea surface temperature (SST) anomalies on the rainfall variability over northern West Africa on interannual to decadal timescales and on the North Atlantic Oscillation (NAO) on decadal timescales. Rainfall variability is a crucial factor in food production, water resource planning and ecosystems, especially in regions with scarce freshwater resources (Paeth and Hense 2004). The NAO can affect food production, energy consumption (Figure 5.1), and other economic factors (see Introduction). Understanding the processes which are relevant for sub-Saharan West African rainfall and the North Atlantic Oscillation variability are not only of academic, but also of

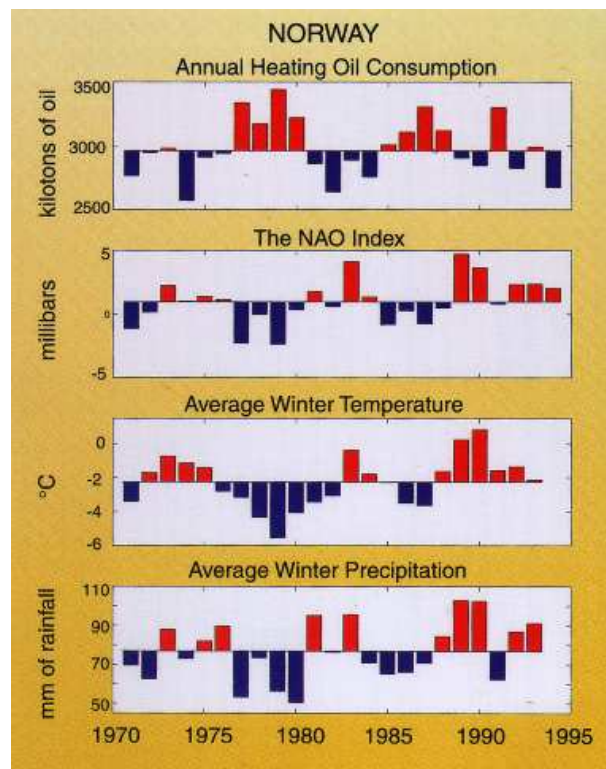


Figure 5.1: Figure shows the anti-correlation between the NAO index and the oil consumption in Norway. A strong NAO index is associated with relatively warm winters in Norway and vice versa. Figure downloaded at <http://ugamp.nerc.ac.uk/predicate/>.

direct interest for societies in the context of climate prediction. An overview of the results – based basically on simulations with the atmospheric general circulation model ECHAM4.5 – run in stand-alone mode – and the global ocean-atmosphere-sea ice model MPI-OM/ECHAM5 – is presented. In addition to the conclusions given at the end of Chapters 2 to 4, the results are in the following summarized in order to answer the scientific objectives raised in the introduction:

- *Is the drying trend over the West Sahel in particular driven by changes in only one ocean basin? Is it possible to restrict the region of SST anomalies to the Tropical Atlantic, Pacific or Indian Oceans? What kind of SST pattern in the individual ocean basins is the most important one? What is/are the basic physical atmospheric process(es) which lead(s) to the rainfall change over the West Sahel?*

By conducting a set of numerical experiments with an atmospheric general circulation model I found that the Indian Ocean warming in the last decades is of paramount importance in driving the recent observed drying trend over the West Sahel. When sea surface temperatures were changed in one ocean basin at a time, it was the Tropical Indian Ocean that dominated. The warming of the Indian Ocean produced mid-tropospheric large-scale subsidence over sub-Saharan West Africa. The anomalous descending motion suppressed convective activity.

- *Which ocean basin is the most important for the trend of the NAO? What is the mechanism responsible for the change of the NAO, since a clear mechanism of how the tropical SSTs impact the NAO was not given by Hoerling et al. (2001)?*

Additionally, it is found that the warming of the tropical Indian Ocean

has also likely contributed to the strengthening of the North Atlantic Oscillation observed during the recent decades. The response patterns of the experiments in which the tropical Indian Ocean SST is warmed/cooled project strongly upon the positive/negative polarity of the NAO index.

By analyzing the model simulations we found that the South Asian Jet can act as a waveguide with circumglobal teleconnection in the Northern Hemisphere. The meridional wind pattern – associated with this circumglobal teleconnection – is linked to the North Atlantic Oscillation. A warming/cooling in the Indian Ocean, especially in the western Indian Ocean, produces anomalies in the South Asian Jet. The waveguiding effect of the South Asian Jet carries the perturbation into the North Atlantic sector and leads to a NAO-like response.

Our analysis – confirmed by the observed trend in the western South Asian Jet and the anomaly pattern of the 300hPa winter meridional wind – indicates that the change of the NAO may be via the circumglobal pattern.

- *Sub-Saharan summer rainfall anomalies are mainly characterized by two distinctive patterns: A "dipole" and a "monopole" rainfall anomaly pattern between Sahel and Guinea Coast rainfall anomalies (see Introduction). The identification of key ocean areas for driving these two basic rainfall anomaly patterns over sub-Saharan West Africa in summer is another major aim of this thesis. This could improve the ability to predict sub-Saharan West African rainfall variability on interannual time-scales that is so vital for the society.*

We have identified the Indian and eastern tropical Atlantic Oceans as two key ocean areas for driving the two basic rainfall anomaly patterns over sub-Saharan West Africa in summer. By changing the SSTs in these two ocean areas simultaneously in atmosphere model experiments we are able to simulate the two observed basic patterns of the boreal summer rainfall variability over sub-Saharan West Africa. The dominant SST forcing along Guinea Coast are the SST anomalies of

the eastern tropical Atlantic and the associated anomalous water vapor content of the lower troposphere. The impact of these SST anomalies in the eastern tropical Atlantic on the boreal summer rainfall over sub-Saharan West Africa is confined to approximately 10°N . The rainfall north of this latitude (e. g. , over the West Sahel) is linked via changes in the large-scale atmospheric circulation to changes of the Indian Ocean SST. These findings are confirmed by our correlation analysis between the observed July to September rainfall indices of our two regions and the observed July to September sea surface temperatures. The out-of-phase rainfall anomaly pattern is associated with SST anomalies of the same sign in the eastern tropical Atlantic and the Indian Ocean. Opposite SST changes in these two ocean areas lead to a monopolar rainfall change over the whole west sub-Saharan region.

Intensity and position changes of the intertropical convergence zone (ITCZ) are referred to as the main causes for rainfall changes over West Africa in the literature. Our analysis shows that rainfall intensity changes – originating in different ocean basins – can ”mimic” a shift of the ITCZ in summer. Hence, position changes of the ITCZ over sub-Saharan West Africa can partly be deduced from intensity changes caused by SST anomalies in different oceans.

Our simulations indicate that a rainfall enhancement/reduction over the West Sahel is not necessarily linked to a supply of exceptionally wet/dry air to West Africa from the tropical Atlantic.

Since tropical SSTs appear to be predictable at least one season ahead, our results imply a great deal of predictability in sub-Saharan West African rainfall.

5.2 Discussion

I have identified the warming of the Indian Ocean as the primary cause for the drying trend in the West Sahel and as a principal contributor to the recent strengthening of the North Atlantic Oscillation.

An important question is whether the observed warming of the Indian Ocean may have been a consequence of anthropogenic climate change associated

with increased concentrations of anthropogenic greenhouse gases and aerosols. If it were to be demonstrated that anthropogenic climate change was the principal cause of the Indian Ocean warming – and therefore the cause of the drought in the Sahel – the responsibility for the drought would be transferred to the industrialized nations responsible for the majority of historical greenhouse gas emissions and aerosols, raising questions of attribution and liability (see Hulme 2001).

The performed experiments all used constant values of greenhouse gases and aerosols. Their capacity to qualitatively explain the NAO trend and the west sub-Saharan recent drying trend indicates that the direct atmospheric effect of those anthropogenic greenhouse gases and aerosols is not a necessary condition. However, the history of prescribed SSTs is likely to bear a footprint of the climate response to changes in the atmospheric chemical composition. Thus, the existence of an impact of anthropogenic greenhouse gases/aerosols on the mean state and variability of the oceans cannot be discounted. That the recent Indian Ocean warming contains a signature of anomalous greenhouse gas/aerosol forcing is suggested through analyses of historical integrations with coupled ocean-atmosphere climate models (Horerling et al. 2004).

It has to be tested further whether the Indian Ocean warming is due to anthropogenic climate change and when the warming might end.

We have identified the Indian and eastern tropical Atlantic oceans as two key ocean areas for driving the two basic rainfall anomaly patterns over sub-Saharan West Africa in summer. These findings could improve the ability to predict sub-Saharan West African rainfall variability on interannual time-scales that is so important for society. This shows the need to monitor sea surface temperatures for climate prediction. In the Introduction it was also emphasized that not only sea surface temperatures modulate sub-Saharan West African rainfall, but also natural vegetation processes (Zeng et al. 1999), and land use changes whose impacts in the Sahelian region are likely to increase rapidly in the coming years (Taylor et al. 2002). These processes have likely acted synergistically to produce the unusual recent drought in the Sahel (Zeng 2003).

The land-ocean-atmosphere processes that influence the West African Mon-

soon (WAM) variability will be addressed in the international upcoming African Monsoon Multidisciplinary Analysis (AMMA) project. The AMMA project has three overarching aims:

- To improve our understanding of the WAM and its influence on the physical, chemical and biological environment regionally and globally.
- To provide the underpinning science that relates climate variability to issues of health, water resources and food security for West African nations and defining relevant monitoring strategies.
- To ensure that the multidisciplinary research is effectively integrated with prediction and decision making activity

5.3 Additional Results

In the following some preliminary results are very briefly presented. They will be subject of two forthcoming papers. The results are based on the coupled model experiments – for model and experiment description see Chapter 4.

5.3.1 **Is there a relation between the secular rainfall variability over West Africa north and south of the Sahara desert?**

The rainfall in both Morocco and the sub-Saharan West Sahel region is characterized by a decline since about the 1970s, with the sub-Saharan reduction being a continuation of a trend that started in the 1950s (Figure 5.2; Lamb and Pepler 1991). The source of the pronounced decadal variability in these regions is one of the most pressing questions in climate dynamics today (Ward et al. 1999).

Both Morocco and sub-Saharan West Sahel experience very pronounced and well defined rainy seasons that are strongly out of phase with each other. The rainy season in the West Sahel is in the July to September (JAS) period

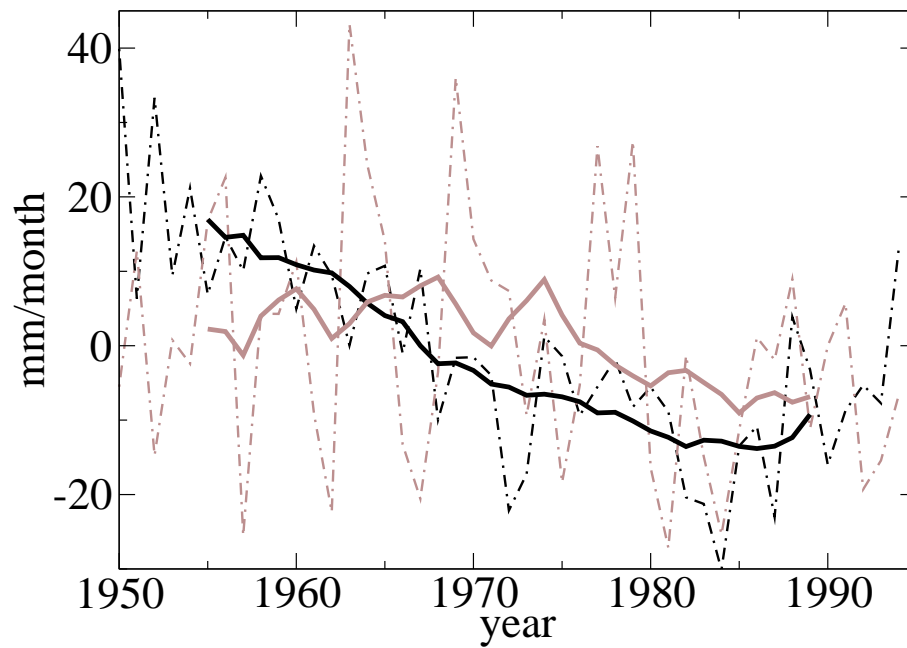


Figure 5.2: Observed rainfall anomaly over the West Sahel (black curves; area-average from 10° W to 10° E and from 12° N to 20° N) and Morocco (grey curves; area-average from 10° W to 3° W and from 31° N to 36° N) during the rainy seasons (July to September for the West Sahel and December to February for Morocco), based on the Climate Research Unit (CRU) dataset [mm/month]. The dot-dashed curves denote the seasonal means, the solid curves the 11-yr running mean.

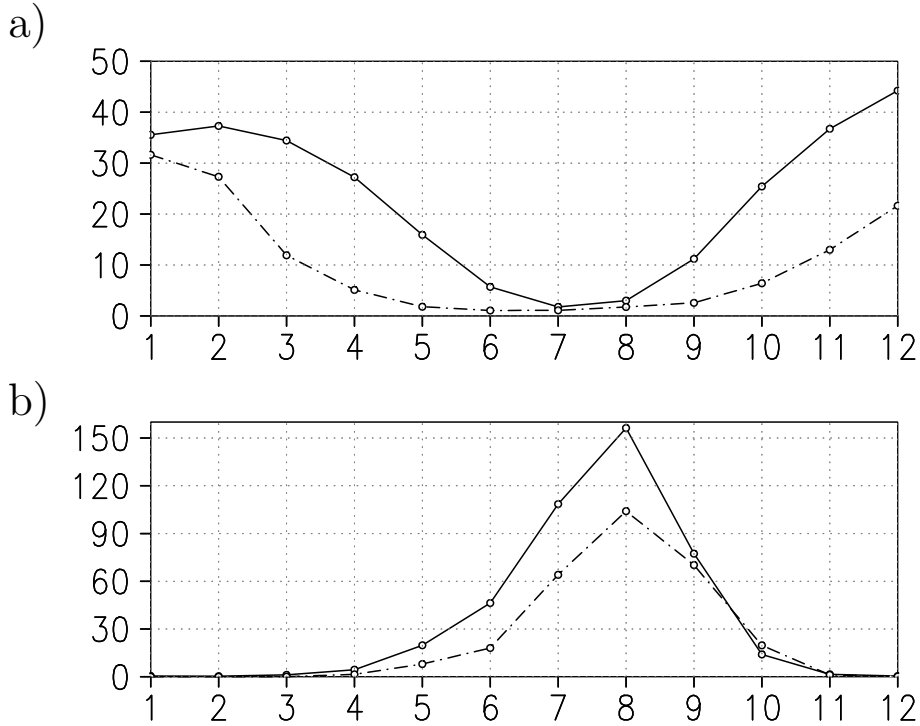


Figure 5.3: Annual cycle of the precipitation averaged over a) the Moroccan region (area-average from 10° W to 3° W and from 31° N to 36° N) and b) the West Sahel (area-average from 10° W to 10° E and from 12° N to 20° N); solid line: observation (GPCC); dot dashed line: simulated rainfall of the CTRL integration; units: mm/month.

(solid curve in the lower Figure 5.3). The rainy season in Morocco is approximately from November to March (solid curve in the upper Figure 5.3; Lamb and Pepler 1991). These contrasting annual rainfall marches are the products of very different components of the global atmospheric circulation pattern. On the northern side of the Sahara desert, the intensity of the summer subtropical high pressure system precludes almost any precipitation during JAS (Ward et al. 1999). At this time, to the south of the Sahara, the intertropical convergence zone (ITCZ) has reached its most northerly position. Sub-Saharan rainfall is produced by westward propagating lines of thunderstorms "West African disturbances lines" with north-south orientation. These systems are displaced to the south of the sub-Saharan zone

during the other season of the year.

Most Moroccan rainfall is associated with the extratropical cyclonic storm systems that move eastward off the North Atlantic and onto Western Europe and the Mediterranean during the northern Hemisphere winter half-year. The tracks of those systems are too far north during the rest of the year to affect Morocco – which is the result of the extension of the subtropical High onto Morocco.

The Moroccan rainfall is significantly anti-correlated to the state of the NAO. During negative NAO index values the "storm track" has a west-east orientation. This is favorable for cyclonic and frontal systems to affect north-west Africa. During positive NAO winter months the "storm track" is more north steering weather systems away from Morocco.

I have shown that the Indian Ocean warming/cooling produces a rainfall reduction/enhancement over the West Sahel and a stronger/weaker NAO. Figure 5.4a shows the mean winter (DJF) precipitation anomaly over north-west Africa (relative to the control integration) for the "warm Indian Ocean" and figure 5.4b for the "cold Indian Ocean" experiment. Additionally, figures 5.5a and 5.5b show the mean July to September Sahelian rainfall anomalies for the same experiments. These experiments show that the Indian Ocean forces West African rainfall both north and south of the Sahara desert. The experiments indicate that the observed warming in the Indian Ocean may have contributed to the secular West African rainfall decline both north and south of the Sahara desert. The observed Indian Ocean warming may be a common cause for the rainfall decline over West Africa north and south of the Sahara desert.

5.3.2 Indian Ocean impact on the thermohaline circulation (THC)

I have shown that the Indian Ocean warming is a principal contributor to the recent trend of the NAO. The trend in the NAO is associated with convection intensity changes in the Labrador and the Greenland-Iceland Seas (Dickson et al., 1996) which influence the strength and character of the Atlantic meridional overturning circulation. Hence, I would like to test whether the tropical

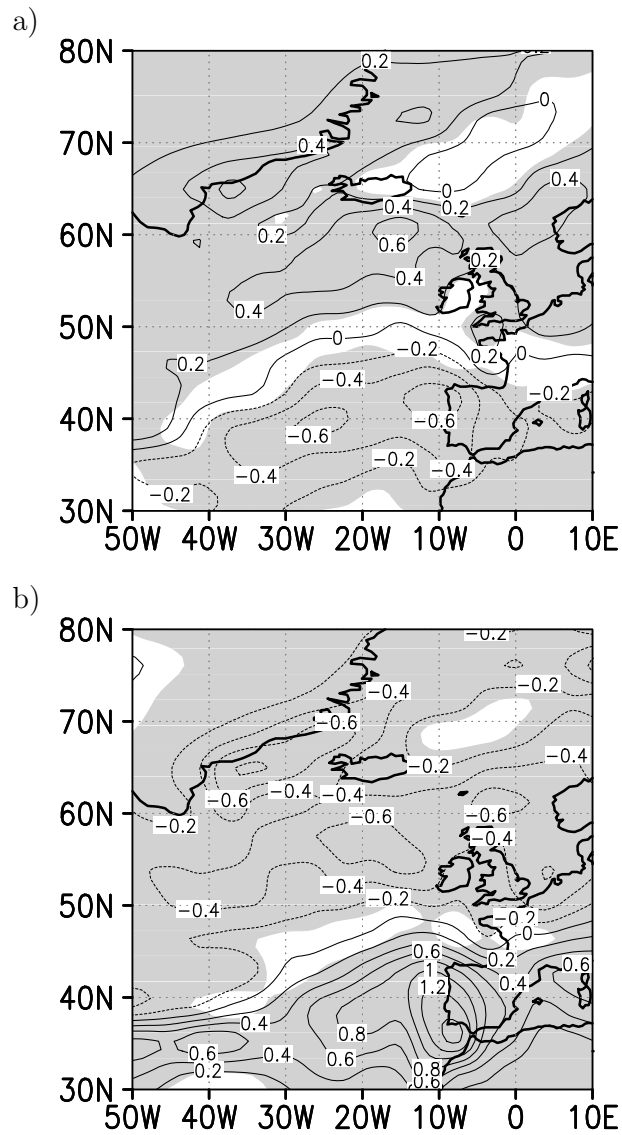


Figure 5.4: Mean DJF precipitation anomaly (relative to control integration): a) for the SST-sensitivity experiment "warm Indian Ocean"; b) for the SST-sensitivity experiment "cold Indian Ocean"; shading indicates significant changes at the 95% confidence level according to a two-tailed t-test; [mm/day].

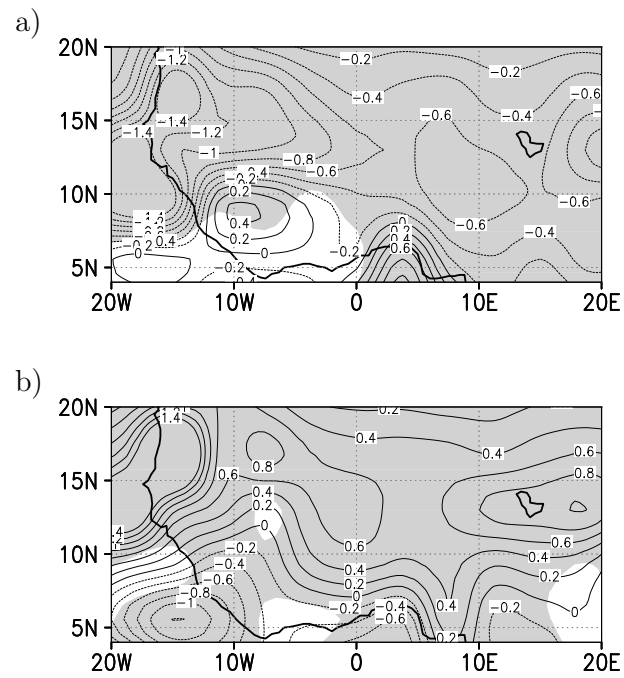


Figure 5.5: Mean JAS precipitation anomaly (relative to control integration): a) for the SST-sensitivity experiment "warm Indian Ocean"; b) for the SST-sensitivity experiment "cold Indian Ocean"; shading indicates significant changes at the 95% confidence level according to a two-tailed *t*-test; [mm/day].

Indian Ocean may force the Atlantic thermohaline circulation (THC).

The Atlantic thermohaline circulation (THC) is an important component of the global climate system (Broecker 1991). In the North Atlantic the Gulf Stream transports enormous amounts of heat poleward ($\approx 1.2PW$) as part of the THC, thereby warming western Europe. The THC is forced by convection at high latitudes, which causes dense surface waters to sink to deeper ocean layers, forming the so-called North Atlantic Deep water (NADW). Strong and rapid changes in the intensity of the NADW formation have been reported from paleoclimatic records (Broecker et al. 1985), and it is well established that such changes exert a strong impact on the climate over large land areas (e.g., Manabe and Stouffer 1995, 1999; Schiller et al. 1997). Several papers have suggested that the THC may weaken in response to greenhouse warming (e.g., Mikolajewicz et al. 1990; Manabe et al. 1991; Stocker and Wright 1991; Cubasch et al. 1992; Manabe and Stouffer 1994; Rahmstorf 1995, 1997, 1999; Wood et al. 1999). Most greenhouse-gas simulations show a weakening of the North Atlantic thermohaline circulation (THC) in response to enhanced surface warming and freshening in the subpolar regions. Here results are presented from a state-of-the-art global coupled climate model that the observed warming of the Indian Ocean may provide stabilizing feedbacks.

Delworth et al. (2000) analyzed the impact of the recent trend in the Arctic/North Atlantic Oscillation for the North Atlantic thermohaline circulation. Using ensembles of numerical experiments with a coupled ocean-atmosphere model, Delworth et al. (2000) show that a weakening of the THC due to greenhouse gases could be delayed by several decades in response to a sustained upward trend in the Arctic/North Atlantic oscillation during winter, such as has been observed over the last 30 years. I have shown that the observed warming of the Indian Ocean played/plays a crucial role for the recent trend of the NAO. So it is possible that the Indian Ocean warming has also important implications on the Atlantic thermohaline circulation via its impact on the NAO.

The control run simulates a meridional overturning circulation of about 15 Sv ($1\text{ Sv}=10^6\text{m}^3\text{s}^{-1}$) at 30°N (black curve in Figure 5.6). In the SST sensitivity experiments the THC changes. A warm Indian Ocean leads to an increase in the meridional overturning of about 3 Sv (red curve in Figure 5.6). A cold

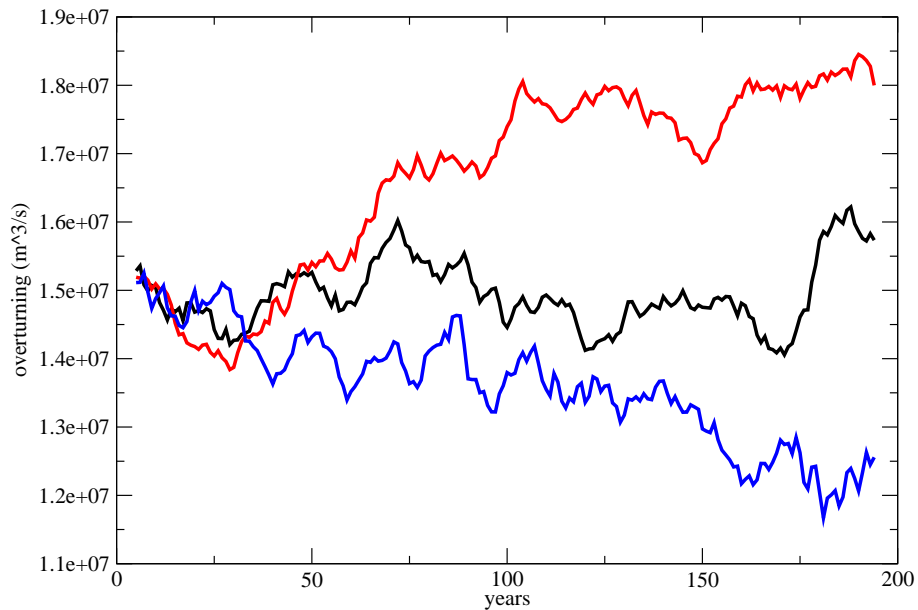


Figure 5.6: *Atlantic meridional overturning at 30°N (11-year running mean): for the control integration (black curve); for the SST-sensitivity experiment "warm Indian Ocean" (red curve); for the SST-sensitivity experiment "cold Indian Ocean" (blue curve); units [m³/s].*

Indian Ocean produces a reduction in the meridional overturning circulation of about 3 Sv (blue curve in Figure 5.6). The physics responsible for the change of the THC in our model is mainly related to tropical air-sea interactions and not to changes in the NAO. It is found that the rather strong observed warming in the Tropical Indian Ocean influences the fresh water budget of the Tropical Atlantic, and this affects the THC.

Large-scale air sea interactions in the Tropics lead to anomalous high salinities in the Tropical Atlantic involving anomalous fresh water fluxes in this region. These are advected into the sinking region, thereby increasing the surface density. The time lag between the changes in tropical SSTs and the THC is of the order of several decades (see Figure 5.6). The mechanism is similar to that described in Latif et al. (2000).

5.4 References

- Broecker, W. S., D. M. Peteet, and D. Rind, 1985: Does the ocean-atmosphere system have more than one stable mode of operation?, *Nature*, **315**, 21-26
- Broecker, W. S., 1991: The great ocean conveyor, *Oceanography*, **4**, 79-89
- Cubasch, U., K. Hasselmann, H. Höck, E. Maier-Reimer, U. Mikolajewicz, B. D. Santer, and R. Sausen, 1992: Time-dependent greenhouse warming computations with a coupled ocean-atmosphere model, *Climate Dynamics*, **8**, 55-69.
- Delworth, T. L., and K. W. Dixon, 2000: Implications of the recent trend in the Arctic/North Atlantic Oscillation for the North Atlantic Thermohaline Circulation, *Journal of Climate*, **13**, 3721-3727
- Dickson, R. R., J. Lazier, J. Meincke, P. Rhines, and J. Swift, 1996: Long-term co-ordinated changes in the convective activity of the North Atlantic, *Progress in Oceanography*, **38**, 241-295.
- Hoerling, M.P., J.W. Hurrell, T.Y. Xu, 2001: Tropical origins for recent North Atlantic climate change, *Science*, **292**, 90-92.
- Hoerling, M. P., J. W. Hurrell, T. Xu, G. T. Bates, and A. Phillips, 2004, Twentieth century North Atlantic climate change. Part II: Understanding the effect of Indian Ocean warming, *Climate Dynamics*, **23**, 391-405.
- Hulme, M., 2001: Climatic perspectives on Sahelian desiccation: 1973-1998, *Global Environmental Change*, **11**, 19-29.
- Kumar A., F. Yang, L. Goddard, and S. Schubert, 2004: Differing trends in the tropical surface temperatures and precipitation over land and oceans, *Journal of Climate*, **17**, 653-664.
- Lamb, P. J. and R. A. Pepler, 1991: West Africa, *Teleconnections linking worldwide climate anomalies*, M. Glantz, R. Katz and N. Nicholls, Eds., Cambridge University Press, 121-189.

- Latif, M. E. Roeckner, U. Mikolajewicz, and R. Voss, 2000: Tropical stabilization of the thermohaline circulation in a greenhouse warming simulation, *Journal of Climate*, **13**, 1809-1813.
- Manabe, S. , and R. J. Stouffer, M. Spelman, and K. Bryan, 1991: Transient responses of a coupled ocean-atmosphere model to gradual changes of atmospheric CO_2 , *Journal of Climate*, **4**, 785-818.
- Manabe, S. , and R. J. Stouffer, 1994: Multiple-century response of a coupled-atmosphere model to an increase of atmospheric carbon dioxide, *Journal of Climate*, **7**, 5-23.
- Manabe, S. , and R. J. Stouffer, 1995: Simulation of abrupt climate change induced by freshwater input to the North Atlantic Ocean, *Nature*, **378**, 165-167.
- Manabe, S. , and R. J. Stouffer, 1999: The role of thermohaline circulation in climate, *Tellus*, **51**, 91-109
- Mikolajewicz, U. , B. D. Santer, and E. Maier-Reimer, 1990: Ocean response to greenhouse warming, *Nature*, **345**, 589-593.
- Mikolajewicz, U. , and R. Voss, 2000: The role of the individual air sea flux components in CO_2 -induced changes of the oceans circulation and climate. *Climate Dynamics*, **16**, 627-642.
- Paeth, H. , and A. Hense, 2004: SST versus climate change signals in West African rainfall: 20th Century variations and future projections, *Climatic Change*, **65**, 179-208.
- Rahmstorf, S., 1995: Bifurcations of the Atlantic thermohaline circulation in response to changes in the hydrological cycle, *Nature*, **378**, 145-149.
- Rahmstorf, S., 1997: Risk of sea-change in the Atlantic, *Nature*, **388**, 825-826.
- Rahmstorf, S., 1999: Shifting seas in the greenhouse?, *Nature*, **399**, 523-524.

- Schiller, A., U. Mikolajewicz, and R. Voss, 1997: The stability of the thermohaline circulation in a coupled oceanatmosphere model, *Climate Dynamics*, **13**, 325-348.
- Stocker, T. F., and D. G. Wright, 1991: Rapid transitions of the ocean's deep circulation induced by changes in surface water fluxes, *Nature*, **351**, 729-732.
- Taylor C. M., E. F. Lambin, N. Stephenne, R. J. Harding, R. L. H. Essery, 2002: The influence of land use change on climate in the Sahel, *Journal of Climate*, **15**, 3615-3629.
- Ward, M.N., P. J. Lamb, D. H. Portis, M. el Hamly, and R. Sebbari, 1999: Climate variability in northern Africa. Understanding droughts in the Sahel and the Maghreb. *Beyond el Niño: Decadal and interdecadal climate variability*, A. Navarra, Ed., Springer-Verlag, 119-140.
- Wood, R. A., A. B. Keen, J. F. Mitchell, and J. M. Gregory, 1999: Changing spatial structure of the thermohaline circulation in response to atmospheric CO_2 forcing in a climate model, *Nature*, **399**, 572-575.
- Zeng, N., J. D. Neelin, K. M. Lau, C. J. Tucker, 1999: Enhancement of interdecadal climate variability in the Sahel, *Science*, **286**, 1537-1540.
- Zeng, N., 2003: Drought in the Sahel, *Science*, **302**, 999-1000.

List of Figures

| | | |
|-----|---|----|
| 1.1 | Observed JJAS rainfall anomaly over the West Sahel, based on the Climate Research Unit dataset (mm/month). The rainfall is averaged from 10 ⁰ W to 10 ⁰ E and from 12 ⁰ N to 20 ⁰ N. The black curve denotes the seasonal mean, the red curve the 11-yr running mean. | 2 |
| 1.2 | Illustration of the two extreme phases of the North Atlantic Oscillation (NAO) with some climatic impacts. Figure a) shows the positive and b) the negative NAO phase. Figures are available at http://www.ldeo.columbia.edu/~visbeck/misc | 7 |
| 1.3 | Winter (December to March) index of the NAO based on the difference of normalized pressures between Lisbon, Portugal, and Stykkishólmur/Reykjavik, Iceland from 1864 through 2000. The heavy solid line represents the meridional pressure gradient smoothed to remove fluctuations with periods less than 4 years. From Hurrell et al. (2001). | 9 |
| 2.1 | a) Observed JJAS rainfall anomaly over the West Sahel, based on the Climate Research Unit dataset (mm/month), b) observed winter (DJFM) NAO index defined by Hurrell (1995), c) observed tropical Indian Ocean SST Index for the JJAS season (in Celsius), based on the Reynolds SSTs; averaged from the east coast of Africa to 120 ⁰ E and from 30 ⁰ S to 30 ⁰ N. The black curves denote the seasonal means, the red curves the 11-yr running mean or the linear trend. | 25 |

| | | |
|-----|--|----|
| 2.2 | a) SST difference field: JJAS SST anomaly in the tropics (Wet-Mode (1951-1960) minus Dry-Mode (1979-1995)) (in Kelvin) and b) SST anomaly for the "Indian Ocean minus 1K" experiment (in Kelvin) | 28 |
| 2.3 | a) Simulated JJAS rainfall anomaly (relative to control integration) for the experiments with: Full SST anomaly of Figure 2.2a ("Global Tropics"); b) Indian Ocean portion of Figure 2.2a ("Indic"); c) SST anomaly of Figure 2.2b ("Indian Ocean minus 1K"); units: mm/month; the box indicates the West Sahel. | 30 |
| 2.4 | a) Simulated DJF sea level pressure (SLP) anomaly (relative to control integration) for the experiments with: Full SST anomaly of Figure 2.2a ("Global Tropics"); b) Indian Ocean portion of Figure 2.2a ("Indic"); c) SST anomaly of Figure 2.2b ("Indian Ocean minus 1K"); units: hPa. | 32 |
| 3.1 | Empirical Orthogonal Function (EOF) analysis loading patterns of the observed July to September rainfall; (a) EOF1, (b) EOF2. | 42 |
| 3.2 | Correlation coefficients between the observed JAS rainfall averaged over the box with the observed JAS rainfall over West Africa. | 43 |
| 3.3 | Correlation between the observed JAS SST and the observed JAS rainfall averaged over: a) the Guinea Coast area (indicated by the box) ; b) the West Sahel region (indicated by the box). | 44 |
| 3.4 | Annual cycle of the precipitation averaged over a) the Guinea Coast region and b) the West Sahel; solid line: observation (CRU); dot dashed line: simulated rainfall of the CTRL integration; units: mm/month. | 46 |
| 3.5 | Illustration of the SST anomaly in the individual experiments. | 47 |

- 3.6 Empirical Orthogonal Function (EOF) analysis loading patterns of the simulated July to September rainfall in an atmospheric model driven with climatological SSTs; (a) EOF1, (b) EOF2. 49
- 3.7 Simulated JAS rainfall anomaly (relative to control integration) for the experiments with: a) eastern tropical Atlantic reduced by one Kelvin; b) eastern tropical Atlantic enhanced by one Kelvin; units: mm/month. 50
- 3.8 Simulated 1000hPa JAS humidity anomaly (relative to control integration) for the experiments with: a) eastern tropical Atlantic reduced by one Kelvin; b) eastern tropical Atlantic enhanced by one Kelvin; units: g/kg; shading indicates significant changes at the 95% confidence level according to a two-tailed t-test. 51
- 3.9 Simulated JAS rainfall anomaly (relative to control integration) for the experiments with: a) Indian Ocean reduced by one Kelvin; b) Indian Ocean enhanced by one Kelvin; units: mm/month. 53
- 3.10 Simulated 500 hPa JAS vertical velocity (ω) anomaly (relative to control integration) for the experiments with: a) Indian Ocean reduced by one Kelvin; b) Indian Ocean enhanced by one Kelvin; units: Pa/s; shading indicates significant changes at the 95% confidence level according to a two-tailed t-test). 54
- 3.11 Coloring shows vertical velocity anomaly (in Pa/s; multiplied by $(-1) \times 10^2$) and vectors the zonal and vertical wind anomaly (u-component in m/s; z-component in Pa/s but multiplied by $(-1) \times 10^2$) for the experiments with: a) Indian Ocean reduced by one Kelvin; b) Indian Ocean enhanced by one Kelvin; u- and z-component averaged from 12°N to 20°N. 55
- 3.12 Simulated JAS rainfall anomaly (relative to control integration) for the experiments with: a) Indian Ocean and eastern tropical Atlantic reduced by one Kelvin; b) Indian Ocean and eastern tropical Atlantic enhanced by one Kelvin; units: mm/month. 57

| | | |
|------|--|----|
| 3.13 | Correlation between the observed JAS SST averaged over the eastern tropical Atlantic area (indicated by the box) and the observed JAS SST. | 58 |
| 3.14 | Simulated 1000hPa JAS humidity anomaly (relative to control integration) for the experiment with Indian Ocean and eastern tropical Atlantic enhanced by one Kelvin; units: g/kg; shading indicates significant changes at the 95% confidence level according to a two-tailed t-test. | 59 |
| 3.15 | Observed area-averaged SST Index for: a) eastern tropical Atlantic; b) tropical Indian Ocean; both for the JAS season (in Celsius), based on the Reynolds SSTs; the black curves denote the JAS means; the red curves the linear trend. | 60 |
| 3.16 | Simulated JAS rainfall anomaly (relative to control integration) for the experiments with: a) Indian Ocean enhanced and eastern tropical Atlantic reduced by one Kelvin; b) Indian Ocean reduced and eastern tropical Atlantic enhanced by one Kelvin; units: mm/month. | 62 |
| 4.1 | Observed winter (DJFM) NAO index defined by Hurrell (1995). The black curve denotes the seasonal mean, the red curve the 11-yr running mean. | 71 |
| 4.2 | Observed annual tropical Indian Ocean SST Index (in Celsius), based on the Reynolds SSTs; averaged from the east coast of Africa to 120°E and from 30°S to 30°N. The black curve denotes the annual means, the red curve the linear trend. | 73 |
| 4.3 | Red coloring shows the area of the tropical Indian Ocean in which the sea surface temperatures are prescribed for the individual OAGCM SST-sensitivity experiments. | 74 |
| 4.4 | Annual sea surface temperatures averaged over the tropical Indian Ocean: for the control integration (black curve); for the SST-sensitivity experiment "warm Indian Ocean" (red curve); for the SST-sensitivity experiment "cold Indian Ocean" (blue curve); units [Kelvin]. | 75 |

| | | |
|------|--|----|
| 4.5 | First Empirical Orthogonal Function (EOF) loading pattern of the simulated winter (DJF) sea level pressure of the OAGCM control integration. | 76 |
| 4.6 | SST anomaly for a) the Indian Ocean minus 1K AGCM experiment; b) the western Indian Ocean minus 1K AGCM experiment. | 77 |
| 4.7 | Mean DJF sea level pressure anomaly (relative to control integration): a) for the SST-sensitivity experiment "warm Indian Ocean"; b) for the SST-sensitivity experiment "cold Indian Ocean"; units [hPa]. | 79 |
| 4.8 | Correlation of winter (DJF) 300hPa meridional wind averaged over the black box and winter 300hPa meridional wind in the Northern Hemisphere. | 80 |
| 4.9 | The leading EOF of Northern Hemisphere 300hPa winter (DJF) meridional wind [m/s per standard deviation]. | 81 |
| 4.10 | Correlation of winter (DJF) 300hPa meridional wind with the first principal component of winter (DJF) sea level pressure over the North Atlantic sector (NAO index) in the control integration. The crosses mark the centers of the ten lobes in the EOF1 plot of the meridional wind in Figure 4.9. | 81 |
| 4.11 | Correlation of winter (DJF) 300hPa zonal wind with the first principal component of winter (DJF) meridional wind in the control integration. | 82 |
| 4.12 | Correlation of winter (DJF) 300hPa zonal wind with the first principal component of winter (DJF) sea level pressure over the North Atlantic sector (NAO index) in the control integration. | 83 |
| 4.13 | Mean simulated winter (DJF) zonal wind anomaly (relative to control integration): a) for the SST-sensitivity experiment "warm Indian Ocean"; b) for the SST-sensitivity experiment "cold Indian Ocean"; [m/s]. | 84 |
| 4.14 | Mean simulated winter (DJF) precipitation anomaly (relative to control integration): a) for the SST-sensitivity experiment "warm Indian Ocean"; b) for the SST-sensitivity experiment "cold Indian Ocean"; units [mm/month]. | 85 |

- 4.15 Simulated 11-yr running mean timeseries of the winter (DJF)
 a) zonal wind anomaly index in the South Asian Jet region
 and b) NAO index (relative to the mean of the control in-
 tegration) for the control integration (black curve); for the
 SST-sensitivity experiment "warm Indian Ocean" (red curve);
 for the SST-sensitivity experiment "cold Indian Ocean" (blue
 curve). 86
- 4.16 Observed winter (DJF) zonal wind anomaly index (see text
 for details) in the South Asian Jet region, based on the NCEP
 reanalysis data. The dotted-dashed curve denotes the seasonal
 means, the thick solid black curve the 11-yr running mean. . . 88
- 4.17 Observed meridional 300hPa winter (DJF) wind anomaly be-
 tween the mean of the years ((1982-1993) minus (1949-1960)),
 based on the NCEP reanalysis data; [m/s]. 89
- 4.18 Mean DJF sea level pressure anomaly (relative to control in-
 tegration): a) for the SST-sensitivity experiment "Indian Ocean
 minus 1K"; b) for the SST-sensitivity experiment "western
 Indian Ocean minus 1K experiment"; [hPa]. 90
- 4.19 Meridional 300hPa winter (DJF) wind response for the "west-
 ern Indian Ocean minus 1K" experiment; [m/s]. 91
- 5.1 Figure shows the anti-correlation between the NAO index and
 the oil consumption in Norway. A strong NAO index is asso-
 ciated with relatively warm winters in Norway and vice versa.
 Figure downloaded at <http://ugamp.nerc.ac.uk/predicate/>. . . 96
- 5.2 Observed rainfall anomaly over the West Sahel (black curves;
 area-average from 10°W to 10°E and from 12°N to 20°N) and
 Morocco (grey curves; area-average from 10°W to 3°W and
 from 31°N to 36°N) during the rainy seasons (July to Septem-
 ber for the West Sahel and December to February for Mo-
 rocco), based on the Climate Research Unit (CRU) dataset
 [mm/month]. The dot-dashed curves denote the seasonal means,
 the solid curves the 11-yr running mean. 102

- 5.3 Annual cycle of the precipitation averaged over a) the Moroccan region (area-average from 10°W to 3°W and from 31°N to 36°N) and b) the West Sahel (area-average from 10°W to 10°E and from 12°N to 20°N); solid line: observation (GPCC); dot dashed line: simulated rainfall of the CTRL integration; units: mm/month. 103
- 5.4 Mean DJF precipitation anomaly (relative to control integration): a) for the SST-sensitivity experiment "warm Indian Ocean"; b) for the SST-sensitivity experiment "cold Indian Ocean"; shading indicates significant changes at the 95% confidence level according to a two-tailed t-test; [mm/day]. . . . 105
- 5.5 Mean JAS precipitation anomaly (relative to control integration): a) for the SST-sensitivity experiment "warm Indian Ocean"; b) for the SST-sensitivity experiment "cold Indian Ocean"; shading indicates significant changes at the 95% confidence level according to a two-tailed t-test; [mm/day]. . . . 106
- 5.6 Atlantic meridional overturning at 30°N (11-year running mean): for the control integration (black curve); for the SST-sensitivity experiment "warm Indian Ocean" (red curve); for the SST-sensitivity experiment "cold Indian Ocean" (blue curve); units [m^3/s]. 108

Acknowledgements

I am very grateful to Professor Dr. Mojib Latif for giving me the opportunity to accomplish this Ph. D. at the Max-Planck-Institut für Meteorologie, for his encouragement, and his continuous support. Furthermore, I am very grateful to Professor Dr. Hartmut Graßl for examining this dissertation.

I would like to thank my colleagues, especially Dr. Noel Keenlyside, Dr. Christian Reick, Dr. Johann Jungclaus, Dr. Helmuth Haak, David Schröder, Katja Lohmann, Daniela Matei, Holger Pohlmann, and Caroline Narayan.

I also thank my family for their support and encouragement.

This work was supported by the Federal German Ministry of Education and Research (BMBF) under grant No. 01 LW 0301A (Glowa), and the Ministry of Science and Research (MWF) of the state of Northrhine-Westfalia under grant No. 223 - 212 00 200.